Future energy consumption of passenger vehicles in Europe: effects of powertrain choice, fleet composition, and temperature variability

SET3901: Thesis Project SET

Georgios Margonis

Delft University of Technology

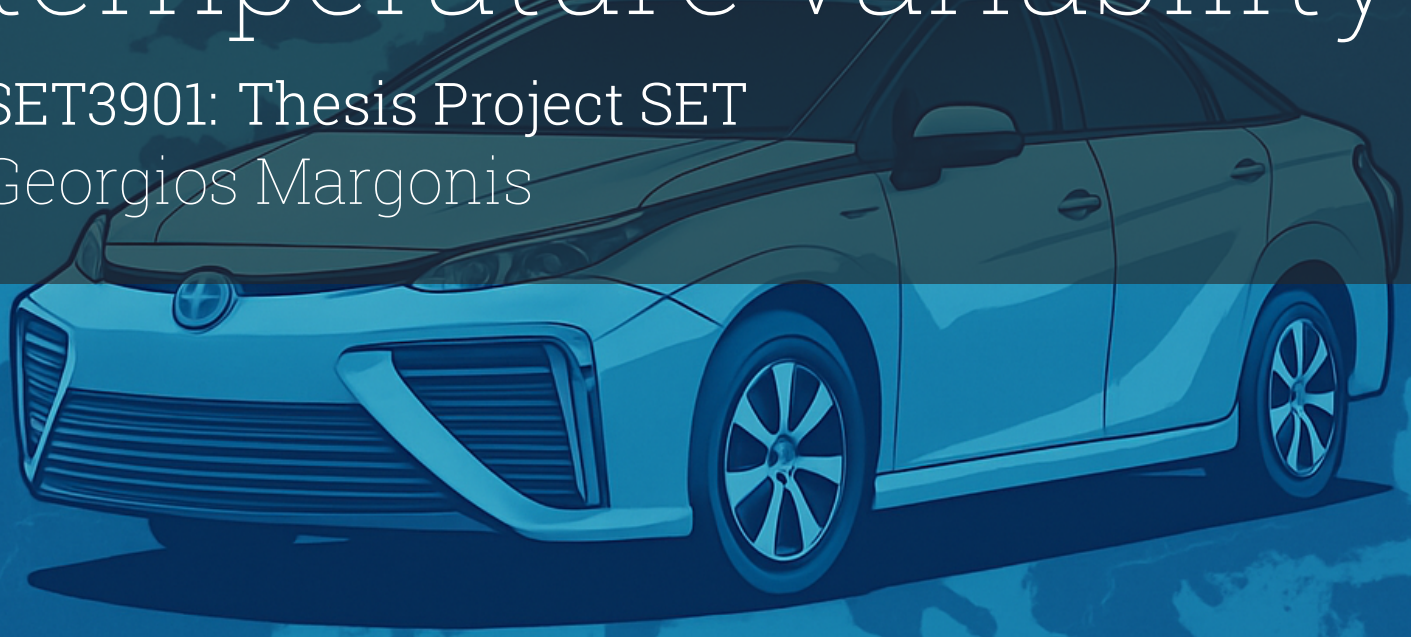

TU Delft

Future energy consumption of passenger vehicles in Europe: effects of powertrain choice, fleet composition, and temperature variability

by

Georgios Margonis

to obtain the degree of Master of Science
at the Delft University of Technology,
to be defended publicly on Tuesday July 14, 2025 at 03:15 PM.

Student number:	5955602	
Project duration:	December 5, 2024 – July 14, 2025	
Thesis committee:	Dr. S.J. Pfenninger-Lee,	TU Delft, supervisor
	Dr. Baiba Pudāne,	TU Delft
Daily supervisor:	Dr. Francesco Sanvito,	TU Delft

TU Delft

Preface

This thesis is the final product of my Master's degree in Sustainable Energy Technology at Delft University of Technology. It represents not only the culmination of months of dedicated work and research but also the end of a rewarding academic journey that has significantly shaped my professional and personal development.

The research presented here explores the modeling and assessment of hydrogen fuel cell electric vehicles (FCEVs) within the broader context of European transport decarbonization. The work builds upon the Vehicle Consumption Assessment Model (VCAM) and reflects my deep interest in the intersection of energy systems, mobility, and climate resilience. The process has challenged me technically and intellectually, and it has provided valuable insights into the complexities of future transport planning under climate constraints.

I would like to express my sincere gratitude to my supervisors, Francesco Sanvito and Stefan Pfenninger-Lee, for their continuous guidance, critical feedback, and encouragement throughout this project.

Special thanks go to my family and friends, whose patience and encouragement helped me stay focused and motivated. Their support, both emotional and practical, has been indispensable.

I hope this thesis contributes meaningfully to the growing body of knowledge on sustainable mobility and inspires further work toward low-carbon, efficient transport systems.

Georgios Margonis
Delft, July 2025

Summary

The transition to de-fossilized energy systems plays a central role in achieving climate neutrality in Europe, and the transport sector is pivotal in this transformation. Nowadays, passenger vehicles represent an important share of the final energy consumption and the greenhouse gas emissions. As internal combustion engine vehicles (ICEVs) are gradually phased out and replaced by battery electric vehicles (BEVs), and hydrogen fuel cell electric vehicles (FCEVs), understanding the evolving energy demand profile of passenger transport becomes more and more critical. This thesis addresses this challenge by quantifying the way in which the differences in powertrain technologies, in the vehicle types, and in weather conditions influence the energy consumption and the total energy demand across European regions.

The core of this research is the enhancement of the Vehicle Consumption Assessment Model (VCAM), a simulation platform capable of evaluating the energy consumption of different powertrains under various environmental and operational conditions. The model was extended to include a detailed representation of FCEVs and used under dynamic weather profiles and region-specific fleet compositions. These advancements allowed the simulation of real-world driving scenarios by using both historical and projected climate data, as well as the assessment of policy pathways and fleet evolution trends through 2050.

The methodological framework followed a multi-layered approach. First, a powertrain comparison for BEVS, FCEVs, and ICEVs has been made to evaluate them across different vehicle segments, considering performance under different driving cycles. Second, a temperature sensitivity analysis has been made for forty years of temperature data for Greece, Germany, and Finland, which were used to quantify the impact of cold and hot conditions on energy consumption and range for each powertrain technology. Lastly, a scenario-based analysis has been performed to scrutinize the effects of different IEA policy pathways (STEPS, SDS, NZE) and IPCC climate scenarios (RCP 2.6, 4.5, 8.5), as well as the influence of the growing SUV market share, on the passenger vehicle energy demand in 2050.

The results show that the energy demand is highly sensitive to the selection of powertrain technology, with BEVs offering the highest efficiency, as well as the highest sensitivity to ambient temperature. The FCEVs perform more consistently across extreme temperatures, but consume more energy than BEVs. ICEVs are the least efficient vehicles, but they present a moderate sensitivity to temperature because of their capability to use the engine's waste heat to cover the thermal loads. Vehicle size can significantly alter consumption, especially for electrified vehicles in extreme climates.

Regarding the regional effects, the projections for the passenger vehicle energy demand differ substantially. Germany's demand remains the highest due to population and mobility volume, while Finland shows the greatest sensitivity to climate conditions. Greece, where the most moderate climate conditions exist, presents the lowest variability. Across all technologies, BEVs offer the highest efficiency but also the greatest vulnerability to temperature extremes, with the energy consumption rising to more than 40% in cold conditions. FCEVs, which are less efficient overall, keep a more stable performance across temperature variations. The scenario analysis made shows that the ambitious decarbonization strategies (STEPS, SDS, NZE) could reduce total passenger vehicle energy demand by more than 60% relative to 2019 levels. However, this reduction is sensitive to fleet composition. To be more specific, for example, an annual SUV market growth of 2 percent could increase energy demand by up to 19% in Germany compared to a no-growth baseline. Similarly, consumptiom in the coldest years can exceed the warmest by 8 - 15 % for FCEVs and BEVs, depending on the region.

In conclusion, this thesis provides a detailed and geographically differentiated understanding of the passenger vehicle energy demand during the energy transition. It underlines the need to plan, while considering climate conditions, segments, and technologies to ensure that the electrification of the transport sector aligns with the broader goals.

Contents

List of Figures

List of Tables

Nomenclature

If a nomenclature is required, a simple template can be found below for convenience. Feel free to use, adapt or completely remove.

Abbreviations

Abbreviation	Definition
AFIR	Alternative Fuels Infrastructure Regulation
ANL	Argonne National Laboratory
BEV	Battery Electric Vehicle
BTMS	Battery Thermal Management System
Cd	Drag Coefficient
CMIP5	Coupled Model Intercomparison Project Phase 5
CMEM	Comprehensive Modal Emissions Model
CO_2	Carbon Dioxide
COPERT	Computer Programme to Calculate Emissions from Road Transport
DC	Driving Cycle
EC	European Commission
EEA	European Environment Agency
EU	European Union
EV	Electric Vehicle
FASTSim	Future Automotive Systems Technology Simulator
FCEV	Fuel Cell Electric Vehicle
GHG	Greenhouse Gas
GPS	Global Positioning System
HBEFA	Handbook of Emission Factors for Road Transport
HEV	Hybrid Electric Vehicle
HVAC	Heating, Ventilation, and Air Conditioning
H_2	Hydrogen
ICE	Internal Combustion Engine
ICEV	Internal Combustion Engine Vehicle
IEA	International Energy Agency
IPCC	Intergovernmental Panel on Climate Change
ISA	International Standard Atmosphere
IVE	International Vehicle Emissions model
km	Kilometer
kWh	Kilowatt-hour
kW	Kilowatt
LHV	Lower Heating Value
MPGe	Miles Per Gallon equivalent
MOVES	Motor Vehicle Emission Simulator
NAF	Norwegian Automobile Federation
NEXO	Hyundai Nexo Fuel Cell Vehicle
NREL	National Renewable Energy Laboratory
NRMSE	Normalized Root Mean Squared Error
NZE	Net Zero Emissions by 2050 Scenario
PHEM	Passenger car and Heavy duty Emission Model
PHEV	Plug-in Hybrid Electric Vehicle

Abbreviation	Definition
PEM	Proton Exchange Membrane
pkm	Passenger Kilometer
RCP	Representative Concentration Pathway
RMSE	Root Mean Squared Error
SDS	Sustainable Development Scenario
SOC	State of Charge
SUV	Sport Utility Vehicle
STEPS	Stated Policies Scenario
TWh	Terawatt-hour
TU	Technische Universiteit
UDDS	Urban Dynamometer Driving Schedule
UK	United Kingdom
US	United States
VCAM	Vehicle Consumption Assessment Model
VISSIM	Verkehr In Städten – SIMulationsmodell (Traffic in Cities Simulation Model)
VSP	Vehicle Specific Power
VT-CPFM	Virginia Tech Comprehensive Power-based Fuel Consumption Model
VT-CPEM	Virginia Tech Comprehensive Power-based Emissions Model
vkm	Vehicle Kilometer
WLTP	Worldwide Harmonised Light Vehicles Test Procedure

Symbols

Symbol	Definition	Unit
a	Vehicle acceleration	$\mathrm{m\,s^{-2}}$
A_f	Frontal area of the vehicle	$\mathrm{m^2}$
C_d	Aerodynamic drag coefficient	–
F_{max}	Maximum measured tractive force	N
$F_{\text{measured},i}$	Measured traction force at time step i	N
F_{min}	Minimum measured tractive force	N
$F_{\text{modeled},i}$	Modeled traction force at time step i	N
F_{trac}	Tractive force	N
g	Acceleration due to gravity	$9.81\,\mathrm{m\,s^{-2}}$
H_{real}	Measured hydrogen consumption	$\mathrm{kg/\,100km}$
H_{sim}	Simulated hydrogen consumption	$\mathrm{kg/\,100km}$
LHV	Lower heating value of hydrogen	$\mathrm{kW\,h\,kg^{-1}}$ or $\mathrm{MJ\,kg^{-1}}$
m	Vehicle mass	kg
N	Number of time steps or data points	–
$NRMSE$	Normalized Root Mean Squared Error	$\%$
P	Power	W or kW
P_{aux}	Auxiliary system power draw	W
P_{fc}	Fuel cell power output	kW
P_{idle}	Fuel cell idle consumption	kW
r	Wheel radius	m
$RMSE$	Root Mean Squared Error	N
SOC	State of charge of the battery	$\%$
T_{amb}	Ambient temperature	$^\circ\mathrm{C}$

Symbol	Definition	Unit
v	Vehicle speed	$\mathrm{m\,s^{-1}}$ or $\mathrm{km\,h^{-1}}$
VSP	Vehicle Specific Power	$\mathrm{kW\,t^{-1}}$
W	Energy or work	J or $\mathrm{kW\,h}$
Δt	Time step duration	s
Error	Relative deviation from measured value	$\%$
α	Road slope angle (grade)	rad or $\%$
δ	Road inclination angle	rad
η_{fc}	Fuel cell system efficiency	–
η_{overall}	Overall drivetrain efficiency	–
η_{trans}	Transmission efficiency	–
ρ	Air density	$\mathrm{kg\,m^{-3}}$

1

Introduction

This chapter provides the foundation of this thesis by first presenting the role of the transport sector in global and European greenhouse gas emissions. Following this, it examines the most important developments in electric mobility and the broader energy transition. It continues by examining the way in which the different powertrain technologies interact with climate conditions to influence vehicle energy use. The last section defines the core research questions, sets the boundaries of the research, and previews the organization of the remaining chapters. Together, these sections provide the context and rationale for the modeling and scenario analysis that follow.

1.1. Transport sector emissions and challenges

The transport sector plays a crucial role in global greenhouse gas emissions since it is responsible for approximately a quarter of energy-related CO_2 emissions, totaling around 8 Gt of CO_2 annually (OWD, 2021). The highest share of these emissions comes from road transport, which contributes about 74.5% of the transport sector. while the rest are divided into aviation, shipping, and rail, as depicted in Figure 1.1.

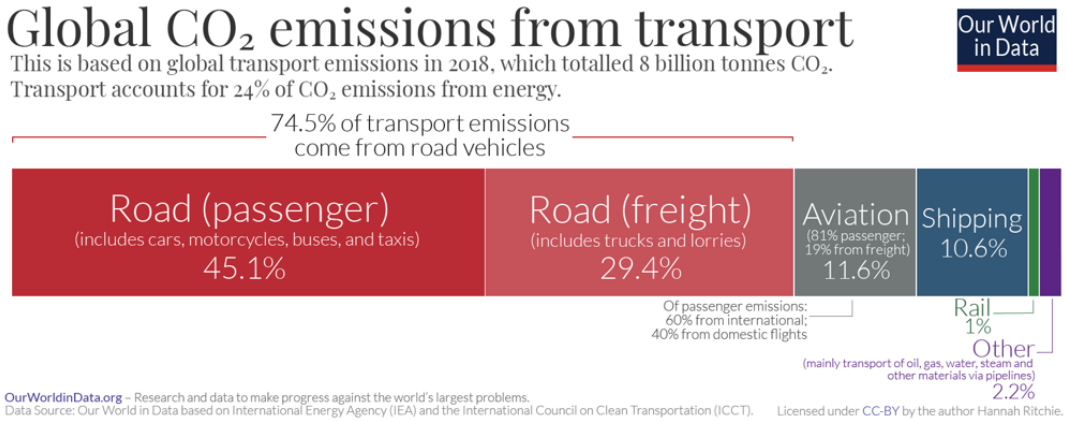

Figure 1.1: Global CO_2 emissions from transport (OWD, 2021)

Passenger vehicles, such as cars, motorcycles, and buses, constitute the majority, as they are responsible for around 45% of the transport sector's CO_2 emissions and 10% of the global CO_2 emissions (IEA, 2024). This positions the passenger transport sector as a top priority target for climate change mitigation efforts.

In Europe, the situation is similarly critical. Transportation is responsible for 25% of the EU's total greenhouse gas emissions, making the sector the second largest one in terms of emissions, with passenger transport, and especially cars, being responsible for around 15% of the EU's CO_2 emissions

(Agency, 2023; Eurostat, 2025). Surprisingly, transport sector emissions in the EU have not decreased since 1990, in contrast with other sectors, a fact that makes it one of the most difficult sectors towards decarbonization (Eurostat, 2025).

One of the main obstacles to overcome is the high dependence of the transport sector on fossil fuels. The vast majority of the passenger cars moving continue to use internal combustion engines (ICEs), which consume petrol or diesel. Petroleum-based fuels constitute more than 95% of the energy consumption in the transport sector, making it a crucial pollutant source (IEA, 2024). This long-term dependence on ICE vehicles resulted in continuously increasing petroleum consumption and relevant CO_2 emissions (IEA, 2024). In addition, the total CO_2 output of the passenger vehicles is significantly impactful because of the increased number of vehicles and the kilometers driven. Around the world, the passenger car fleet exceeds one billion vehicles, and demand for mobility keeps rising. These pipe emissions not only degrade air quality, but also contribute to the accumulation of CO_2 in the atmosphere, undermining all efforts to limit the global warming effect.

Technological shifts in the automotive sector are now underway to address these challenges. There is a clear trend in low or zero-emission technologies as alternatives to conventional ICEs. Battery electric vehicles (BEVs) are rapidly increasing because of the technology improvements and increased political support. The global sales of BEVs have increased from around 4% in 2020 to around 18% in 2023 (IEA, 2023). Europe is a pioneer in this transition: electric vehicles (including plug-in hybrid vehicles) constituted around 18% of the new entries in EU in 2021 and continued to increase over 20% until 2023 (Eurostat, 2025). Concurrently, fuel-cell electric vehicles (FCEVs), which directly produce electric energy by using hydrogen, are evolving with their use; however, they remain limited because of the increased cost and the lack of refueling infrastructure. At the same moment, conventional vehicles are becoming more and more efficient by using hybrid systems and enhancing the combustion process, decreasing the consumption and the CO_2 emissions. Still, to align with climate objectives, studies indicate that the electrification of road transport must accelerate further and reach near-total adoption of zero-emission vehicles in the coming decades (IEA, 2023). However, the increase in larger and heavier vehicles (e.g., SUVs) has partially offset efficiency gains, showing that both technology and consumer choices will determine how quickly emissions can decline. Overall, the powertrain landscape is rapidly evolving, with BEVs leading the decarbonization charge, supported by hybrids in the interim, and FCEVs being explored for the longer term – all in response to the pressing need to mitigate transport's environmental impact.

These technology trends are strongly driven by environmental and regulatory pressures, especially in Europe. The EU has posed ambitious targets in the context of the European Green Deal and the "Fit for 55" package, which compels significant CO_2 emissions reduction in the transport sector. The Green Deal aims to achieve climate neutrality by 2050, including decreasing transport emissions by 90% in relation to 1990 (Commission, 2023b). To reach this long-term vision, the EU introduced the Fit for 55 package, which tightens interim targets: the EU aims to reduce overall GHG emissions by at least 55% by 2030 (from 1990 levels)(Commission, 2023b). For road transport, this means strict CO_2 emission limits for the new vehicles. In 2023, the EU officially adopted a regulation requiring that by 2035, all new cars and vans sold must be zero-emission, effectively phasing out the sale of new gasoline and diesel cars. Before that, until 2030, manufacturers have to decrease the average CO_2 emissions of new cars by 55% in relation to 2021 levels (Commission, 2023b). These regulations aim to facilitate and accelerate electric transport and enhance innovation in clean mobility.

Many European countries set their own national goals beyond the mutual plan. Norway, for example, aims to have 100% zero-emission new passenger cars by the end of 2025, way earlier than the rest of the European Union (on Clean Transportation, 2023). The Netherlands, Ireland, and Sweden aim to phase out new ICE vehicles by 2030, while countries such as the United Kingdom and Denmark by 2035 (on Clean Transportation, 2023). These regulatory interventions, coupled with incentives such as subsidies and tax breaks, and infrastructure investment (e.g., expanding charging networks), are rapidly reshaping the passenger car market. They create a market pull for BEVs and other zero-emission vehicles driven by policies while making the high-emitting vehicles less attractive or even non-compliant with the regulations.

In summary, the transport sector, and especially passenger cars, faces a significant challenge to comply with the global and European climate goals. The increased percentage of CO_2 emissions makes

the decarbonization of this sector crucial. The powerful regulatory frameworks, such as the European Green Deal and Fit for 55, set clear end-dates for conventional vehicles, and technological adoption trends indicate an ongoing shift toward electrification. This context of a mandated energy transition in mobility sets the stage for the detailed analyses to follow. In the following sections of this introduction, the path to the transition to more sustainable powertrains will be explained, as well as the way to quantitatively assess it through energy modeling and scenario analysis. Understanding the current emissions landscape and the forces driving change is a necessary first step before delving into the modeling of future transport energy systems and evaluating pathways to achieve climate-neutral mobility.

1.2. Background on the energy transition and mobility trends

A milestone in the energy transition of the transport sector in Europe is the rapid growth of electric mobility. In recent years, the adoption of electric vehicles (EVs) - and especially battery electric vehicles and Plug-in Hybrid Electric Vehicles (PHEVs) - has steadily increased. According to recent data, in 2023 EVs constituted around 22.7% if the total new entries of passenger cars in the EU, whereas a decade ago this number was at zero levels. This means that 2.4 million new electric cars were sold in 2023, an increased number from the 2.0 million in 2022 (Agency, 2024).

The majority of these vehicles were BEVs, with a share of around 15%, whereas PHEVs covered around 8% of the new sales (Agency, 2024). Battery electric vehicle sales overcame those of PHEVs, with an increase of 37% in 2023, while plug-in hybrid sales plateaued or even declined slightly (Agency, 2024; Commission, 2023a). This trend reflects the advancements in battery technologies and the stricter regulations that aid electric vehicles' growth. Because of the increased adoption of EVs, the average CO_2 emissions of new cars in Europe have decreased by around 27% between 2019 and 2022 (Commission, 2023a).

Europe is a global leader in the EV market in the new cars market share, second only to China in absolute numbers. In Norway, electric vehicles constituted around 88-91% of new sales in 2023 (Agency, 2024). In Sweden, the relevant percentage was 61%, while in Germany, which is the biggest car market in Europe, it reached 31% (Agency, 2024).

This dynamic is not limited to passenger cars. Light-duty vehicles, such as vans, are starting to be electrified: around 7.7% of new van entries in the EU in 2023 were electric (Agency, 2024). Accordingly, many cities invest in electric buses, whereas manufacturers have introduced new electric trucks for short-distance transportation.

While electric mobility with the use of batteries represents the main pole in decarbonization, there are other technologies, such as fuel-cell electric vehicles, that use hydrogen to produce electricity in the vehicle. FCEVs offer increased autonomy and faster refueling, a fact that makes them perfect for heavy-duty vehicles or long distances. However, they remain in the early development stage in Europe: only a thousand new entries annually and less than six thousand by the end of 2023 (Europe, 2023). The main obstacles are the cost, the lack of refueling stations, and the low efficiency in comparison with BEVs.

The growth of EVs also requires the growth of the relevant charging infrastructure. By 2023, Europe had around 632,000 public charging points built ((ACEA), 2024). However, the infrastructure increased only six times between 2017 and 2023, while electric vehicle sales increased by 18 times ((ACEA), 2024). In addition, 60% of the charging points are in three main countries (the Netherlands, France, and Germany), and other regions have sparse coverage ((ACEA), 2024).

To address these gaps, the EU has introduced the Alternative Fuels Infrastructure Regulation (AFIR) as part of the Fit for 55 package, setting binding targets for charger availability. For example, AFIR requires that by 2025, fast-charging stations ($\geq 150kW$) be installed every 60 km along core TEN-T transport corridors. The European Commission estimates that roughly 3.5 million public charging points will be needed by 2030 to support the envisioned EV growth and meet the 55% emissions-cut target for cars (Commission, 2023a). The European Commission suggests that around 3.5 million public charging points will be required by 2030, while others increase this number to around 6-8 million, taking into account more promising EV adoption scenarios ((ACEA), 2024).

Finally, electric vehicles' effectiveness relies on a cleaner energy supply and broader shifts in transport

habits. As the renewable energy sources' share is increasing in Europe, electric vehicles become "cleaner" per kilometer driven (Agency, 2025). In parallel, other sustainable alternatives such as vehicle sharing, multi-modal transport integration, and active travel (cycling, walking) are being promoted to reduce vehicle demand and energy use.

1.3. Relevance of powertrain technologies and weather impacts

The decarbonization of passenger transport leads the way to transition from conventional internal combustion engine vehicles to alternative powertrain technologies, such as battery electric vehicles, plug-in hybrids, and fuel-cell electric vehicles. Each of these powertrains operates with different energy sources and efficiencies, and importantly, each is affected differently by external conditions like ambient temperature and seasonal weather. Understanding the way weather influences energy consumption and vehicle autonomy is crucial not only for evaluating their real-world performance but also for planning sustainable energy systems, especially in Europe, where there are various climate conditions, such as the cold winters in the North and the mild Mediterranean conditions, influence how each powertrain performs throughout the year.

Regarding battery electric vehicles, they are highly sensitive to ambient temperature fluctuations and present a significant range in autonomy and efficiency between summer and winter (U.S. Department of Energy, 2024). In lower temperatures, the electrochemical reactions of the battery slow decelerating, whereas systems such as cabin heating and battery consume even more energy. For example, in -7°C, a typical BEV can present a decrease in autonomy by 39-41% in comparison with a temperature of 25 $^{\circ}$C (U.S. Department of Energy, 2024). Under certain circumstances, even two-thirds of the additional consumption in winter is solely due to cabin heating (U.S. Department of Energy, 2024).

Even in milder conditions, the effect is visible: a study in the United Kingdom showed the EVs' autonomy in urban driving routes in temperatures of range 0-15 $^{\circ}$C was around 28% lower than in temperatures of range 15-25°C (Y. Al-Wreikat et al., 2022). In summer, the losses are lower - around 10-15% because of the use of air conditioning and battery cooling (Henning et al., 2019). This fluctuation varies significantly according to the EV model: newer BEVs, which use heat pumps, can retain up to 95% of the rated autonomy, whereas older models without such systems can decrease even down to 63%, with an average of 80% in cold conditions (Norwegian Automobile Federation, n.d.). This seasonality is crucial for Europe: a BEV that easily achieves its advertised range in a Southern European summer might struggle to do so during a Scandinavian winter, necessitating more frequent charging and careful route planning for drivers.

As far as plug-in hybrid vehicles are concerned, they combine electric and thermal motion, and so they are doubly affected by weather conditions. When these vehicles use electricity to move, they present the relevant losses of the BEVs in lower temperatures. In addition, in cold conditions, the thermal system kicks in more often either to supplement power or provide the heating demand, thus reducing the electric autonomy. On the other hand, when the combustion engine is running, a PHEV's behavior resembles that of a hybrid ICE vehicle. In low temperatures, the engine must overcome increased friction and suboptimal thermal efficiency, and it may idle to provide cabin heat – factors which lead to higher fuel consumption per kilometer (U.S. Department of Energy, 2024). Studies show that hybrid vehicles can present a decrease in fuel consumption by 30-34% during winter, more than conventional ICEs (U.S. Department of Energy, 2024). In warm conditions, their efficiency is less influenced, as the air conditioning can be supported by the engine and the battery (Henning et al., 2019). Overall, PHEVs provide flexibility under varying weather conditions. Instead, the impact of weather on PHEVs shifts the balance between electric and engine use, affecting fuel consumption and electric demand in ways that must be accounted for in energy models.

Regarding fuel-cell electric vehicles, which use hydrogen fuel cells to generate electricity in the vehicle, they exhibit a different set of weather sensitivities. They use the waste heat of the fuel cell for cabin heating, thus reducing the need for additional energy, and because of this, they can offer increased autonomy in cold conditions in comparison with the BEVs (Henning et al., 2019). However, in this study, both FCEVs and BEVs were modeled using the same HVAC energy demand profiles in VCAM. This simplification was chosen due to the lack of robust data for HVAC modeling in FCEVs. For instance, in temperature ranges from 15 to -5 $^{\circ}$C, the autonomy of a BEV had decreased by 37.8%, whereas

in a FCEV this decrease was only 23.1% (Henning et al., 2019). However, in extremely cold weather conditions, hydrogen consumption increases a lot to provide heating and prepare the systems. In a tryout in Canada, hydrogen consumption increased by 40% in below-zero temperatures (Martin, 2024). During summer, the need to cool down the fuel cell and the cabin adds a little bit to the consumption, but the effect is deemed limited. In addition, FCEVs are not affected by temperature in refueling time, thus offering functionality advantages in extreme weather conditions. However, the total hydrogen consumption per kilometer is significantly increased in both hot and cold weather extremes.

Conventional petrol or diesel vehicles remain the baseline for weather performance comparisons. ICEVs present lower affection in consumption due to weather conditions. In low temperatures, engine oil and drivetrain fluids become viscous, and it takes longer for the engine to reach optimal operating temperature, leading to higher fuel burn in winter, especially during short trips (U.S. Department of Energy, 2024). However, unlike BEVs, ICEVs can utilize waste heat from engine operation to meet cabin heating demands, making winter HVAC loads effectively ”free” in energy terms and reducing the relative impact on fuel economy. Despite this, the average efficiency decrease is around 10-20%, and this number can rarely reach 24-33% (U.S. Department of Energy, 2024). In warm weather conditions, air conditioning increases the load on the engine. Studies show around a 14% drop in range or fuel economy at 35 $^{\circ}\mathrm{C}$ (Henning et al., 2019). Consequently, even while ICEVs' drivers are not directly affected, seasonal fluctuations in consumption are crucial for computing the fleet's fuel needs and emissions.

The varying climate zones in Europe make the relationship between technology and weather critical. Northern European countries like Norway, Sweden, and Finland face long, harsh winters with mean temperatures well below freezing. BEVs there can lose up to 30% of their autonomy even in milder winter conditions (Norwegian Automobile Federation, n.d.). This requires a more dense charging infrastructure and careful energy planning, especially as Northern European countries lead in EV adoption rates. By contrast, Southern European countries such as Greece, Italy, and Spain have milder winters, where BEV performance remains close to optimal for most of the year, but they experience very hot summers. High temperatures can affect battery performance and increase the use of air conditioning. While according to Henning et al. (2019) and Norwegian Automobile Federation (n.d.) the summer range loss for EVs is generally smaller than winter losses, heatwaves in southern Europe could induce additional stress on both electric and combustion vehicles.

Finally, factors such as precipitation, snow, and road conditions affect the consumption of all types of vehicles through increased rolling resistance and aerodynamic drag. The effect of weather on consumption has significant consequences for energy and transport policy, as it affects both the everyday driving experience and the seasonal energy demand planning. For instance, BEV fleets in Scandinavia require significantly more electricity in January than in July, whereas FCEVs and PHEVs have increased seasonal fuel demands. These phenomena are crucial in modeling energy consumption in the transport sector and in strategic planning and evolving the required technologies per geographic region (Henning et al., 2019; Martin, 2024).

1.4. Problem statement, scope, and thesis outline

As the transport sector becomes an increasingly central component of the global energy transition, accurately modeling the energy consumption of emerging vehicle technologies has become essential not only for estimating demand but also for understanding their role in energy system flexibility. In decarbonized systems, which are heavily relying on variable renewable energy sources like wind and solar, periods of low generation, such as the Dunkelflaute in winter, when both solar irradiance and wind availability are low, can strain the balance between supply and demand. In countries such as Switzerland, these events often lead to increased electricity imports and system dependency. In such contexts, passenger electric vehicles represent both a significant load and a potential flexibility asset through demand-side management (DSM), such as smart charging. However, the extent in which the EVs can support or stress the grid heavily depends on accurate estimations of their consumption in different regions, climates, and driving conditions. The misrepresentation of this load, especially during extreme weather conditions or congestion scenarios, has the risk of underestimating grid vulnerabilities and flexibility needs.

The core problem addressed in this thesis is the lack of comprehensive modeling tools that can represent the energy consumption of different passenger vehicle powertrains, including battery electric vehicles (BEVs), plug-in hybrid electric vehicles (PHEVs), internal combustion engine vehicles (ICEVs), and FCEVs, under realistic conditions of European driving, climate, and fleet composition. While BEVs are expected to be the dominant technology in the future market, FCEVs are included due to their potential to offer system-level benefits in niche but critical use cases. For instance, FCEVs can decouple electricity consumption spatially and temporally, by allowing hydrogen production in regions with low grid congestion, which relocates the energy demand geographically. Moreover, in regions that have highly limited transmission infrastructure, hydrogen mobility could provide an alternative pathway towards decarbonization, which eases grid stress. Existing models often oversimplify or omit these interdependencies, which leads to limited insight into energy demand patterns and weakens the integration between transport modeling and broader energy system analysis.

This research is driven by the overarching question: ***To what extent is the energy demand from passenger mobility influenced by variations in powertrain technologies, vehicle types, and weather conditions?*** In order to address this question, the thesis investigates three supporting sub-questions:

1. **What are the quantified differences in consumption and range between various powertrain technologies across vehicle segments?**
2. **To what degree does weather variability impact the energy consumption of passenger vehicles with different powertrains?**
3. **To what extent does the energy demand for passenger mobility differ across European regions, and what role do vehicle fleet compositions and climate zones play?**

To address these questions, the thesis focuses on extending and applying the Vehicle Consumption Assessment Model (VCAM). The work involves modeling and comparing the energy consumption of BEVs, FCEVs, and ICEVs, while explicitly incorporating temperature variability to reflect weather conditions across Europe. The analysis is geographically focused on European countries and uses regional data on fleet composition and ambient conditions, whereas standardized driving cycles are used. The outputs are designed to support integration into broader energy system models, enabling cross-sectoral assessments of future transport energy demand. While the study emphasizes physical and environmental determinants of consumption, it does not explicitly model behavioral factors such as driver habits, traffic congestion, or long-term technological evolution beyond the defined fleet scenarios.

The thesis is structured into six chapters. Chapter 1 introduces the motivation, background, and structure of the research. Chapter 2 presents a literature review of existing vehicle consumption models, identifying gaps related to hydrogen powertrains and environmental effects. Chapter 3 describes the methodology, including the extension of VCAM to cover additional technologies and the integration of regional data. In this Chapter, Section 3.3 presents the model quality assessment that has been made in order to validate the model against real-world data. Chapter 4 presents the simulation results, comparing powertrains under different temperatures, regions, and use cases. Chapter 5 discusses the findings in light of decarbonization goals and energy system planning and reflects on the limitations of

the study, while offering key insights and recommendations for future research. Chapter 6 concludes the thesis by answering the research questions posed.

2

Literature Review

This chapter presents a complete examination of the current vehicle fuel consumption approaches and tools. Firstly, it categorizes the models into macroscopic, mesoscopic, and microscopic frameworks, examining their theoretical foundations, their typical applications, and the relevant advantages and limitations. The following section offers a comparative analysis of the most used simulation platforms as far as the computational efficiency, the powertrain coverage, the incorporation of environmental conditions, the accessibility and customizability, and the overall level of detail are concerned. Using this comparative analysis as a baseline, the review identifies research gaps, which mostly have to do with the poor representation of the fuel cell electric vehicles, the limited treatment of weather fluctuations, and the European regional demand. It concludes by positioning the Vehicle Consumption Assessment Model as a promising foundation in order to deal with these gaps in the present thesis.

2.1. Overview of vehicle consumption models

Studying energy consumption in road vehicles has emerged into three crucial modeling frameworks: macroscopic, mesoscopic, and microscopic (Chen et al., 2024). Each of these approaches offers a different level of detail and range, and their understanding is crucial in order to select the most appropriate tool to evaluate energy demand under various conditions. Figure 2.1 illustrates this categorization, while Table 2.1 includes a comparison of the frameworks. This section examines these categories, focusing on European studies, highlighting their historical development, their advantages and their limitations, as well as the way they handle different vehicle types, driving patterns, and environments in estimating energy use.

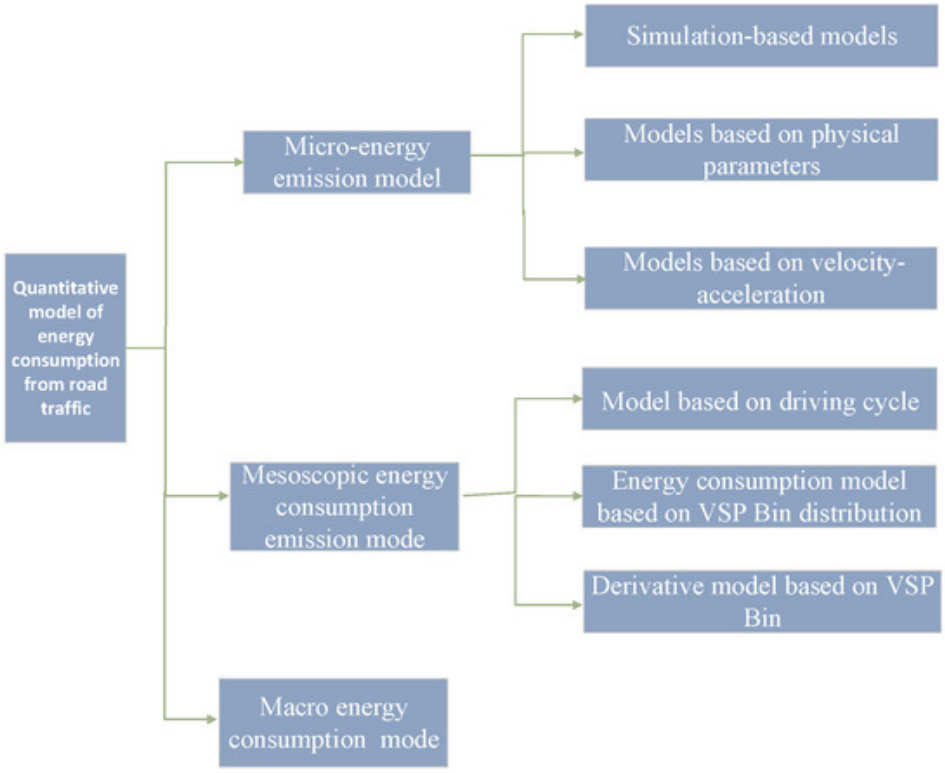

Figure 2.1: Modeling frameworks (Chen et al., 2024).

2.1.1. Macroscopic energy consumption models

Macroscopic models operate at the highest level of aggregation, treating an entire road network or region as the unit of analysis over extended periods (typically months or years) (Chen et al., 2024). In these models, vehicle energy consumption is calculated using complete statistical data, such as the total kilometers driven, the fleet composition, and the average fuel economy for each vehicle type (Chen et al., 2024). For instance, a typical formulation will sum energy use across vehicle categories k and fuel types i by multiplying the number of vehicles, their average annual distance, and an average energy intensity (fuel per distance) for each category.

Classic macroscopic models include national inventory tools, such as COPERT (Computer Program to Calculate Emissions from Road Transport) in Europe, which offers standardized fuel consumption and emission factors for different vehicle types (passenger cars, vans, trucks, etc.) based on European data inputs such as total mileage, fleet composition, average speed, and environmental parameters like external temperature and humidity (Chen et al., 2024). These models have been extensively used in policy analysis and emissions inventories to track trends and assess mitigation strategies (Ntziachristos et al., 2009).

Macroscopic models offer various advantages and thus are widely used. Their main one is their simplicity and applicability in large-scale scenarios. They require relatively coarse input data (often obtainable from travel surveys or registration statistics) and are computationally light, making them suitable for national energy demand projections or long-term scenario modeling. Due to their extended scope, they are useful in order to analyze trends. For example, they can be used to evaluate how total passenger transport energy consumption changes with fleet electrification or fuel economy improvements on a country basis (Chen et al., 2024).

On the other hand, these models present some limitations. The high degree of spatial and temporal aggregation means macroscopic approaches cannot capture fine-grained variations in driving behavior or road conditions. Geographical or operational details, such as the differences between urban traffic and highway driving, are averaged out in these models. As a result, macroscopic tools are inadequate for real-time or localized analysis. Another disadvantage is the accuracy loss that can happen due to

their reliance on default or test-cycle-based factors, as consumption factors often come from laboratory driving cycles and do not fully represent real driving conditions. This can lead to systematic errors – for example, older European inventory methods using steady-state cycles underestimated the impact of aggressive acceleration or congestion (Chen et al., 2024).

2.1.2. Mesoscopic energy consumption models

Mesoscopic models represent an intermediate scale between macro and micro, capturing vehicle energy consumption at the level of specific road types, traffic situations, or time periods (e.g., corridor-level or city-scale over minutes to hours). Instead of simulating each vehicle independently, mesoscopic approaches use aggregated descriptions of vehicle standards in a given road part or network slice, such as the average speed, frequency of stops/starts, or statistical distributions of acceleration in order to estimate energy use (Chen et al., 2024). They try to integrate some dynamics of traffic conditions without the full complexity that microscopic models have.

Early mesoscopic methods were based on standardized driving cycles for characterizing typical driving conditions. For example, the European model Artemis used libraries of driving cycles to represent urban, rural, and highway driving, assigning fuel consumption or emission factors based on the cycle that best fit the average speed and driving aggression of the scenario (Mądziel, 2023). More specifically, Artemis, which was developed in the 2000s, is notable for selecting representative driving cycles by clustering real-world driving patterns and then computing emissions and consumption factors for each cluster, applying additional correction factors to improve accuracy (Chen et al., 2024).

This approach enhanced the simplified average speed models by understanding, for instance, that driving in an urban environment with starts and stops at 50 km/h presents a different energy behavior than driving in steady state speed. However, even purely cycle-based mesoscopic models still struggle with highly localized effects, such as the extra fuel used near traffic lights or bus stops, since a single cycle averages over many driving events (Chen et al., 2024).

A major advance in mesoscopic modeling was the introduction of Vehicle Specific Power (VSP) as a unifying parameter in the late 1990s. VSP, developed by Jimenez-Palacios (1999) at MIT, measures the instantaneous power demand per unit vehicle mass in kW per tonne required to move the vehicle, considering speed, acceleration, road grade, and aerodynamic drag (Chen et al., 2024). Researchers found out that the distribution of VSP over time is a strong indicator of fuel consumption, better than using mean speed or acceleration statistics, because it is related to the engine load. VSP-based models work by dividing vehicle operating modes into VSP bins, such as idle, low power cruise, high power demand, and assigning each bin an energy consumption rate. The American model MOVES (Motor Vehicle Emission Simulator) is an example of this approach, since it specifies the working modes of the vehicles related to VSP regions and estimates the fuel consumption in accordance with the time spent in each operating mode (Chen et al., 2024). By taking advantage of big databases with driving data, second by second, MOVES achieves higher accuracy than older mean speed methods, as it captures the effect of aggressive driving or road grade via VSP without micro-simulation (Chen et al., 2024). The trade-off is the increased needs for data and calibration, since MOVES is strongly based on extensive local data, a fact which makes its use outside the U.S. a challenge (Chen et al., 2024). A similar international model, IVE (International Vehicle Emissions), has been developed in order to extend VSP-bin modeling on a global scale, but it requires detailed inputs and has suffered from data aging in regions where the data are not well updated (Chen et al., 2024).

In Europe, mesoscopic modeling has also advanced through projects and tools that incorporate detailed vehicle simulations in broader traffic contexts. The Handbook of Emission Factors for Road Transport (HBEFA) is one such tool, which is widely used in European countries. HBEFA provides fuel consumption and emissions factors for a broad range of traffic conditions based on a mesoscopic philosophy: use data produced by micro-simulations and calculate average fuel consumption rates for every driving pattern (Mądziel, 2023). In practice, HBEFA and similar models, such as earlier versions of COPERT and Artemis, offer analysts the possibility to estimate energy use and emissions by applying the calibrated factors, thus bridging the gap between aggregate national models and highly detailed simulations. These approaches are invaluable in Europe for ”eco-driving” studies, where different routes or traffic management strategies on energy demand are evaluated (Mądziel, 2023).

Mesoscopic models have many strengths, but the one that stands out is the balance they succeed between realism and complexity. They integrate more driving details than macroscopic models, capturing the way speed variability, road grade, and starts-and-stops affect consumption, but they still remain way more computationally efficient than simulating every vehicle movement. This makes them well-suited for policy analysis and network planning. Many mesoscopic methods are also based on empirical data, a fact that adds to increased accuracy (Chen et al., 2024; Ye et al., 2019).

Despite the advantages, mesoscopic models also have limitations. They are still relying on aggregate representations of driving. They usually assume that an average driving pattern or a mean distribution can represent all types of vehicles in a given road segment, which omits the extreme behaviors or the interactions between vehicles. They cannot capture the real-time coupling between vehicles because they typically leave out the vehicle-to-vehicle interactions, in contrast with the complete microscopic simulations. In addition, their accuracy is strongly connected to the quality of calibration data (Chen et al., 2024).

2.1.3. Microscopic energy consumption models

Microscopic energy models simulate vehicle energy use at the finest level of detail, as the individual vehicles are modeled on a second-by-second basis, while they move along a driving cycle or a traffic simulation. These models usually use physical equations of motion and powertrain response to estimate the instantaneous fuel or energy consumption, or they use empirical relations calibrated for specific vehicles. The development of microscopic models for vehicle consumption started earlier than mesoscopic and macroscopic approaches, because understanding vehicle dynamics represents the basis for all the higher-level models(Chen et al., 2024). Innovative works at the start of the 1980s introduced fuel consumption modeling based on power. Post et al. (1984) formulated fuel consumption as a function of the engine power demand, taking into account the losses and the efficiency, while Akçelik and Biggs (1989) refined this by integrating vehicle parameters such as drag force and rolling resistance. By the early 1990s, researchers An and Ross (1993) had further improved these formulations and complete texts, such as Wong (2001), had consolidated the physics of vehicle energy use into computational models. These efforts concluded in more flexible frameworks such as the Virginia Tech Comprehensive Power-Based Fuel Consumption Model (VT-CPFM), which was developed by Rakha et al. (2011). VT-CPFM offered a generic parametrized equation to estimate fuel rate based on the instantaneous speed and acceleration of the vehicle, as well as vehicle-specific constants such as vehicle mass and engine size (Rakha et al., 2011). This marked a significant milestone, since the need to perform extensive real-world calibration for every new vehicle was overcome, thus making microscopic models based on physics more practical and extendable in different passenger car models.

In parallel, purely empirical microscopic models have been developed, using statistical fits to driving data and not detailed mechanics. A significant example is the VT-micro model by Ahn et al. (2004), which expresses the instantaneous fuel consumption as a polynomial equation of speed and acceleration. These models are typically derived from a large set of test data to find the best formula. They have the advantage of simplicity and easy integration, since they require only kinematic variables as inputs, and can be easily plugged into traffic simulations or fed with recorded drive cycle data to estimate fuel consumption (Chen et al., 2024).

Another branch of microscopic modeling includes software that fully simulates vehicles. Tools like the PTV, VISSIM, SUMO, AIMSUN, and others focus on creating realistic vehicle trajectories, taking into account car following and lane changing, while complementary models like CMEM (Comprehensive Modal Emissions Model) or the aforementioned VT-CPFM compute instantaneous fuel use for these trajectories (Chen et al., 2024). CMEM, developed in UC Riverside, is a typical micromodel example based on simulation, as it uses vehicle parameters and instantaneous driving inputs such as speed, acceleration, and road grade, to compute the engine load and then the fuel rate (Scora & Barth, 2006). This model and its successors have been widely applied in research in order to evaluate the way vehicles consume fuel in different driving patterns and routes (Chen et al., 2024; Kan et al., 2018). European researchers also significantly contributed to this sector. For example, PHEM (Passenger car and Heavy Duty Engine Model), developed by TU Graz, is a microscopic energy/emission simulation, which uses engine maps for different vehicle segments to predict the fuel consumption under any driving pattern. PHEM's results have significantly contributed to creating HBEFA factors, showing that

microscopic tools underpin mesoscopic ones (Chen et al., 2024). Nowadays, microscopic simulations are frequently used to create virtual test drives for new powertrain technologies. Users can model hybrid-electric or battery-electric vehicles through a standardized driving cycle to evaluate energy consumption and range under certain conditions. This practice is at the core of evaluating the impacts of powertrain technologies on energy demand, and is one of the reasons why the Vehicle Consumption Assessment Model (VCAM) in this thesis is built to do.

Microscopic models offer the highest analysis and physical realism. They can conceive the effects of the differences in the vehicles and operating conditions that other models have to simplify. For example, a microscopic model can directly simulate the way a heavier vehicle consumes more energy when going up a hill or the way the use of an HVAC system on a warm day increases fuel consumption. Experiments have quantified effects under extreme weather conditions, when vehicles can consume significantly more energy than under milder conditions (Giechaskiel et al., 2021). These can be incorporated into a microscopic simulation, allowing weather impacts on energy consumption to be evaluated. Microscopic approaches are also required to assess new powertrain technologies and control strategies, such as when hydrogen fuel cell vehicles or advanced driver-assistance features are introduced. All these make microscopic models crucial for research and innovation.

On the other hand, there is complexity. Microscopic models require a handful of input data and detailed calibration against experimental data. Composing a trustworthy micromodel can be work-intensive, and simulating a large number of vehicles through second-to-second simulations is computationally demanding. This makes microscopic modeling less practical in modeling country fleets or future scenarios, where the uncertainty is high and many parameters have to be evaluated. In addition, while microscopic models can include almost any effect, such as grade, weather, and traffic, they are only as accurate as the assumptions that are being made and the data provided. A detailed model can misestimate fuel consumption if the engine map or the rolling resistance is not representative of the real world. Furthermore, many times the models are developed and validated for one specific vehicle, and then this model is used for all vehicles of this type, which can cause errors in the results. However, despite these challenges, the trend in Europe and globally is to continuously improve microscopic tools and integrate them into wider modeling frameworks, since computing power grows and more empirical data become available (He et al., 2023).

Table 2.1: Comparison of Macroscopic, Mesoscopic, and Microscopic Vehicle Energy Consumption Models

Criterion	**Macroscopic**	**Mesoscopic**	**Microscopic**
Temporal Resolution	Year, Month	Hours or Days	Hours or Seconds
Spatial Resolution	National / Regional level	Urban network / Road segments	Individual vehicles and routes
Inputs	Average speeds, number of vehicles	VSP, road type, typical conditions	Speed, acceleration, load, temperature
Vehicle Types	Fleet categories	Typical driving profiles per class	Individual technical specifications
Computational Demand	Low	Moderate	High
Suitability for New Technologies	Limited	Moderate	High
Examples	COPERT, HBEFA	MOVES, ARTEMIS, HBEFA	CMEM, VT-CPFM, PHEM

2.2. Comparative evaluation of key tools

The field of vehicle energy consumption modeling has seen the development of several frameworks, each excelling in particular areas while facing specific limitations. Instead of merely listing these tools, this section highlights key aspects of modeling frameworks—computational efficiency, powertrain diversity, environmental integration, and accessibility—and evaluates how various tools address these challenges.

Computational efficiency

Efficient simulations are essential for large-scale fleet analyses and time-sensitive studies. FASTSim, developed by NREL, achieves computational efficiency by simplifying vehicle dynamics while maintaining accurate results with errors under 10% (Holden et al., 2015). This balance makes it highly suitable for analyzing large fleets. In contrast, ADVISOR, another tool from NREL, provides detailed and accurate results using backward-forward simulation techniques but requires significant computational resources due to its dependence on engine maps and extensive parametrization (Masclans Abelló, 2021). Similarly, VT-CPFM and VT-CPEM adopt power-based methodologies, offering high accuracy for steady-state conditions but struggling with transient or large-scale dynamic simulations (Fiori et al., 2016).

Powertrain diversity

Modeling frameworks must account for diverse powertrain technologies, including ICEVs, BEVs, PHEVs, and FCEVs. FASTSim supports ICEVs, BEVs, and PHEVs effectively, allowing for a broad range of powertrain analyses, although it does not fully address hydrogen fuel cell vehicles (FCEVs) (Bi et al., 2021; Grubwinkler et al., 2016). ADVISOR, while historically significant for hybrid and electric vehicle modeling, faces challenges adapting to emerging technologies. VT-CPFM and VT-CPEM are tailored to ICEVs and BEVs, respectively, but lack features to evaluate hybrid or hydrogen technologies comprehensively (Park et al., 2013).

Integration of environmental factors

Environmental conditions, particularly temperature variability, significantly affect vehicle energy consumption, especially for electrified powertrains with sensitive battery thermal dynamics. Many frameworks, including FASTSim, offer limited capabilities for modeling these external factors (Bi et al., 2021). For instance, while FASTSim allows for user-defined speed profiles and vehicle parameters, it struggles to model temperature impacts or road-grade variability comprehensively (Grubwinkler et al., 2016). VT-CPEM focuses primarily on steady-state conditions and overlooks transient environmental effects (Fiori et al., 2016). Innovative approaches, such as Grubwinkler et al. (2016) real-time data-driven model, incorporate environmental factors effectively, achieving estimation errors as low as 7%. However, these approaches rely heavily on large datasets, limiting their adaptability.

Accessibility and customizability

Open-source and customizable frameworks are vital for researchers and policymakers. FASTSim and ADVISOR are freely available, making them accessible for a wide range of studies (Holden et al., 2015; Markel et al., 2002). FASTSim's simplicity and support for user-defined inputs further enhance its versatility, enabling a wide range of scenarios to be modeled. Customizability remains a key strength of FASTSim, while other tools often rely on predefined datasets or require complex reconfiguration to adapt to new scenarios.

Level of detail

Balancing model simplicity and accuracy remains a persistent challenge. FASTSim strikes a practical balance, providing sufficient detail for energy consumption studies without overwhelming computational resources (Holden et al., 2015). ADVISOR and CMEM, on the other hand, are highly detailed, enabling accurate simulations of specific vehicle dynamics, but their complexity and extensive input requirements hinder broader or real-time studies (Boriboomsin et al., 2012; Masclans Abelló, 2021). VT-CPFM and VT-CPEM excel in power-based modeling but are less capable of representing diverse driving behaviors or integrating weather variability (Fiori et al., 2016).

Limitations and research gaps

Despite the advances in vehicle energy modeling, important gaps exist in integrating external factors and powertrain diversity. Most models find it difficult to consider weather variability, which has a remarkable effect on EV efficiency, mainly because of the sensitivity of the battery to temperature fluctuations and the increased HVAC loads in extreme conditions (Ahn et al., 2002; Fiori et al., 2016). Furthermore, hydrogen fuel cell vehicles (FCEVs) and hybrid technologies, critical to achieving decarbonization in specific sectors, remain poorly represented in most tools (Masclans Abelló, 2021). Moreover, modeling regional demand, mainly in Europe, requires tools capable of integrating localized driving cycles, fleet compositions, and regulatory contexts that are rarely present in current frameworks (Bi et al., 2021; Yue et al., 2013).

Positioning the Vehicle Consumption Assessment Model (VCAM)

The Vehicle Consumption Assessment Model (VCAM) addresses many critical gaps in the already established transport energy models, offering a highly flexible platform that can simulate vehicle energy consumption under various conditions. Its ability to recreate almost any vehicle, using certain inputs, such as powertrain type, allows researchers to analyze a wide range of vehicle configurations and performance characteristics. Additionally, VCAM integrates external factors, such as ambient temperature and driving profiles, making it extremely effective for analyzing BEV performance under varying real-world scenarios.

However, despite its flexibility, VCAM currently lacks features for hydrogen vehicle modeling and advanced regional demand integration, particularly in European contexts where localized mobility patterns and environmental conditions play a critical role in achieving transport decarbonization goals (Masclans Abelló, 2021). By enhancing VCAM's capabilities to include these factors, this thesis aims to bridge the identified gaps, providing a more comprehensive and adaptable tool for transport energy modeling and system-level analysis.

2.3. Gaps and their connection to research objectives

The gaps identified in the existing vehicle energy consumption frameworks highlight critical limitations that must be dealt with to support the energy transition. The limited capacity of current tools to fully integrate hydrogen vehicles and to take into account weather variability is a significant obstacle to accurately evaluating future energy demands. This is important for regions such as Europe, where diverse climates, regulatory landscapes, and mobility patterns require detailed and region-specific analyses.

Moreover, most models struggle to bridge the gap between vehicle-level simulations and regional demand assessments, limiting their relevance in broader energy system planning. This disconnect seems particularly problematic in scenarios that require holistic integration of transport and renewable energy systems, as decreasing emissions in the transport sector should align with the evolving dynamics of energy generation and consumption at the system level.

To address these gaps, this thesis aims to enhance the Vehicle Consumption Assessment Model (VCAM) with the following objectives:

1. **Incorporate Hydrogen Vehicle Modeling:** Develop and integrate features for simulating hydrogen fuel cell vehicles (FCEVs), enabling VCAM to represent a broader range of powertrain technologies and assess their contributions to decarbonization.
2. **Model Weather Variability:** Extend VCAM's capabilities to simulate the impacts of external conditions, such as extreme temperatures, on vehicle energy consumption and range, particularly for BEVs and other electrified powertrains.
3. **Regional Demand Integration for Europe:** Adapt VCAM to account for localized driving cycles, fleet compositions, and climate variability across European regions, providing actionable insights into regional transport energy demand and emissions.

By addressing these gaps, this thesis will bridge the divide between vehicle-level and system-level modeling, offering a complete tool that evaluates different powertrain technologies and supports strategic energy planning. This thesis is directly connected to the continued effort to decarbonize the transport systems while ensuring the effective integration of renewable energy sources.

3

Methodology

The Methodology section provides a complete description of the steps followed in order to extend and apply the Vehicle Consumption Assessment Model in evaluating fuel cell electric vehicles in real-world European conditions (see Figure 3.1. In Section 3.1, the architecture of the original model is enhanced by integrating the new entry of hydrogen fuel cell electric vehicles, which is complete with detailed fuel cell efficiency maps, idle mode behavior, and HVAC system modeling. In this section, the complete description of the governing equations is provided. In Section 3.2, the data collection procedure is described, which includes the collection of data for each of the European countries' fleet composition, the selection of driving cycles, and the compilation of different weather year time series.

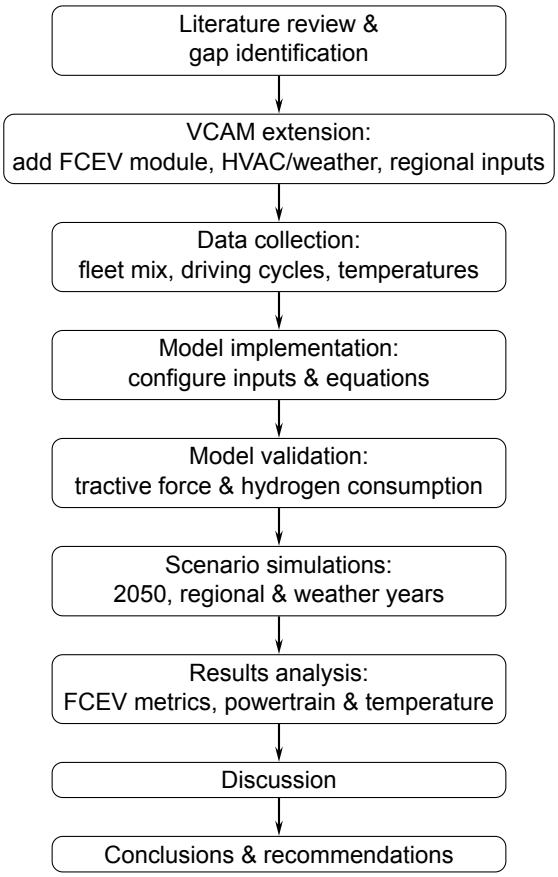

Figure 3.1: Flowchart of the thesis methodology

3.1. VCAM structure

This section presents the main features, capabilities, and structure of the established Vehicle Consumption Assessment Model. VCAM acts as a virtual test bench, simulating energy consumption based on specific inputs. These inputs can be organized by vehicle specifications and external factors. Model specifications define crucial efficiency characteristics, such as curb weight, maximum power, and drag coefficient. Respectively, external factors such as driving cycle profiles and outer temperature are independent of the vehicle model.

VCAM functions mainly as a backward simulation model, which means that it computes vehicle consumption based on predefined driving cycles, without taking into account any interaction with the driver. However, it integrates some forward modeling elements by including dynamic constraints, such as power or torque limitations, which introduce feedback loops into the consumption calculation.

The current model structure is represented in Figure 3.2 and has been developed and thoroughly explained by Sanvito (2022). The model structure varies depending on the powertrain type that is being simulated. In the figure, current inputs and outputs concerning BEVs and ICEVs are depicted. On top of these, there are other inputs and outputs concerning FCEVs that will be discussed.

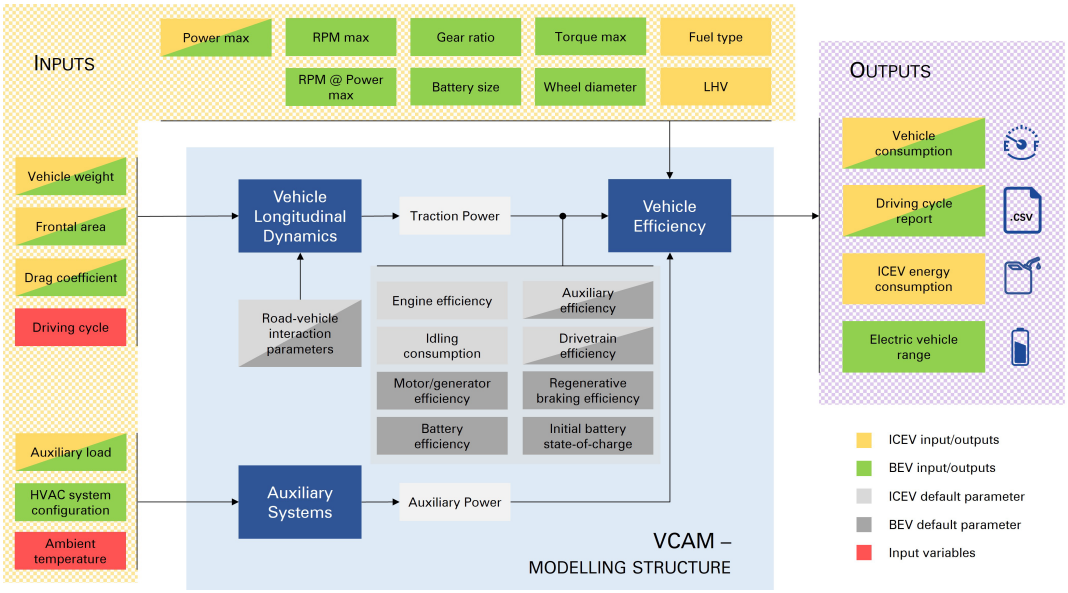

Figure 3.2: VCAM modeling structure

3.1.1. FCEV inputs

As already said, the model inputs are categorized by vehicle-dependent and vehicle-independent variables. The latter are present in all types of powertrains:

- **Driving Cycle (DC):** The driving cycle serves as the model's demand component and is composed of various profiles: (i) the time profile of the driving cycle (DC), (ii) the speed profile, (iii) the acceleration profile, and (iv) the road grade. To maintain consistency in units of measurement, the inputs follow specific conventions: timestep are customizable, speed is given in $m \cdot s^{-1}$, acceleration in $m \cdot s^{-2}$, and road grade in percentage, which corresponds to the tangent of the road angle multiplied by 100. Driving cycles may either be standard ones, used for vehicle certification, or custom-defined according to user requirements.
- **External Temperature:** the ambient temperature varies throughout the year. The model can take as input a specific temperature or time series data related to countries and different weather years

There are also some common inputs between FCEVs and other powertrain types. These are:

- **Vehicle Weight:** expressed in kilograms [kg] and accounts for the curb weight plus driver/passengers (on average),
- **Frontal Area:** expressed in [m^2],
- **Drag Coefficient:** a parameter that concerns the aerodynamic efficiency of the vehicle,
- **Auxiliary load:** This variable accounts for the additional electrical load generated by various vehicle components, including power steering, onboard controllers, windshield wipers, infotainment systems, and other auxiliary devices. It is represented as a constant power load, measured in watts [W].

The unique inputs for FCEV modeling are:

- **Fuel Cell Max Power:** it represents the maximum power output in [kW] that the fuel cell can provide,
- **Fuel Cell Efficiency Map:** it expresses the efficiency of the fuel cell for each power output
- **Battery Size:** overall battery capacity in [kWh],
- **Idle Power:** the power consumed by the fuel cell when the vehicle is idle in [kW],
- **Fuel Cell Ramp-up Time:** the time that the fuel cell needs to reach peak power.
- **Hydrogen Tank Size:** the size of the tank for the stored hydrogen expressed in [kg]

3.1.2. Model outputs

The model has some default outputs:

- **Vehicle Consumption:** the output result computed is the FCEV consumption expressed in [$kg_{H_2}/100km$], as well as the fuel efficiency in MPGe,
- **Driving Cycle Report:** a .csv output file containing all the driving cycle variables relevant to each time step,
- **Fuel cell electric vehicle range:** the total range in [km] is computed.

3.1.3. Governing equations

This section covers the equations used to simulate Fuel Cell Electric Vehicles, as well as vehicle dynamics in the software.

Vehicle longitudinal dynamics

The initial modeling block transforms the driving cycle inputs into corresponding forces and power demands. The longitudinal dynamics of a vehicle are typically modeled by summing four primary resistive forces: aerodynamic drag, rolling friction, road grade, and inertial forces. This modeling framework is well established in the literature and has been widely applied in vehicle propulsion and control studies (Guzzella & Sciarretta, 2013; Muneer et al., 2004; Rajamani, 2012; Tate & Boyd, 2000; X. Wu & Peng, 2005). To begin, the traction power is determined using Equation 3.1:

$$F_{\text{traction}} = F_{\text{aerodynamic}} + F_{\text{rolling friction}} + F_{\text{road grade}} + F_{\text{inertia}} \tag{3.1}$$

where $F_{\text{aerodynamic}}$ represents the aerodynamic resistance (Equation 3.2), $F_{\text{rolling friction}}$ accounts for the interaction between the tires and the road (Equation 3.3), $F_{\text{road grade}}$ corresponds to the force exerted due to road incline (Equation 3.5), and F_{inertia} denotes the inertial force (Equation 3.6).

Each force component is described as follows:

$$F_{\text{aerodynamic}} = \frac{1}{2} \cdot \rho_{\text{air}} \cdot A_f \cdot C_d \cdot v^2 \tag{3.2}$$

where ρ_{air} is the air density, A_f is the vehicle's frontal area, C_d is the aerodynamic drag coefficient, and v represents the vehicle speed. The rolling friction force is calculated using Equation 3.3:

$$F_{\text{rolling friction}} = m \cdot g \cdot C_r \cdot \cos\delta \tag{3.3}$$

where m represents the vehicle mass, including the driver and passenger contributions, g is the gravitational acceleration, C_r is the rolling friction coefficient, and δ is the road angle in radians. The rolling friction coefficient varies as a function of vehicle speed and external temperature, as detailed in Table A.1.

The conversion from road slope to road angle is expressed in Equation 3.4:

$$\delta = \arctan\alpha \tag{3.4}$$

where α denotes the road slope in percentage.

The force due to road grade is given by Equation 3.5:

$$F_{\text{road grade}} = m \cdot g \cdot \sin\delta \tag{3.5}$$

The inertia force is determined as follows:

$$F_{\text{inertia}} = m \cdot a \tag{3.6}$$

Finally, the computed forces are transformed into power by multiplying them by the vehicle speed.

Auxiliary systems

This section focuses on the modeling of the auxiliary Heating, Ventilation, and Air Conditioning (HVAC) system in Fuel Cell Electric Vehicles (FCEVs). The HVAC modeling determines the heating or cooling load based on external temperature conditions, assuming steady-state operation. The fundamental equations used for this modeling approach are derived from the study of Lajunen (2017). This methodology is consistent with the HVAC modeling applied to BEVs, ensuring a unified framework for evaluating auxiliary thermal loads.

For FCEVs, different HVAC system configurations can be selected, including:

- **Heat Pump with Waste Heat Recovery (HP-WH):** If the HVAC system utilizes a heat pump with waste heat recovery (hvac_mode $=$ ”hp_wh”), the COP is computed as a function of the external temperature:
$$\text{COP} = \max(1, \text{cop}_{\text{HP-WH}}(T_{\text{out}})) \tag{3.7}$$
- **Heat Pump with PTC Heating (HP-PTC):** If the HVAC system integrates a Positive Temperature Coefficient (PTC) heater alongside a heat pump (hvac_mode $=$ ”hp_ptc”), the COP follows:
$$\text{COP} = \max(1, \text{cop}_{\text{HP-PTC}}(T_{\text{out}})) \tag{3.8}$$
- **Heat Pump with PTC Heating and Waste Heat Recovery (HP-PTC-WH):** In this case, the HVAC system combines a heat pump, a PTC heater, and waste heat recovery (hvac_mode $=$ ”hp_ptc_wh”), leading to a COP defined as:
$$\text{COP} = \max(1, \text{cop}_{\text{HP-PTC-WH}}(T_{\text{out}})) \tag{3.9}$$

The thermal load from the HVAC system is converted into an electrical power demand using the coefficient of performance:

$$P_{\text{HVAC}} = \frac{P_{\text{th}}}{\text{COP}} \tag{3.10}$$

Additionally, Fuel Cell Electric Vehicles (FCEVs) require an extra thermal management load associated with the battery (BTMS), which ensures proper temperature. The total auxiliary thermal load is computed as:

$$P_{\text{th, aux}} = P_{\text{HVAC, aux}} + P_{\text{BTMS}} \tag{3.11}$$

The auxiliary efficiency (η_{aux}) in FCEV modeling accounts for:

- The DC/DC converter efficiency used to supply the HVAC system.
- The round-trip efficiency of the auxiliary fuel cell power system.

Vehicle modeling

Fuel Cell Electric Vehicles (FCEVs) present a unique powertrain architecture that combines a fuel cell system, a battery pack, and an electric drivetrain to provide traction power while maintaining optimal energy efficiency. This section details the computational approach used to model power demand, power split strategy, and efficiency characteristics in FCEVs. The conceptual layout of an FCEV, as depicted in Figure 3.3, illustrates the key power flow pathways between the fuel cell system, battery, and electric motor.

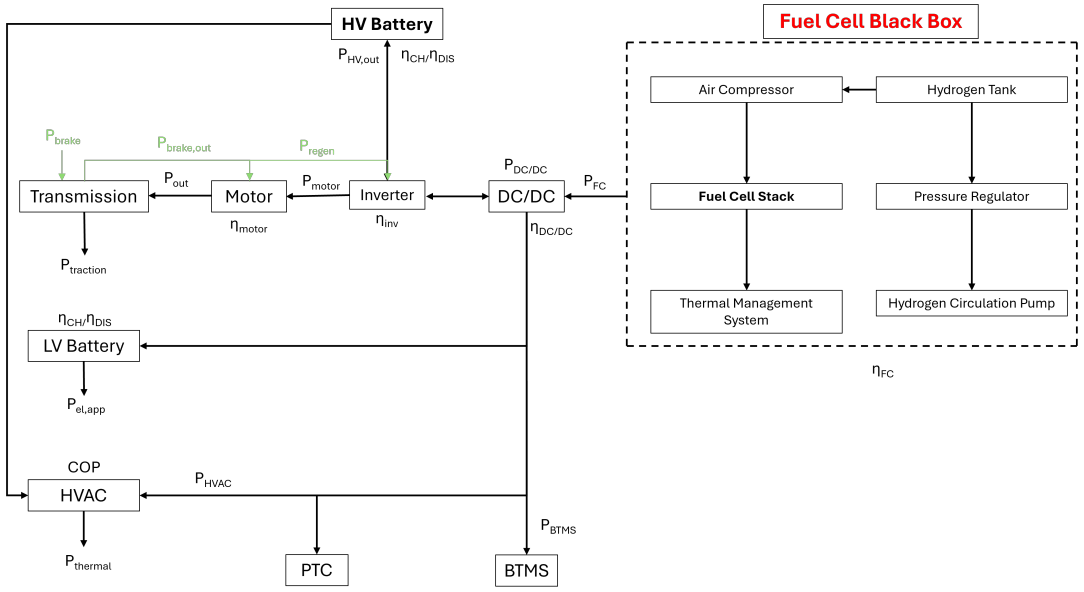

Figure 3.3: Conceptual architecture of an FCEV drivetrain, illustrating power flow pathways.

As depicted in the Figure, the fuel cell system is modeled as a black box with the efficiency used containing all the components present in the fuel cell (e.g., air compressor, pressure regulator, hydrogen circulation pump, etc.) as well as the necessary inverters/converters. The power management strategy in an FCEV balances fuel cell output and battery contribution, ensuring that the fuel cell operates efficiently. The fuel cell system operates at optimum power output to achieve increased efficiency, as outlined by Purnima and Jayanti (2020):

$$P_{\text{FC, max}} \cdot 0.1 \leq P_{\text{FC}} \leq P_{\text{FC, max}} \cdot 0.9 \tag{3.12}$$

The power split strategy is implemented as follows:

- If the total power demand is low, the battery provides power while the fuel cell operates at idle,
- If the demand exceeds the fuel cell's optimal efficiency range, the battery supplements additional power,
- If regenerative braking occurs, excess energy is stored in the battery.

Battery power contribution is determined dynamically, ensuring that State of Charge (SOC) remains within predefined limits:

$$SOC_{\text{min}} \leq SOC \leq SOC_{\text{max}} \tag{3.13}$$

where the lower limit prevents excessive discharge, and the upper limit ensures the battery does not overcharge.

The fuel cell efficiency varies depending on output power levels. An example of Toyota Mirai's fuel cell system and stack efficiencies is shown in Figure 3.4. The fuel cell system efficiency ($\eta_{\text{FC,sys}}$) is generally lower than the fuel cell stack efficiency ($\eta_{\text{FC,stack}}$) due to additional system losses, including compressors, thermal management, and DC/DC conversion losses.

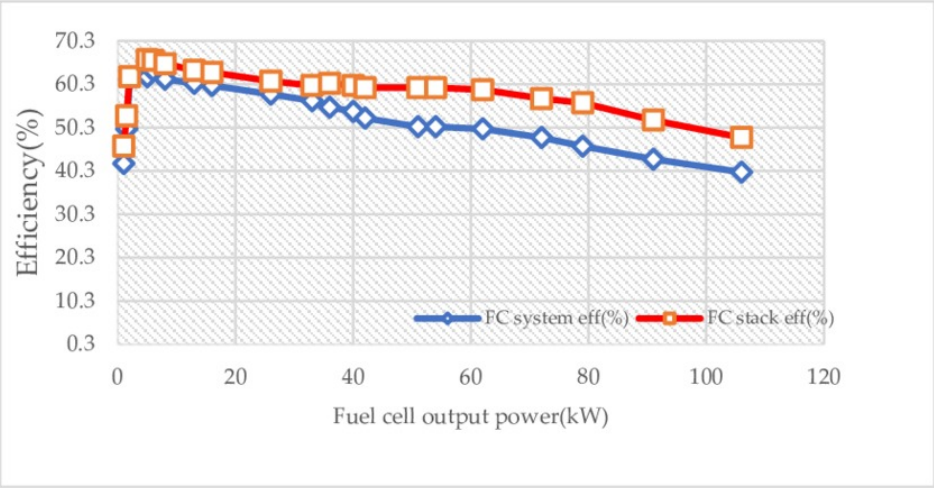

Figure 3.4: Fuel cell efficiency map: stack efficiency vs. system efficiency as a function of output power (Q. Wu et al., 2025).

Fuel cell efficiency is interpolated from empirical data, ensuring accurate performance prediction:

$$\eta_{\text{FC}} = f(P_{\text{FC}}) \tag{3.14}$$

where $f(P_{\text{FC}})$ is a function derived from test data. The efficiency declines at higher power outputs due to increased parasitic losses and reactant flow constraints.

The power at the motor outlet is given by equation 3.15:

$$P_{out} = \frac{P_{traction}}{\eta_{dt}} \tag{3.15}$$

while motor's power is computed as:

$$P_{motor} = \frac{P_{out}}{\eta_{motor}} \tag{3.16}$$

The motor efficiency, η_{motor}, is dependent on the vehicle's partial load, which is the ratio of the actual motor power demand to the vehicle's maximum power output, P_{max} (Brooker et al., 2015). Additionally, the peak motor efficiency is expressed as a function of the maximum power itself (Basso et al., 2014).

FCEVs recover energy during braking through regenerative braking, where the electric motor acts as a generator to charge the battery. The braking power is given by:

$$P_{brake} = -P_{traction} \tag{3.17}$$

The recovered power is limited by:

- The battery's maximum charge acceptance rate.
- The state of charge (SOC) of the battery.
- The efficiency of the power electronics.

If the battery is full or charging power exceeds system limits, the excess braking energy is dissipated as heat through mechanical brakes, and it is computed as:

$$P_{\text{regen}} = \min(-P_{\text{motor}} \cdot \eta_{\text{regen}}, P_{\text{max, charge}}) \tag{3.18}$$

where: $P_{\text{max, charge}}$ is the maximum allowable battery charging power.

If the battery State of Charge (SOC) is below its upper limit (e.g., 85% SOC), the recovered energy is stored in the battery. When the vehicle requires additional power beyond the fuel cell's or motor's direct supply, the battery discharges to meet the demand. However, this process is subject to a discharge efficiency factor ($\eta_{\text{discharge}}$), accounting for losses.

The actual power supplied by the battery during discharge is adjusted as:

$$P_{\text{batt, out}} = \frac{P_{\text{batt}}}{\eta_{\text{discharge}}}, \quad \text{if } P_{\text{batt}} > 0 \tag{3.19}$$

To prevent overcharging or deep discharge, the battery power output and input are constrained within predefined operational limits:

$$P_{\text{batt}} = \begin{cases} P_{\text{max, discharge}}, & \text{if } P_{\text{batt}} > P_{\text{max, discharge}} \\ -P_{\text{max, charge}}, & \text{if } P_{\text{batt}} < -P_{\text{max, charge}} \\ P_{\text{batt}}, & \text{otherwise} \end{cases} \tag{3.20}$$

where $P_{\text{max, discharge}}$ represents the battery's maximum discharge power.

The SOC of the battery is updated dynamically based on the net power exchange and the battery's total capacity:

$$SOC = SOC_{\text{prev}} - \frac{P_{\text{batt}} \cdot \Delta t}{E_{\text{batt, capacity}}} \tag{3.21}$$

where:

- Δt is the timestep duration.
- $E_{\text{batt, capacity}}$ represents the battery's energy storage capacity (kWh).

Outputs

The estimation of hydrogen consumption for fuel cell electric vehicles (FCEVs) in this study is based on second-by-second power demand from the drive cycle and an interpolated fuel cell efficiency map. The method accounts for traction power, fuel cell system efficiency, auxiliary loads, and the lower heating value (LHV) of hydrogen.

At each time step, the fuel cell power demand P_{fc} is determined from the drive cycle simulation. Fuel cell efficiency η_{fc} is then interpolated from a predefined efficiency map based on the power level. The instantaneous hydrogen consumption in kilograms is computed as:

$$\Delta H_2(t) = \frac{P_{\text{fc}}(t) \cdot \Delta t / 3600}{\eta_{\text{fc}}(t) \cdot \text{LHV}_{H_2}} \tag{3.22}$$

where:

- $P_{\text{fc}}(t)$ is the power provided by the fuel cell in kilowatts (kW),
- Δt is the simulation time step in seconds (typically 1 s),
- $\eta_{\text{fc}}(t)$ is the interpolated fuel cell efficiency at time t,
- LHV_{H_2} is the lower heating value of hydrogen, taken as $33.7\,\text{kW h kg}^{-1}$.

The total hydrogen consumed over the drive cycle is given by the sum of instantaneous hydrogen usage:

$$H_{\text{total}} = \sum_t \Delta H_2(t) \tag{3.23}$$

To express consumption in standard terms, hydrogen use is normalized per 100 kilometers:

$$H_{\text{norm}} = \frac{H_{\text{total}}}{d_{\text{km}}} \cdot 100 \tag{3.24}$$

where d_{km} is the total distance traveled in kilometers, computed from the drive cycle speed profile.

The model also computes the equivalent electric energy delivered by the fuel cell, taking into account efficiency losses:

$$E_{\text{fc,total}} = \sum_t P_{\text{fc}}(t) \cdot \eta_{\text{fc}}(t) \cdot \frac{\Delta t}{3600} \tag{3.25}$$

From this, the average specific energy consumption of the fuel cell system can be derived:

$$e_{\text{fc}} = \frac{E_{\text{fc,total}}}{d_{\text{km}}} \quad \left[\frac{\text{kWh}}{\text{km}}\right] \tag{3.26}$$

Finally, the estimated driving range R in kilometers is calculated based on the onboard hydrogen tank capacity H_{tank}:

$$R = \frac{H_{\text{tank}}}{H_{\text{norm}}} \cdot 100 \tag{3.27}$$

This formulation captures both the physics of fuel cell operation and the vehicle-specific parameters. Auxiliary loads and idle power consumption are included within P_{fc} at each time step. The model can be easily adapted if more vehicle-specific data becomes available.

3.2. Data collection for scenario analysis

In order to be able to evaluate the way in which the passenger vehicle energy demand might evolve in the future, this study is based on a dataset that combines vehicle characteristics and climate projections. This section outlines the key sources and assumptions used to generate the necessary inputs for the scenario analysis that will follow. The data collection process is structured around the current and projected fleet composition in Europe, the historical and future temperature time series, and travel demand statistics.

3.2.1. Vehicle fleet mix in Europe

VCAM generates time-series consumption data for different vehicle segments. In order to have accurate relevance to real-world data, vehicle segments A, C, and E are used, which correspond to the vehicle fleet mix in Europe as small, medium, and large passenger vehicles. This car fleet composition is reported by Eurostat (2025) for the reference year 2023. The classification followed is based on the engine size of petrol and diesel engine vehicles, since they represent the largest share of vehicles currently. To be more specific, small cars correspond to engines of size $Size \leq 1399\text{cm}^3$, whereas medium cars correspond to size $1400\text{cm}^3 \leq Size \leq 1999\text{cm}^3$ and large cars refer to engines of $Size \geq 2000\text{cm}^3$. Figure 3.5 presents the car stock distribution for each country. In cases where fleet composition data is unavailable, values are estimated using a proximity or similarity-based approach. A summary of all assumptions is provided in Table 3.1.

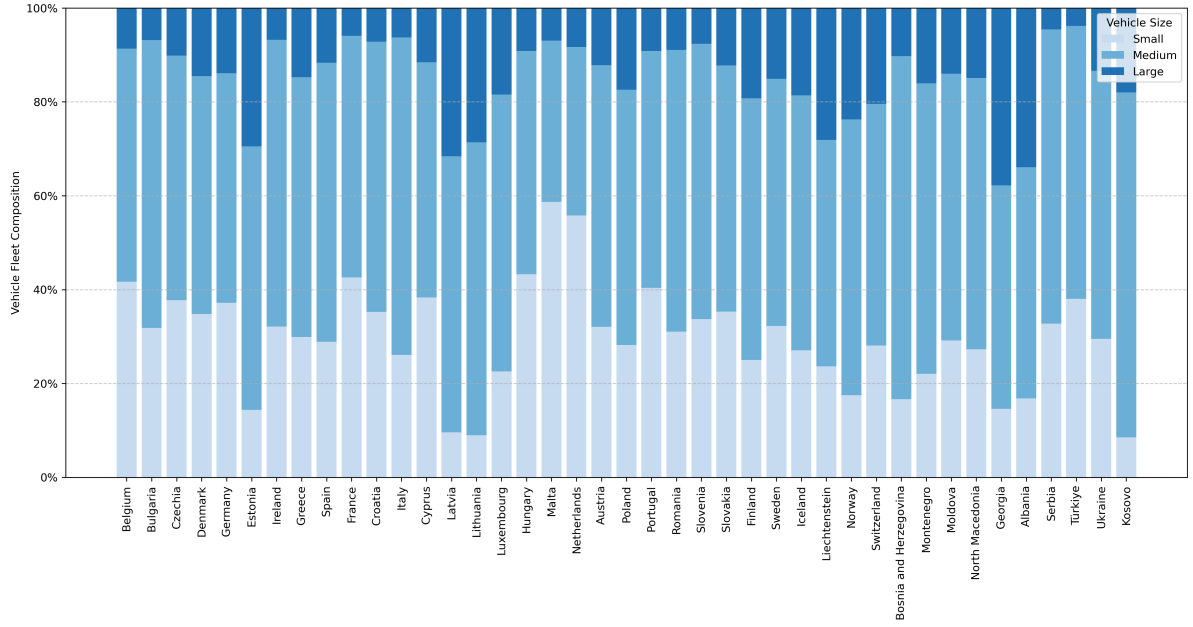

Figure 3.5: Passenger Vehicle Fleet Composition in European Countries

Table 3.1: Data sources and assumptions used for estimating passenger vehicle fleet composition in European countries.

Country	Country Code	Car Fleet Composition Data (2023)	Estimated using neighbors
Albania	AL	✓	-
Austria	AT	✓	-
Belgium	BE	✓	-
Bosnia and Herzegovina	BA	✓	-
Bulgaria	BG	✗	RO, RS, MK
Croatia	HR	✓	-
Czechia	CZ	✓	-
Denmark	DK	✗	DE, SE
Estonia	EE	✓	-
Finland	FI	✓	-
France	FR	✓	-
Germany	DE	✓	-
Greece	GR	✗	AL, IT
Hungary	HU	✓	-
Iceland	IS	✗	NO, DK
Ireland	IE	✓	-
Italy	IT	✓	-
Latvia	LV	✓	-
Lithuania	LT	✓	-
Luxembourg	LU	✓	-
North Macedonia	MK	✗	RS, AL
Moldova	MD	✓	-
Montenegro	ME	✗	BA, RS, AL
Netherlands	NL	✓	-
Norway	NO	✓	-
Poland	PL	✗	DE, CZ, LT
Portugal	PT	✓	-
Romania	RO	✓	-
Serbia	RS	✓	-
Slovakia	SK	✗	CZ, AT, HU, PL
Slovenia	SI	✓	-
Spain	ES	✓	-
Sweden	SE	✓	-
Switzerland	CH	✓	-
Türkiye	TR	✓	-
Ukraine	UA	✗	PL, RO, MD
United Kingdom	GB	✓	-
Kosovo[1]	XK	✓	-

[1] 2021 data used instead of 2023.

3.2.2. Weather year time series data

The weather year temperatures used in this study were obtained from the Renewables Ninja database, an open-access platform created by Professor Stefan Pfenninger. The complete dataset includes forty individual historical years, which cover the period from 1980 to 2019. For each simulation, the ambient temperature input was population-weighted. Using a population-weighted temperature makes sure that the climate conditions driving the vehicle consumption simulations closely reflect the thermal environment experienced by the majority of the population.

3.2.3. Passenger car energy demand calculation

Understanding and projecting passenger vehicle energy demand is crucial for evaluating the effects of transport decarbonization strategies. In this section, the methodology used to compute the current and future energy demand for selected countries is presented. The VCAM model is used to generate segment-specific consumption profiles for different climate conditions and fleet compositions. This analysis aims to quantify the way in which the temperature variations, powertrain mix, and vehicle share affect the energy demand at the national level in the transport sector.

Reference year

For the scenario analysis of this study, three main countries are used: Greece, Germany, and Finland. These countries represent the three main climatic zones that are present in the European territory. In order to compute the energy demand in these countries year 2019 was used as a reference year for the hourly consumption values. It is assumed that the vehicle fleet of these countries consisted of 100 percent Internal Combustion Engine Vehicles. This is justified because Battery Electric Vehicles made up less than 0.5 percent of the fleet at the time.

The core of this analysis is the VCAM tool, which generates the hourly fuel consumption profiles for different vehicle segments A(small), B(medium), and C(large), which correspond to the aforementioned analysis of the vehicle fleet share. All consumption simulations are based on the Worldwide Harmonized Light Vehicles Test Procedure (WLTP) driving cycle, which is assumed to be representative of typical passenger car operation in European conditions.

To accurately represent each country's fleet, the hourly consumption series from VCAM for each segment was combined using country-specific segment weights. That means that for each country, the hourly fleet-average consumption is calculated as a weighted sum of the segment profiles, using the national fleets' share of each segment.

To move from fuel consumption per 100 kilometers to total national passenger car energy demand, the following methodology has been used:

- National statistics for annual passenger kilometers (pkm) were gathered for each country.
- These passenger kilometers total have been converted to vehicle kilometers (vkm) by dividing by the occupancy rate of vehicles for each country.
- To distribute total annual vkm across the year, country-specific hourly mobility profiles were used. These profiles indicate how travel activity is distributed across the 8,760 hours of a year and were normalized so that their sum over all hours equals one. The profiles were provided by Francesco Sanvito and are part of the open-access RAMP-mobility project (Mangipinto et al., 2022).
- For each hour, the total passenger car kilometers driven were allocated using the mobility profile.

The final hourly energy demand has been calculated for each country as a function of the fleet-weighted fuel consumption (l/100km) multiplied by the number of vehicle kilometers driven at the time and the energy content of the fuel. Estimated and European Commission, Joint Research Centre (2021) vehicle km data are presented in Table 3.2. Summing the hourly energy demand over all 8,760 hours gives the annual national passenger car energy demand. These are shown in the following equations:

$$\text{Weighted Consumption}_c(t) = \sum_{\text{seg}} w_{\text{seg},c} \cdot \text{Cons}_{\text{seg},c}(t) \tag{3.28}$$

$$\text{vehicle-km}_c = \frac{\text{passenger-km}_c}{\lambda_c} \tag{3.29}$$

$$\text{vehicle-km}_c(t) = \text{vehicle-km}_c \cdot M_c(t) \tag{3.30}$$

$$E_c(t) = \frac{\text{Weighted Consumption}_c(t)}{100} \cdot \text{vehicle-km}_c(t) \cdot \eta_{\text{fuel}} \tag{3.31}$$

$$E_c^{\text{annual}} = \sum_t E_c(t) \tag{3.32}$$

Where,

- $w_{\text{seg},c}$: Share of vehicle segment seg in country c
- $\text{Cons}_{\text{seg},c}(t)$: Hourly fuel consumption (l/100km) for segment seg in country c at hour t
- λ_c: Average vehicle occupancy (persons per vehicle) in country c
- passenger-km$_c$: Total annual passenger-kilometers in country c
- vehicle-km$_c$: Total annual vehicle-kilometers in country c
- $M_c(t)$: Normalized hourly mobility profile for country c at hour t $\quad(\sum_t M_c(t) = 1)$
- $E_c(t)$: Hourly passenger car energy demand (kWh) for country c at hour t
- E_c^{annual}: Annual passenger car energy demand (kWh) for country c

Table 3.2: Comparison of estimated vehicle kilometers (based on passenger km and occupancy) and JRC IDEES data. Vehicle kilometers are in billions.

Country	Passenger km (billion)	Estimated Vehicle km	JRC IDEES Vehicle km
Greece	60	46.15	40.9
Germany	920	647.89	484.6
Finland	66.8	47.37	38.8

2050 climate scenario projections

To quantify the way in which future temperature increases will affect passenger car energy demand, for the different powertrain technologies, three main scenarios for regional mid-century temperature are applied by the IPCC's Representative Concentration Pathways (RCPs) to each country's 1980-2019 baseline (on Climate Change, 2014). Country-specific projections derived from climate model ensembles, such as CMIP5 and those summarized in the IPCC AR5 Synthesis Report (on Climate Change, 2014) and subsequent regional assessments (IPCC, 2014) are directly applied. First, each country's annual mean temperature baseline is computed by averaging the 365 daily mean values for each year and then averaging those 40 annual means:

$$\overline{T}_{80\text{–}19} \;=\; \frac{1}{40}\sum_{y=1980}^{2019}\left(\frac{1}{365}\sum_{d=1}^{365}\Big(\frac{1}{24}\sum_{h=1}^{24}T_{y,d,h}\Big)\right)$$

Then, for each RCP scenario, regional mid-century temperature projections based on country-level deltas extracted from the literature and IPCC sources are applied. These projections vary by country due to geographic and climatic differences.

$$T_{2050}^{\text{RCP}\,x} \;=\; \overline{T}_{80\text{–}19} \;+\; \Delta T_{\text{RCP}x} \quad (x \in \{2.6, 4.5, 8.5\})$$

The projections, for each RCP scenario, are summarized in Table 3.3.

Table 3.3: Projected mid-century (2041–2060) regional temperature anomalies under IPCC RCP scenarios for selected countries, relative to the 1986–2005 baseline. Ranges reflect the spread across CMIP5 ensemble models (IPCC, 2014).

Country	RCP 2.6 (ΔT in °C)	RCP 4.5 (ΔT in °C)	RCP 8.5 (ΔT in °C)
Greece	1.0 – 1.6	1.4 – 2.1	2.2 – 2.9
Germany	1.4 – 2.1	1.8 – 2.4	2.7 – 3.5
Finland	1.6 – 2.2	2.1 – 2.9	3.5 – 4.5

2050 powertrain share projections

In the data collection part of this thesis, three main scenarios are used for the powertrain share in 2050, obtained from the International Energy Agency (IEA): The Stated Policies Scenario (STEPS), the Sustainable Development Scenario (SDS), and the Net Zero Emissions by 2050 Scenario (NZE). These provide a comprehensive basis in order to model the future fleet composition of Europe, under different policy ambitions.

The IEA Stated Policies Scenario (STEPS) assumes that only the current measures and policies will be followed and projects that the fleet composition will consist of 10% ICEVs, 5% HEVs, 5% PHEVs, 70% BEVs, and 10% FCEVs by 2050 (IEA, 2019a).

According to the IEA Sustainable Development Scenario (SDS), more carbon emission reduction and air-quality policies will be imposed. This will result in a fleet composition of 5% ICEVs, 2% HEVs, 3% PHEVs, 75% BEVs, and 15% FCEVs by 2050 (IEA, 2019b).

In contrast, the IEA Net Zero Emissions by 2050 Scenario (NZE), proposes that the passenger transport sector will be almost completely electrified, while there will be no more ICEV sales after 2035. This will result in a fleet composition with 0% ICEVs, 0% HEVs, 5% PHEVs, 80% BEVs, and 15% FCEVs by 2050 (IEA, 2021).

In order to streamline the temperature-dependent consumption analysis, the five powertrain technologies are consolidated into three main ones: ICEVs, BEVs, and FCEVs. This is done by assuming that PHEVs and HEVs deliver roughly 80 percent of their mileage in combustion mode. The resulting 2050 stock shares are shown in Table 3.4.

Table 3.4: 2050 passenger□car stock shares under IEA scenarios

Scenario	ICEV (% stock)	BEV (% stock)	FCEV (% stock)
STEPS	18%	72%	10%
SDS	9%	76%	15%
NZE	4%	81%	15%

Projection of vehicle shares in 2050

Recent market data and mobility outlooks show a persistent increase in the vehicle share of Sport Utility Vehicles (SUVs) in the European passenger car fleet. According to IEA (2023), the share of SUVs in new passenger car sales in Europe has been increased from about 25 percent in 2015 to approximately 50 percent in 2023. This shows that SUVs are the fastest-growing vehicles in recent years.

To take this into account for the future fleet composition, this thesis includes a scenario where the large segment share continues growing. According to historical data, this growth has been reported to be around 1-2% per year (IEA, 2023). For the purpose of this analysis, this thesis applies a range of yearly growth rates: 1%, 1.5%, and 2%. It assumes that the large segment share linearly increases by the specified annual rate. To maintain the integrity of the total fleet share the shares of the other segments are proportionally decreased. The resulting projected shares are used in the weighted energy consumption calculations for 2050 under all RCP and powertrain mix scenarios.

3.3. Model quality assessment

The credibility and usefulness of every computational model are not only based on its theoretical foundation, but also on the validation, consistency, and transparency of the results it produces. In the context of this thesis, where the VCAM model has been adapted to include and simulate different powertrain technologies under various climate conditions and driving cycles in Europe, it is crucial to evaluate the quality of the model and the produced results. This section offers a structured evaluation of the model's reliability, focusing on its plausibility, transparency, internal consistency, and alignment with empirical data. The aim is to show that the results of the model are robust enough and suitable to support different analyses in the transport sector in the broader context of energy systems. In addition, the limitations of the model are discussed as well as their consequences in translating the findings and for potential future improvements.

3.3.1. Validation of traction force calculation

One of the foundational components in vehicle energy modeling is the calculation of traction force, which determines the required propulsive effort to overcome resistive forces during driving. Since this parameter directly influences energy consumption estimates across all powertrain types, validating its accuracy is essential for ensuring the overall reliability of the model.

The value for traction force computed by the model has been validated against empirical data provided by the Argonne National Laboratory (ANL). The comparison is based on a standard urban driving cycle for a mid-size passenger vehicle using data from ANL's Advanced Powertrain Research Facility. The results are illustrated in Figures 3.6 and 3.7.

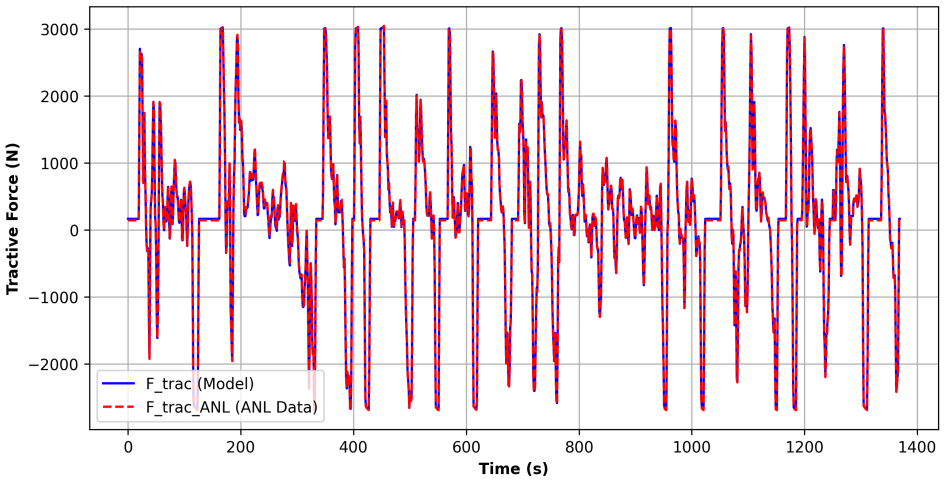

Figure 3.6: Comparison of Modeled Tractive Force vs. ANL's Tractive Force

As depicted in Figure 3.6, the modeled traction force closely aligns with the measurements from ANL. To quantify the level of agreement, both the Root Mean Squared Error (RMSE) and the Normalized RMSE (NRMSE) were calculated.

The RMSE is defined as:

$$\text{RMSE} = \sqrt{\frac{1}{N}\sum_{i=1}^{N}(F_{\text{modeled},i} - F_{\text{measured},i})^2} \tag{3.33}$$

where $F_{\text{modeled},i}$ and $F_{\text{measured},i}$ denote the modeled and measured traction force values at time step i, respectively. RMSE offers an absolute error metric, with lower values indicating better agreement.

To provide a relative metric, the Normalized RMSE (NRMSE) is used:

$$\text{NRMSE} = \frac{\text{RMSE}}{F_{\text{max}} - F_{\text{min}}} \tag{3.34}$$

where F_{max} and F_{min} are the maximum and minimum measured traction forces during the cycle (Blog, 2019). In general, NRMSE values below 10% are indicative of high model accuracy, while values between 10% and 20% suggest acceptable but imperfect alignment.

For this validation case, the calculated RMSE was **17.48 N** and the NRMSE was **0.0209**. These results demonstrate that the modeled outputs fall well within expected bounds, indicating excellent agreement between simulation and experimental data.

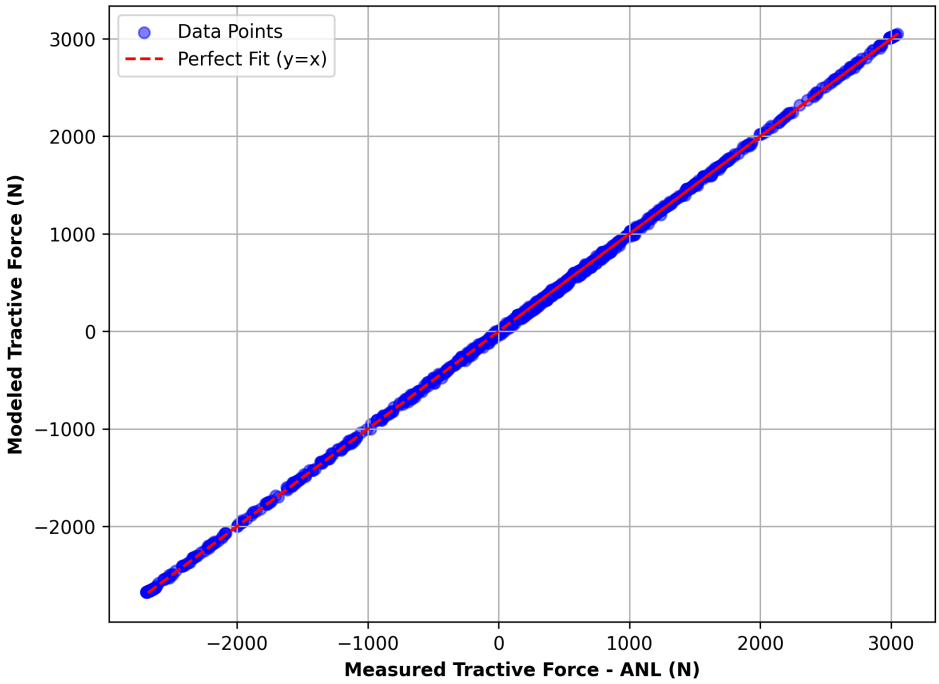

Figure 3.7: Modeled vs. Measured Tractive Force

As shown in Figure 3.7, the observed discrepancies are minimal and can be attributed to reasonable factors such as sensor noise, uncertainty in road load coefficients, or minor simplifications in the modeled physics. The validation confirms that the traction force sub-model used in VCAM performs reliably across realistic urban driving conditions and provides a solid basis for subsequent energy consumption modeling.

3.3.2. Validation of hydrogen consumption estimation

To validate the hydrogen consumption estimates produced by the model, a series of simulation tests were conducted using the Toyota Mirai 2016 fuel cell electric vehicle (FCEV) as a reference platform. All tests were performed under the standard Urban Dynamometer Driving Schedule (UDDS) to ensure consistency in driving conditions. The model's results were compared against empirical data obtained from the Argonne National Laboratory (ANL), focusing on the sensitivity of hydrogen consumption to varying levels of auxiliary power under different ambient temperature scenarios.

Test 1: Baseline conditions (20°C Ambient, HVAC Off)

The first validation test was conducted at an ambient temperature of 20 °C, which represents neutral weather conditions where no HVAC demand is present. Figure 3.8 shows the comparison between the modeled hydrogen consumption and the reference values provided by ANL. As depicted in the graph, the model closely aligns with the empirical data, with the error ranging from **–2.91% to +4.98%** depending on the auxiliary power level. The minimum error occurs near the optimal auxiliary power level of approximately 300 W, where the model and the reference data converge almost exactly.

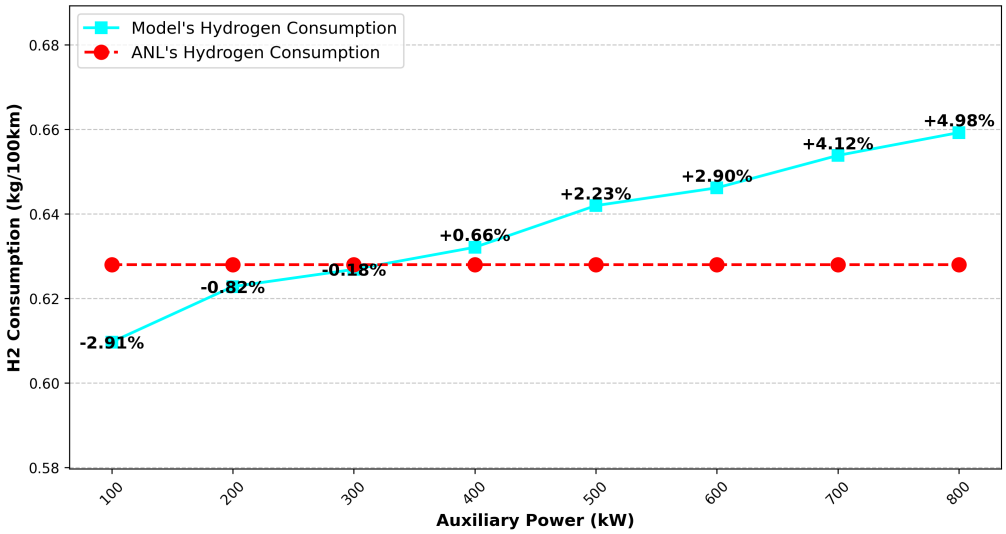

Figure 3.8: Hydrogen consumption validation under neutral weather conditions (20°C ambient)

Test 2: Cold weather conditions (-7°C Ambient, HVAC On)

In the second test, the ambient temperature was set to represent cold weather conditions, simulating HVAC demand for cabin heating and fuel cell system conditioning. As shown in Figure 3.9, the deviation between modeled and measured consumption increased with auxiliary load, reaching up to **+12.34%**. This increased error is attributed primarily to the lack of detailed empirical data on thermal power consumption in FCEVs under low temperatures. The model estimates auxiliary thermal loads based on generic assumptions, which introduces uncertainty in colder scenarios.

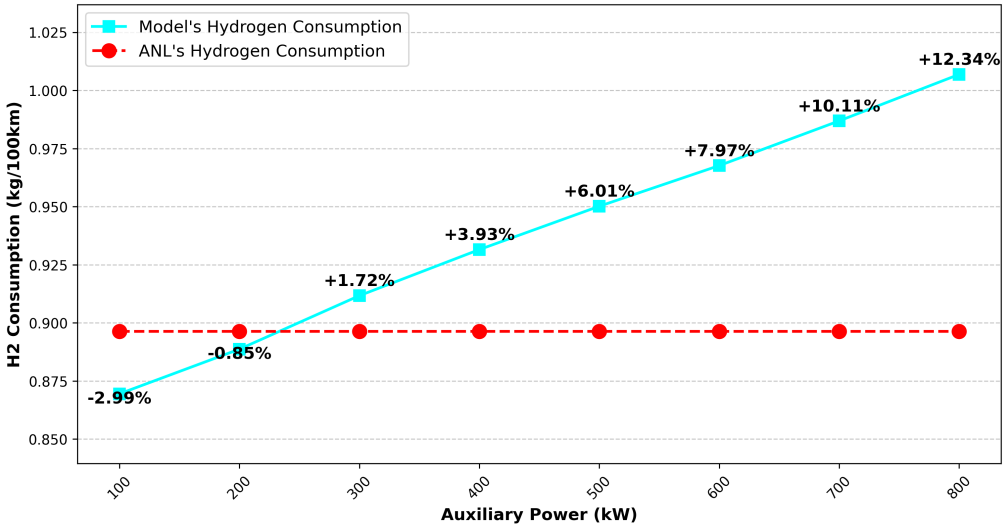

Figure 3.9: Hydrogen consumption validation under cold weather conditions

Test 3: Hot weather conditions (35°C Ambient, HVAC On)
The third validation scenario simulated high ambient temperatures typical of summer operation. In this case, the HVAC system is assumed to draw power for cabin cooling and fuel cell thermal management. As presented in Figure 3.10, the model again shows a rising positive deviation from the reference values, with maximum error reaching **+13.46%**. Similar to the cold weather case, this is mainly due to limited empirical data on the behavior of HVAC and cooling systems in FCEVs during hot operation. Nevertheless, the model maintains a coherent and monotonic trend in response to increasing auxiliary power, which supports its internal consistency.

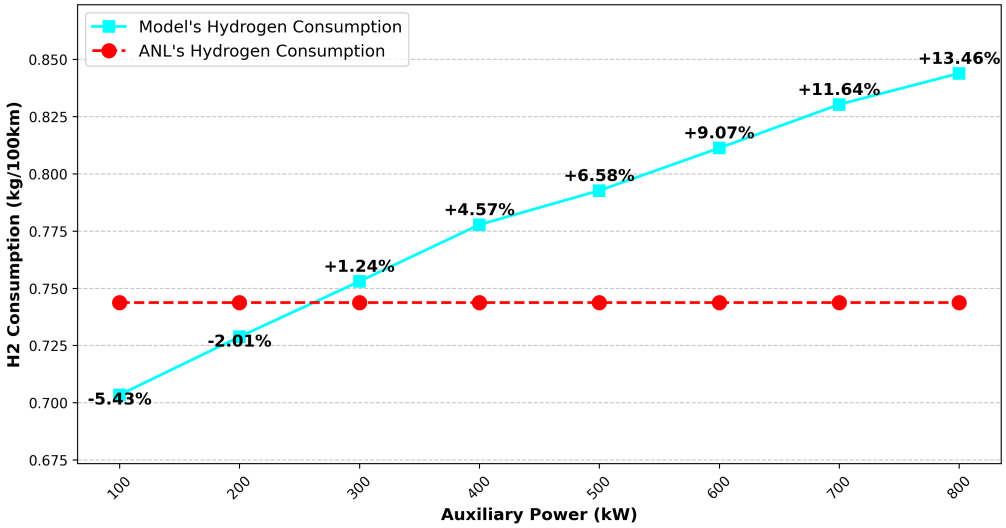

Figure 3.10: Hydrogen consumption validation under hot weather conditions

Overall, the validation results confirm that the hydrogen consumption estimates produced by the model are consistent with known empirical data, particularly under moderate thermal loads. The maximum deviations observed in extreme cold and hot conditions highlight the challenges of modeling HVAC-related energy use in FCEVs due to limited transparency in OEM data. However, across all three scenarios, the model accurately captures the expected trend: hydrogen consumption increases with auxiliary power demand, and deviations remain within an acceptable range for system-level energy modeling.

Toyota Mirai technical specifications

To improve clarity and reproducibility, Table 3.5 summarizes the main technical characteristics of the Toyota Mirai used in the validation process.

Table 3.5: Key Specifications of the Toyota Mirai 2016 FCEV (Argonne National Laboratory, 2016)

Variable	Value / Unit	Notes
Fuel cell max power	$114\,\mathrm{kW}$	Maximum power output of PEM fuel cell
Battery capacity	$1.6\,\mathrm{kW\,h}$	Nominal battery energy capacity
Vehicle weight	$1925.25\,\mathrm{kg}$	Including fuel and passengers
Frontal area	$2.1\,\mathrm{m}^2$	Aerodynamic cross-sectional area
Drag coefficient (C_d)	0.29	Aerodynamic resistance
Wheel radius	$0.3\,\mathrm{m}$	Effective rolling radius
Transmission efficiency	0.90	Drivetrain efficiency
Idle consumption power	$0.94\,\mathrm{kW}$	Fuel cell idle system consumption

Additional validation for FCEVs

To further assess the generalizability of the hydrogen consumption model, two additional FCEV platforms were simulated and compared against measured data under the Worldwide Harmonized Light Vehicles Test Procedure (WLTP). The vehicles tested were the **Hyundai Nexo** and the **Hyundai Tucson FCEV**, both widely used fuel cell vehicles with known physical parameters (Car and Driver, 2015, n.d. Hydrogen Cars Now, n.d.). Table 3.6 summarizes the main technical specifications used for each simulation.

Table 3.6: Specifications of Additional FCEV Models Used in Validation

Parameter	Hyundai Nexo	Hyundai Tucson
Fuel cell max power [kW]	95	100
Battery size [kWh]	1.56	0.95
Vehicle weight [kg]	1854	1882
Frontal area [m^2]	2.577	3.016
Drag coefficient (C_d)	0.32	0.355
Wheel radius [m]	0.336	0.316
Auxiliary power [W]	300	280
Fuel cell idle power [kW]	0.94	0.94
Hydrogen tank capacity [kg]	5.6	5.63

In both cases, it is important to note that the **efficiency map** and **idle power consumption** values used in the simulations were taken from the Toyota Mirai 2016, due to the absence of published manufacturer data for the Hyundai models. These represent key assumptions in the modeling process. If more accurate or vehicle-specific performance maps were available, the model could potentially produce even closer matches to measured consumption.

The simulated and measured hydrogen consumption values are compared below, along with their relative error, computed using the standard formula:

$$\text{Relative Error (\%)} = \frac{H_{sim} - H_{real}}{H_{real}} \times 100 \tag{3.35}$$

Table 3.7: Hydrogen Consumption Validation Results under WLTP

Vehicle	H_{real} [kg/100km]	H_{sim} [kg/100km]	Error (%)
Hyundai Nexo	0.84	0.90	+7.14%
Hyundai Tucson	1.00	1.07	+7.00%

The model shows good alignment with measured data, with errors under 8% in both cases. These results confirm that the simulation framework remains robust when applied to different FCEV architectures. The slightly higher simulated values may be attributed to the use of non-vehicle-specific fuel cell efficiency characteristics and HVAC dynamics. Nonetheless, the accuracy is sufficient for system-level energy analysis, and the model can be easily refined should more detailed performance data become available.

4

Results

This chapter presents a quantitative assessment of hydrogen fuel cell electric vehicles (FCEVS), battery electric vehicles (BEVs), ans internal combustion engine vehicles (ICEVs), focusing on how their energy consumption responds to temperature and how these effects evolve across time, geography, and future scenarios. The analysis begins at the vehicle level, exploring the thermal sensitivity and powertrain behavior of FCEVs under various driving cycles and ambient conditions. It then continues with a comparative analysis between the powertrain technologies, showing the way in which temperature extremes affect energy demand differently for each technology. From then, the analysis is extended into region-specific analysis of long-term weather variability and its influence on the vehicle energy use in three different European countries: Greece, Germany, and Finland, which represent three different climate zones present in Europe. Building on this, the chapter concludes with a scenario-based projection for passenger vehicle energy demand in 2050, incorporating policy and global warming scenarios, and evaluating the impact of changing fleet compositions, especially the rise of SUV penetration. This approach helps in understanding how technical, environmental, and behavioral factors shape the future transport sector.

4.1. FCEV powertrain related results

Figure 4.1 presents the variation of energy consumption and the estimated autonomy of C-Segment FCEVs, under WLTP driving cycle conditions, as a function of ambient temperature, in a range from $-15°\mathrm{C}$ to $35°\mathrm{C}$. The diagram illustrates two main trends. First, the energy consumption, which is shown as a solid blue line and represented by the left y-axis, presents a strong dependence on temperature. On the other hand, the estimated driving range, which is depicted as a red dashed line and represented by the right y-axis, shows an inverse relationship to the consumption. Both lines start their y-axis from zero for clarity.

It is clear from the graph that at low temperatures, especially below $0°\mathrm{C}$, the energy consumption of FCEVs sharply increases, reaching a peak of more than 45 kWh/100km at $-15°\mathrm{C}$. The cause of this significant rise is the increased energy demand in order to heat the cabin and the thermal management systems. As the temperature increases, the consumption decreases steadily, reaching a minimum between $15°\mathrm{C}$ and $25°\mathrm{C}$, when the cooling and heating demand is relatively low. In this optimal condition, the consumption stabilizes at approximately 21-23 kWh/100km. After a specific point, when there is cooling demand, the consumption starts increasing again.

Regarding the estimated driving range, the opposite trend is depicted. To be more specific, the driving range increases as temperature increases from $-15°\mathrm{C}$ to $25°\mathrm{C}$, reaching a peak of 780 km. However, in temperatures above $30°\mathrm{C}$, the driving range starts decreasing because of the increased HVAC loads for cooling, which reduces the available driving range to below 650 km at $35°\mathrm{C}$.

Overall, the results present a significant sensitivity of the efficiency of the FCEVs to ambient temperature. Weather extremes, both cold and hot, result in a marked reduction in efficiency and driving range, showing the increased need for optimal thermal management strategies in FCEV design. This finding

is crucial when examining the possibility of using this powertrain technology in the world and planning the hydrogen mobility infrastructure, especially when considering regions that face extreme seasonal variations.

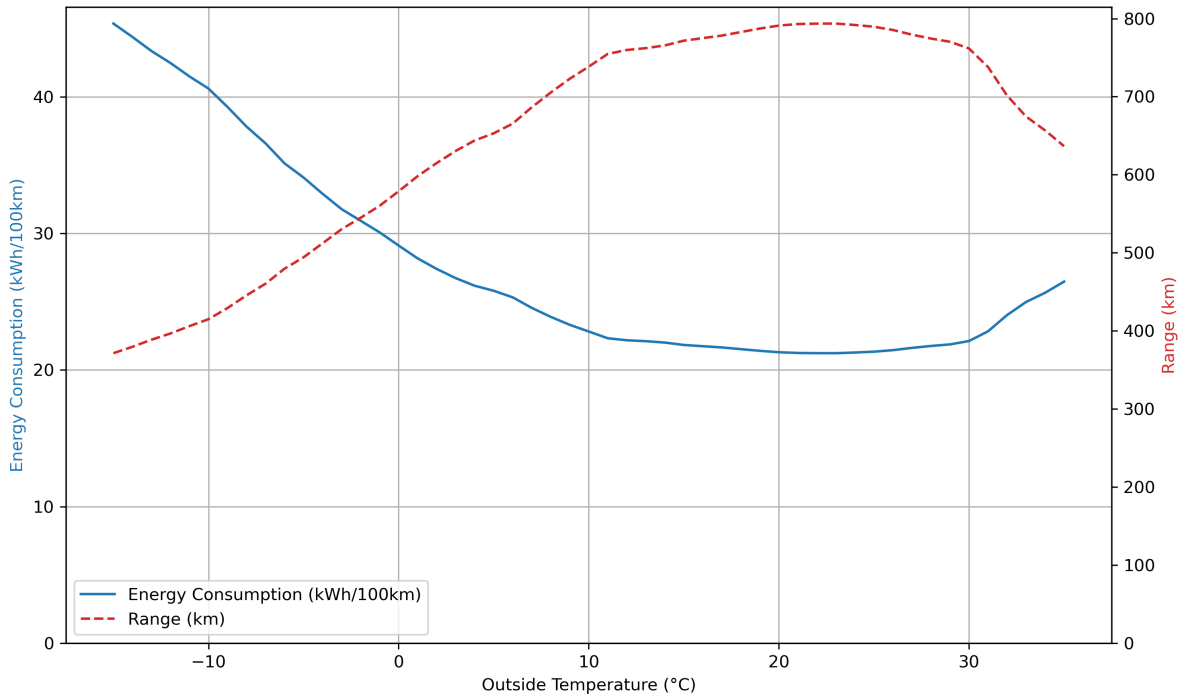

Figure 4.1: Energy consumption and range of FCEV powertrain vs temperature. Reference vehicle: C-Segment. Reference driving cycle: WLTP

Figure 4.2 depicts the temporal distribution of power between the fuel cell system and the battery in the FCEV powertrain, adapted for C-Segment vehicles and the UDDS driving cycle. The chart shows three main power flows in the system over time: the power production of the fuel cell system (blue), the battery discharge (orange), and the battery charge via the regenerative braking (green).

The plot highlights the hybrid nature of the FCEV powertrain technology. The fuel cell system operates as the main power source, offering the majority of the traction power needed for vehicle propulsion, as it is depicted by the large blue spikes, which correspond to accelerating or high-load events. During periods of increased power demand, such as rapid acceleration, the battery provides supplementary power, which results in the positive battery discharge values (orange). This allows the fuel cell system to operate closer to the optimal efficiency range by smoothing out transient power demands.

In contrast, during deceleration events and braking, some part of the kinetic energy of the vehicle is recovered through the regenerative braking technology, which charges the battery. This is shown by the negative green regions of the chart. These charging events happen periodically during the driving cycle and contribute to the improvement of the overall efficiency.

It is worth mentioning that the fuel cell power output does not fluctuate as much as the battery does. This shows that the control strategy followed during the modeling phase of this thesis prioritized fuel cell longevity and efficiency by avoiding continuous changes in the fuel cell load, using the battery to cover short-term fluctuations instead. This kind of strategy enhances fuel cell durability and also allows the system to maximize energy recovery while minimizing hydrogen consumption.

In summary, the power split strategy followed shows the synergy between the fuel cell and the battery systems in FCEVs, which balances the energy efficiency. The effectiveness of this approach in managing power contribution is further reflected in the relatively low hydrogen consumption and the increased autonomy mentioned previously.

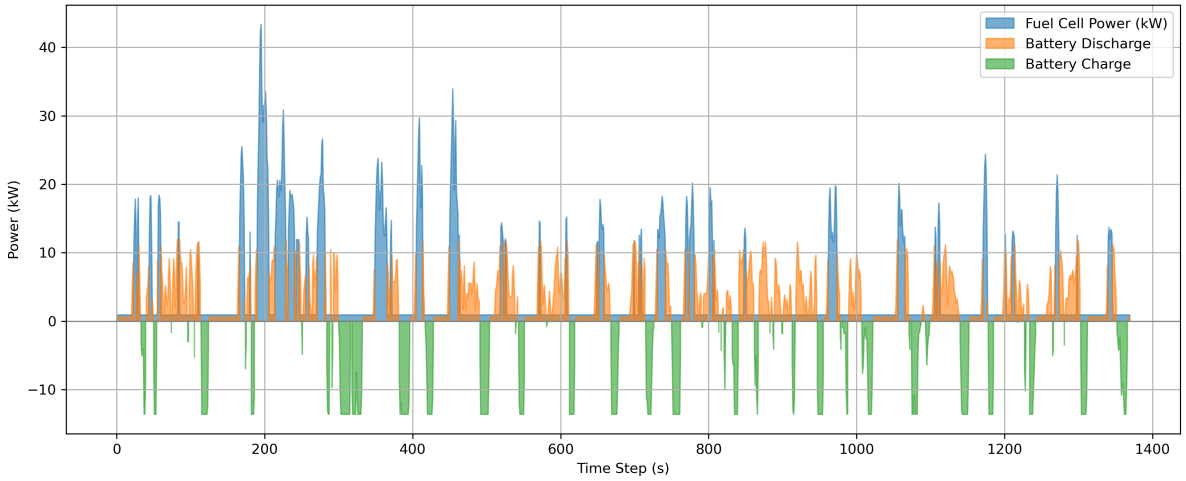

Figure 4.2: Power split between fuel cell (blue), battery discharge (orange), and battery charging (green) in the C-segment FCEV during UDDS driving cycle.

To give further insights into the dynamic power management, Figure 4.3 depicts a zoomed section of the UDDS driving cycle, which now includes the speed profile, with green color taking advantage of the right y-axis, besides the fuel cell and battery power contributions. This detailed view illustrates the way in which the powertrain components respond to transient speed changes and acceleration events. The peaks in fuel cell and battery power lines coincide with the periods of rapid acceleration, while the charging of the battery is happening during decelerating phases, as shown by the drops in the speed signal. This plot clearly shows the complementary roles of the fuel cell and battery, with the latter absorbing the short-term fluctuations and allowing the effective regenerative braking when the vehicle speed decreases.

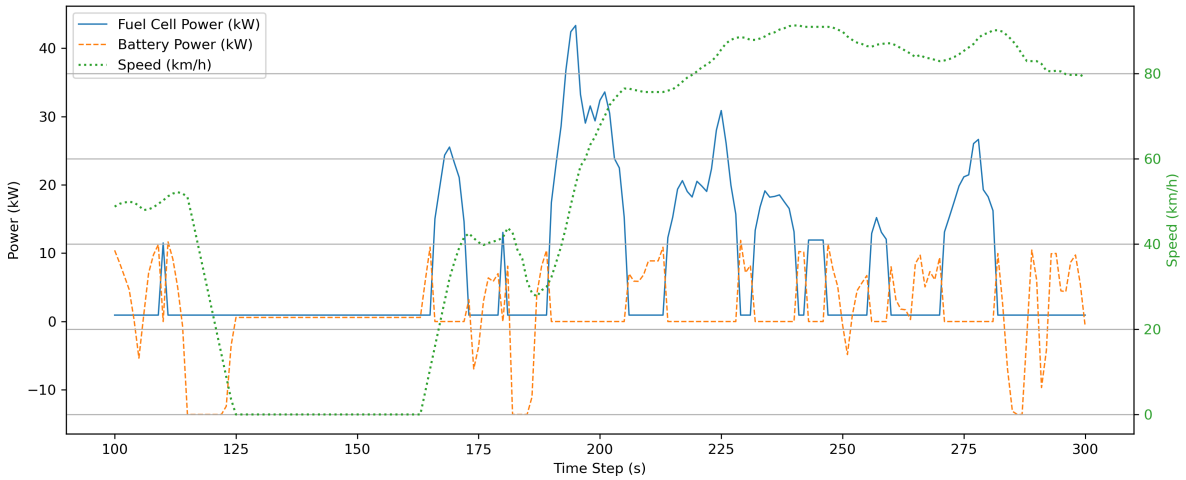

Figure 4.3: Zoomed-in view of fuel cell power, battery power, and vehicle speed over a segment of the drive cycle for the C-segment FCEV

Figure 4.4 depicts the distribution of fuel cell and battery power as a function of the acceleration of the vehicle. The fuel cell power, marked with red scatter points, is close to zero but never reaches it, even during deceleration or zero acceleration events. This happens because of the idle power consumption of the fuel cell, which makes sure that the fuel cell system is constantly operational and ready to adapt to power demands. During positive acceleration, especially in sudden or rapid acceleration peaks, the battery, marked with green scatter points, supplies the extra power, which is clearly depicted in the increased battery power distribution above zero, allowing the fuel cell system to avoid rapid changes

of power demand and operate closer to its optimal range. In contrast, during decelerating events, the battery absorbs the regenerative energy, as shown by the negative values of the battery power, while the fuel cell operates at idle mode. This shows the hybrid control strategy, where the battery buffers short-term power fluctuations and supports the energy recovery as well as the dynamic driving demands.

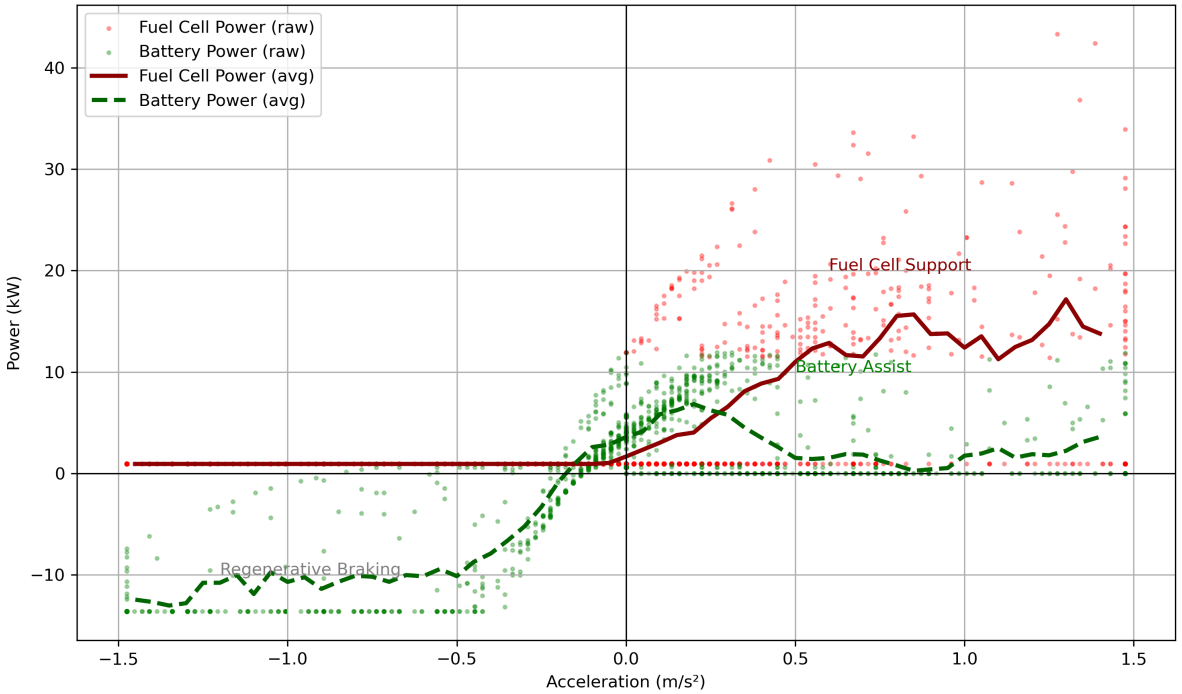

Figure 4.4: Fuel cell and battery power as a function of vehicle acceleration for the C-segment FCEV. Raw data are shown as scatter points, while bold lines indicate moving averages.

Figure 4.5 offers a comparative analysis of two standard driving cycles, UDDS and WLTP, highlighting their influence on the operation of the fuel cell system in C-Segment FCEVs. The speed profiles, depicted in red color, show the time-varying speed demands, with WLTP being characterized by higher peak speeds and increased frequency of aggressive acceleration events in comparison with UDDS. The power output of the fuel cell follows these dynamic demands, with sharp power increases, which correspond to rapid acceleration phases.

In the right-hand panels, the fuel cell power output frequency distributions are depicted for each driving cycle. Both distributions tend to lower power levels, reflecting the prolonged periods of idle power consumption and low speed operation, which are usually present in urban driving scenarios. However, the WLTP distribution presents a wider tail, showing the higher frequency of moderate and high power demands that happen because of the more varying and demanding speed profile.

This analysis also has real-world relevance, as it demonstrates how the different usage patterns, the urban UDDS versus the mixed/real-world WLTP, can significantly alter the operating regime of the fuel cell system. Taking into account that the efficiency and the degradation of the fuel cell system are highly sensitive both to the load level and to the transient dynamics, understanding these patterns is crucial to be able to optimize the fuel cell electric vehicle's system design, to predict hydrogen consumption, and to ensure they are durable under real-world conditions.

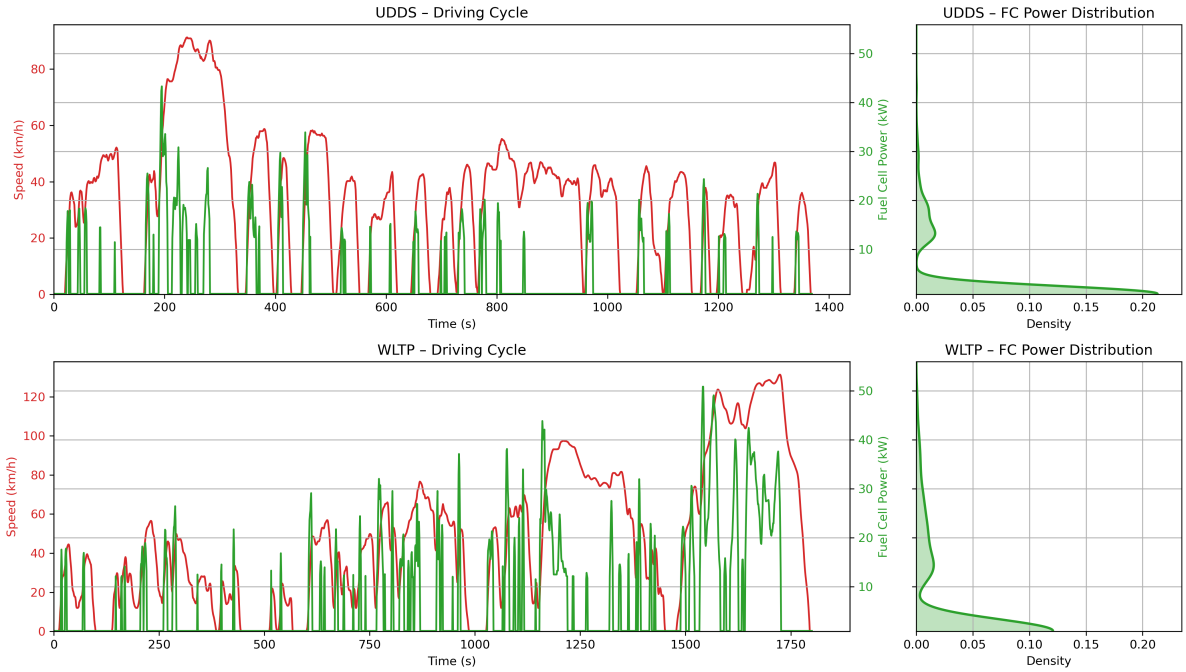

Figure 4.5: Speed profiles (red) and corresponding fuel cell power outputs (green) for the UDDS (top) and WLTP (bottom) driving cycles (left), with fuel cell power probability density distributions (right) for each cycle

Figure 4.6 presents the segment-dependent variability of the FCEV performance as a function of ambient temperature, with hydrogen consumption depicted in subplot (a) and estimated range in subplot (b). These results come by using as reference for the weather variability the country of Greece and a WLTP driving cycle. Furthermore, for this analysis, A-segment FCEVs are assumed to exist and are modeled with a 3kg hydrogen tank, while C and E-segment vehicles represent the typical mid and large size passenger vehicles.

As shown in Figure 4.6 (a), the hydrogen consumption [kg/100km] increases for larger segments and shows a U-shaped curve for temperature dependence across all segments. The minimum consumption occurs at around $20°\mathrm{C}$ - $25°\mathrm{C}$, where the thermal loads are lowest, as discussed previously. Figure 4.6 (b) shows the corresponding estimated driving range for each segment. The range peaks in mild temperatures for all segments and decreases in weather extremes. The total range is also determined by the hydrogen tank size. For example, even though A-Segment vehicles are the most efficient, their range is limited by the smaller 3kg tank.

Regarding the trends, both subplots appear smooth. However, it is worth mentioning the underlying nonlinearities that exist due to vehicle parameters such as weight and frontal area. Heavier vehicles present increased sensitivity in the auxiliary loads, which results in a rapid decrease of autonomy and increased hydrogen use in temperature extremes. Together, these results show the significant impact of vehicle sizing and powertrain configuration on FCEVs' efficiency and usability across different segments.

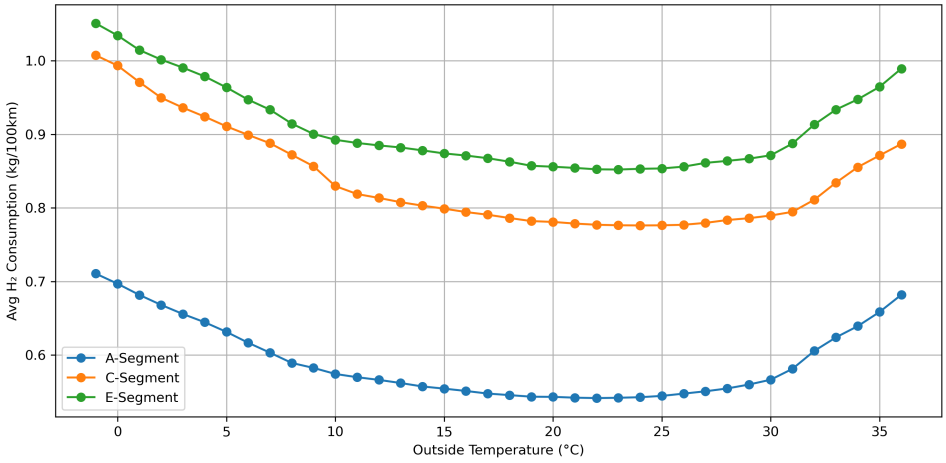

(a) Hydrogen consumption.

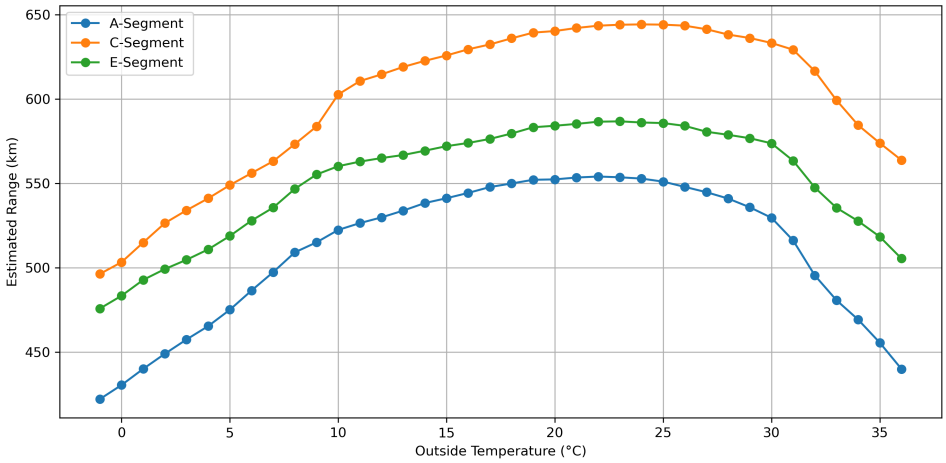

(b) Estimated range.

Figure 4.6: Temperature dependence of (a) hydrogen consumption and (b) driving range for A-, C-, and E-segment FCEVs. Reference country: Greece. Reference drive cycle: WLTP

Figure 4.7 illustrates the relationship between vehicle weight and the mean energy consumption for different FCEV segments, under WLTP driving cycle and a temperature range between $-15°\mathrm{C}$ and $40°\mathrm{C}$. As vehicle weight increases from A-Segment to F-Segment, the mean energy consumption [kWh/100km] also increases. However, this trend is not strictly linear. The increase in energy consumption is caused not only by the increased mass of the vehicle, but also by other critical factors, such as the frontal area, the aerodynamic drag, and the fuel cell system sizing, which are indicated as annotations for each segment in the graph.

The error bars in the diagram represent the minimum and maximum values of energy consumption, which were observed in the given temperature range, highlighting this nonlinearity even more. Heavier and larger vehicles present both higher mean energy consumption and greater variability, a fact that shows their increased sensitivity to changing the operating conditions. This is the result of the complex effects of the mass and aerodynamic drag, as well as the decreased operating efficiency of larger vehicles in temperature extremes.

Consequently, these results show that even though heavier FCEVs inherently consume more energy, the relation between weight and consumption is shaped by a complex, non-linear interaction of design parameters. Therefore, optimizing FCEV performance requires a holistic approach that takes into account not only the mass but also the aerodynamic drag and the powertrain configuration to minimize energy use, especially in larger vehicle segments.

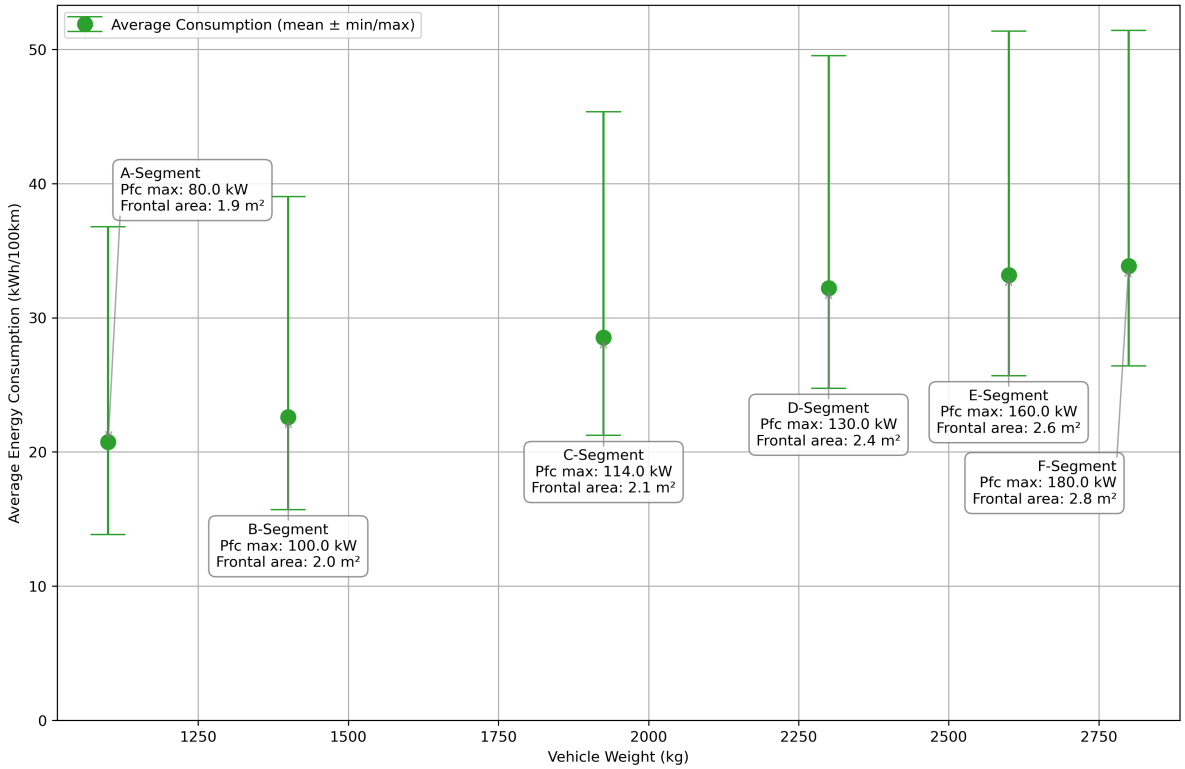

Figure 4.7: Average energy consumption (mean ± min/max) for FCEVs across vehicle segments as a function of vehicle weight. Annotations indicate maximum fuel cell power and frontal area for each segment. Reference driving cycle: WLTP.

4.2. FCEV, BEV, and ICEV powertrain comparison results

Figure 4.8 illustrates the dependence of the energy consumption on temperature for ICEVs and BEVs, which are presented in the subplots (a) and (b) respectively, while the relevant FCEVs results have been discussed previously. In Figure 4.8 (a), the ICEV curve remains relatively flat at low temperatures, with only a slight decrease within the $-20°\mathrm{C}$ to $35°\mathrm{C}$ temperature range, while a notable increase is experienced in higher temperatures. This shows the small influence of the cold weather in conventional vehicles, where the engine's waste heat is enough to cover the cabin's heating demand, and the more significant load from the air-conditioning and the engine cooling at higher temperatures. To quantify this, a "cold penalty" is calculated of roughly 5%, which means that the ICEV consumption at $-20°\mathrm{C}$ is about 5 % higher than at the $20°\mathrm{C}$ baseline. Furthermore, a "hot penalty" is calculated at around 25%, which means that the consumption at $+40°\mathrm{C}$ is approximately 25% above the $20°\mathrm{C}$ level (see Table 4.1).

Figure 4.8 (b) depicts an important U-shaped relationship for BEVs, where the energy consumption is decreased when going from $-20°\mathrm{C}$ to a minimum at $20°\mathrm{C}$ - $25°\mathrm{C}$ and it then increases in higher temperatures. The significant rise in energy consumption in colder temperatures (cold penalty ($\sim$85%) happens due to the increased demand for heating, while higher temperatures allow a milder hot penalty ($\sim$15%), which comes from the cooling demand of the cabin and the battery. BEVs and ICEVs present similar absolute volatility ($\sigma \approx 3.7$ and 3.9 kWh/100 km, respectively), but this represents a much larger percentage of BEVs' baseline, which makes them far more sensitive to temperature variations.

FCEVs present similar qualitative trends to BEVs and, as discussed previously, their energy consumption is similarly extremely sensitive to temperature, with a U-shape and even higher baseline consumption (approximately 26 kWh/100km at $20°\mathrm{C}$). However, FCEVs experience the greatest volatility ($\sigma \approx 77$ kWh/100 km), which means that they nearly double their consumption from $20°\mathrm{C}$ to $-20°\mathrm{C}$. Their hot penalty ($\sim$14%) is comparable to that of BEVs.

These results, which are summarized in Table 4.1 and visualized in Figure 4.8, show that while ICEVs are relatively robust to temperature fluctuations, both BEVs and FCEVs suffer significant increases in

energy consumption at temperature extremes, especially in colder climates. This suggests that the thermal management strategies for electrified vehicles are crucial in making them more efficient.

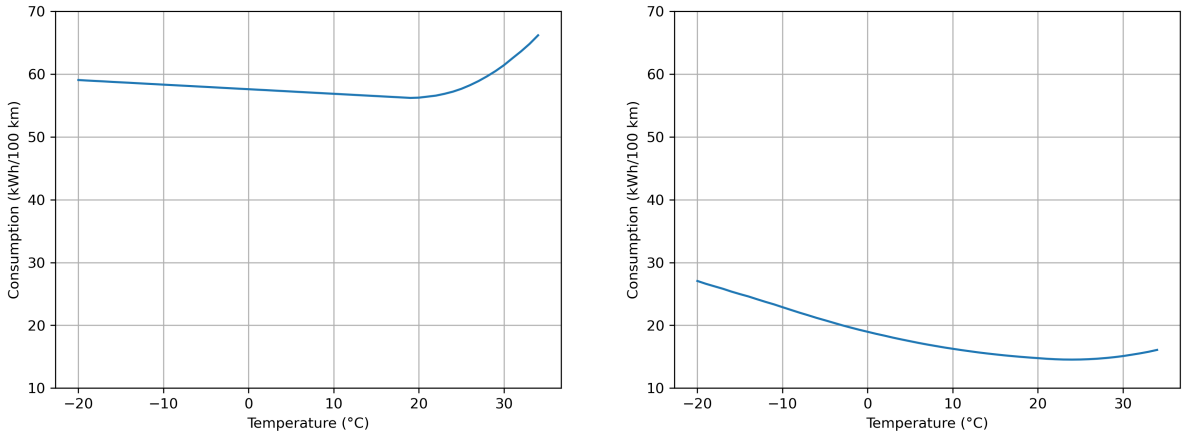

(a) ICEV energy consumption as a function of temperature.

(b) BEV energy consumption as a function of temperature.

Figure 4.8: Temperature dependence of energy consumption for (a) ICEVs and (b) BEVs. Both powertrains display increased consumption at temperature extremes, with BEVs showing much greater relative sensitivity. Reference drive cycle: WLTP.

Table 4.1: Temperature sensitivity of energy consumption for FCEV, BEV, and ICEV powertrains. Metrics shown are the standard deviation (σ) of consumption across the temperature range, and the percentage increase in consumption at $-20\,^{\circ}$C ("cold penalty") and $+40\,^{\circ}$C ("hot penalty") relative to $20\,^{\circ}$C.

Powertrain	σ Consumption (kWh/100 km)	Cold penalty (%)	Hot penalty (%)
FCEV	7.0	87.0	14.3
BEV	3.7	83.3	15.3
ICEV	3.9	5.0	24.9

4.2.1. Consumption variability of FCEVs, BEVs, and ICEVs for different European Countries

In order to perform this analysis, 40 weather years were selected, for the time frame between 1980 and 2019, for three different European countries: Greece, Germany, and Finland, which represent 3 different climate zones. The results consider C-Segment vehicles and the WLTP driving cycle, as reference, in 1-hour time steps. Blank strips are shown in the graph, and they represent non-leap years in correspondence with the missing day.

Figure 4.9 illustrates heatmaps for the hourly energy consumption of FCEVs for C-Segment vehicles for the three countries mentioned previously. Each row in the thermal map corresponds to one weather year, whereas each column represents the months of the year. The color range shows the energy consumption in kWh/100km, with darker colors indicating higher consumption values.

The diagrams reveal significant seasonal fluctuation in hydrogen consumption, which is directly connected to the local climate patterns. In Finland, for example, the impact of cold winters is easily visible as large high-consumption regions during the first months of every year, with some years presenting significantly cold extreme periods. This shows that the below-zero temperatures in Northern Europe can significantly increase FCEV energy use. In contrast, in Greece, the consumption profile is steadier over the 40-year period, with slight increases during the summer peaks and relatively low winter penalties, a fact that reflects the Mediterranean climate. Central European countries, like Germany, present an intermediate pattern, with both summer and winter effects that are visible, but not as extreme as in Finland.

Besides the intra-annual seasonal variability, inter-annual differences are also shown, with certain years presenting periods of significant energy consumption, sometimes even twice that of other years. These points correspond to particularly extreme cold events, or less frequently, extreme summer heatwaves. This variability highlights the need to take into account both yearly and seasonal weather fluctuations when planning hydrogen demand, refueling infrastructure, and vehicle range in the future expansion of FCEVs across Europe.

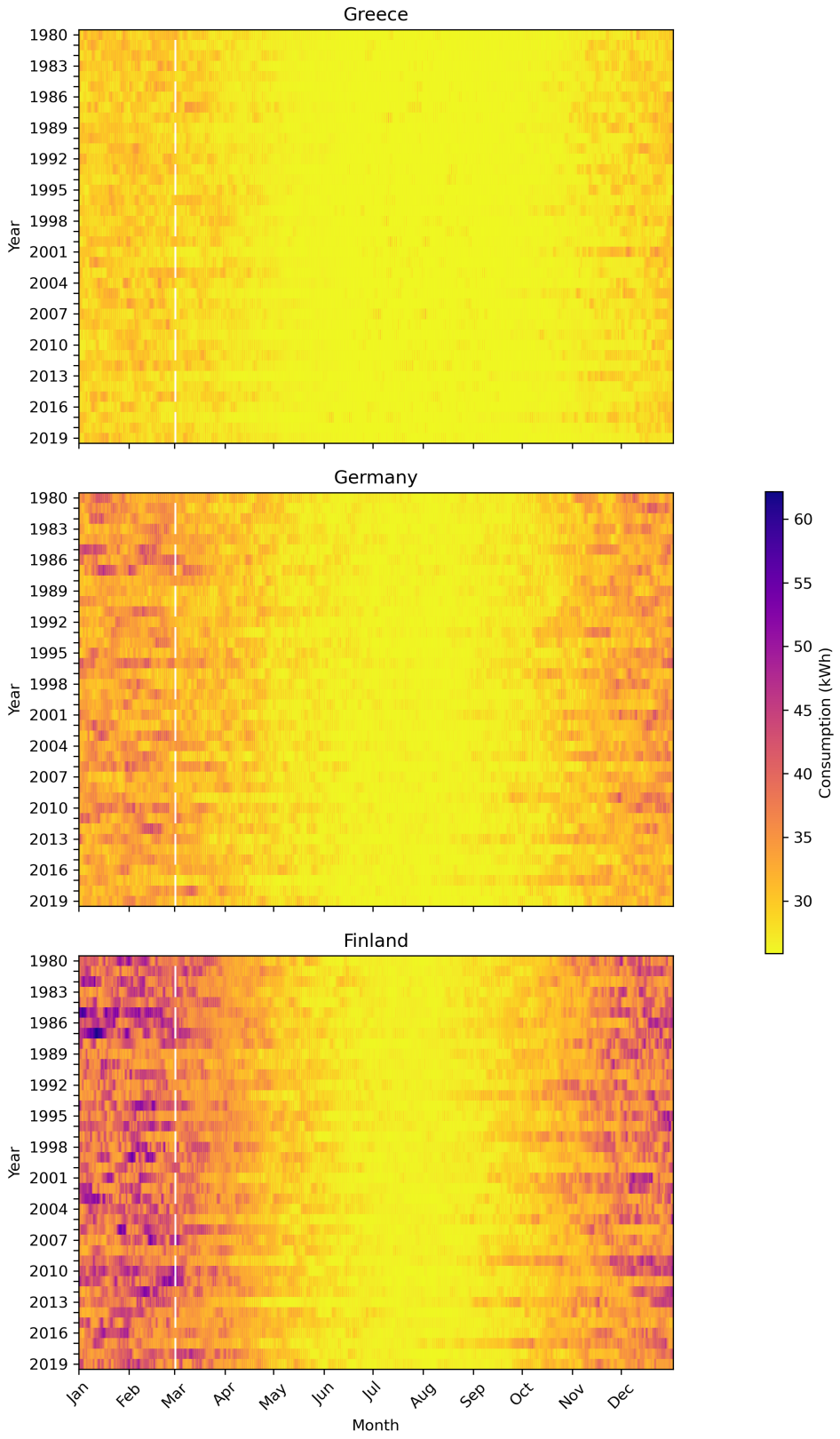

Figure 4.9: Hourly temperature effect on fuel cell electric vehicle consumption considering different weather years from 1980 to 2019. The color code identifies the level of consumption of the FCEV. reference vehicle: C-segment. Countries: Greece, Germany, and Finland. Reference driving cycle: WLTP.

Figures 4.10 and 4.11 present the inter-annual variability of the hourly temperatures and the corresponding energy consumption of the FCEVs for Finland, Germany, and Greece. Figure 4.10 presents the results for Greece, while in Figure 4.11, the results for Finland and Germany are shown. In each figure, the top panel shows the annual distribution of hourly temperatures, highlighting the coldest and the warmest year, whereas the bottom panel shows the distribution of hydrogen consumption in kWh/100km, with darker colors indicating higher mean annual consumption.

A key observation from these plots is that the years with the highest and the lowest mean temperatures do not always correspond to the lowest and the highest energy consumption, respectively. This happens because the entire temperature distribution, which includes the frequency and duration of weather extremes, plays a crucial role in defining the overall vehicle consumption. For example, one year with a short period of extreme cold can lead to higher overall hydrogen use than a year with a lower mean temperature but fewer frequent cold events.

This is more easily observed in Finland, where the extreme cold winters produce large fluctuations both in temperature and in consumption, which result in significant inter-annual variability. Germany presents similar but not so extreme patterns. In Greece, both temperature and consumption distributions are narrower and show smaller yearly variations, which reflects the milder climate conditions. However, the relationship between mean temperature and consumption remains non-trivial because of the influence of the impactful weather extremes.

In summary, these results show that it is important to consider both average climate conditions and frequency and intensity of temperature extremes when assessing the hydrogen demand of the FCEV performance across European countries. This variability must be considered to ensure the FCEVs can operate under different weather conditions reliably.

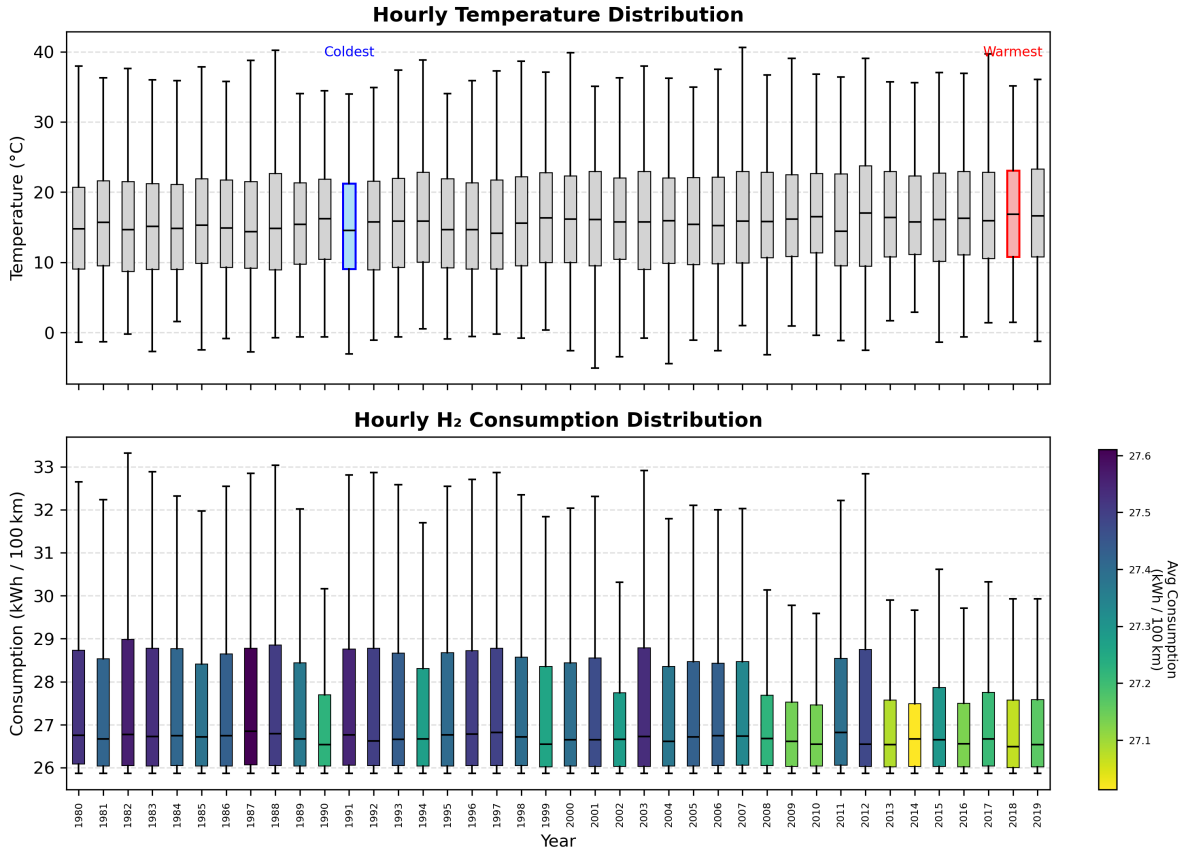

Figure 4.10: Hourly temperature (top) and hydrogen consumption (bottom) distributions for FCEVs in Greece, 1980–2019. C-Segment vehicles. Reference driving cycle: WLTP.

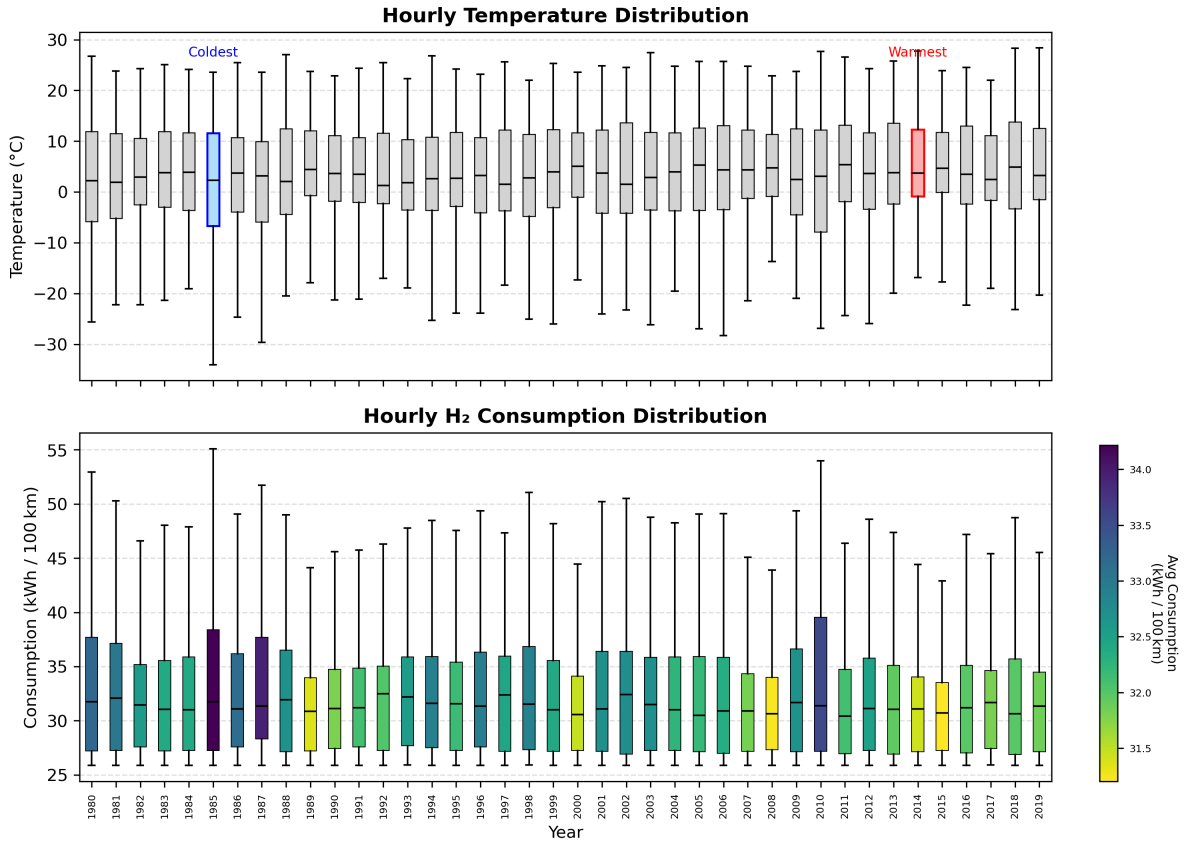

(a) Finland

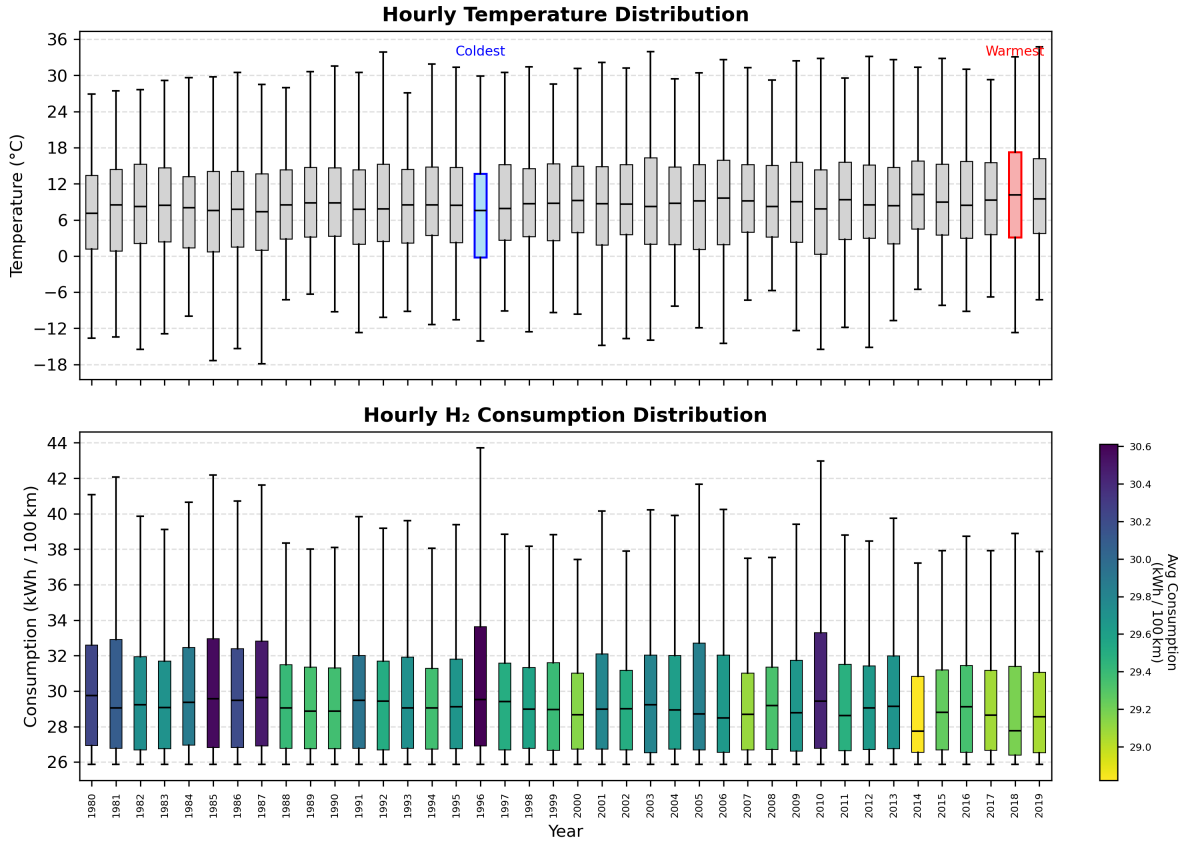

(b) Germany

Figure 4.11: Hourly temperature (top) and hydrogen consumption (bottom) distributions for FCEVs in (a) Finland and (b) Germany, 1980–2019. C-Segment vehicles. Reference driving cycle: WLTP.

To further highlight the impact of temperature variability on vehicles' energy demand, Figures 4.12, 4.13, and 4.14 present the seasonal consumption distributions for the three powertrain technologies for the three countries used as reference. Each panel shows the 100%, 90%, and 50% percentile bands of vehicle consumption (left) and ambient temperature (right) considering different weather years from 1980 to 2019. These percentile tiers show the frequency and the extremity of the temperature conditions that most strongly affect vehicle consumption.

Regarding FCEVs, Figure 4.12 reveals a seasonal pattern, with the strongest variability and highest consumption observed during the winter months, especially in northern climates, such as in Finland. This increased sensitivity to winter happens due to the significant energy demand for cabin heating, and results in wide percentile bands and a strong divergence between the 90th and 10th percentiles. As temperatures become more and more moderate during spring and summer months, both the median and the spread in consumption are decreased, but there are also extremely high values observed in summer due to the cooling demand, especially in warmer countries like Greece.

Comparing the FCEV to BEVs and ICEVs distributions, we see similar trends for the BEVs, with increased winter variability and bigger sensitivity to temperature extremes. In contrast, ICEVs present flatter consumption profiles, with minimal effect due to lower temperatures, because the engine's waste heat is used to warm up the cabin. However, there are some increases observed in consumption during periods with high ambient temperatures, mostly because of the cooling loads.

These results show that considering a constant efficiency for BEVs and FCEVs is not appropriate for weather years, as seasonal and inter-annual variability can cause significant fluctuations in energy consumption. Furthermore, temperature scenarios should be included alongside renewable energy source scenarios to be able to integrate hydrogen and electric vehicles in the energy system. The significant spread, which is observed during winter and the relative risk for high consumption peaks, suggests that there is a need for critical energy planning, especially in regions that face temperature extremes.

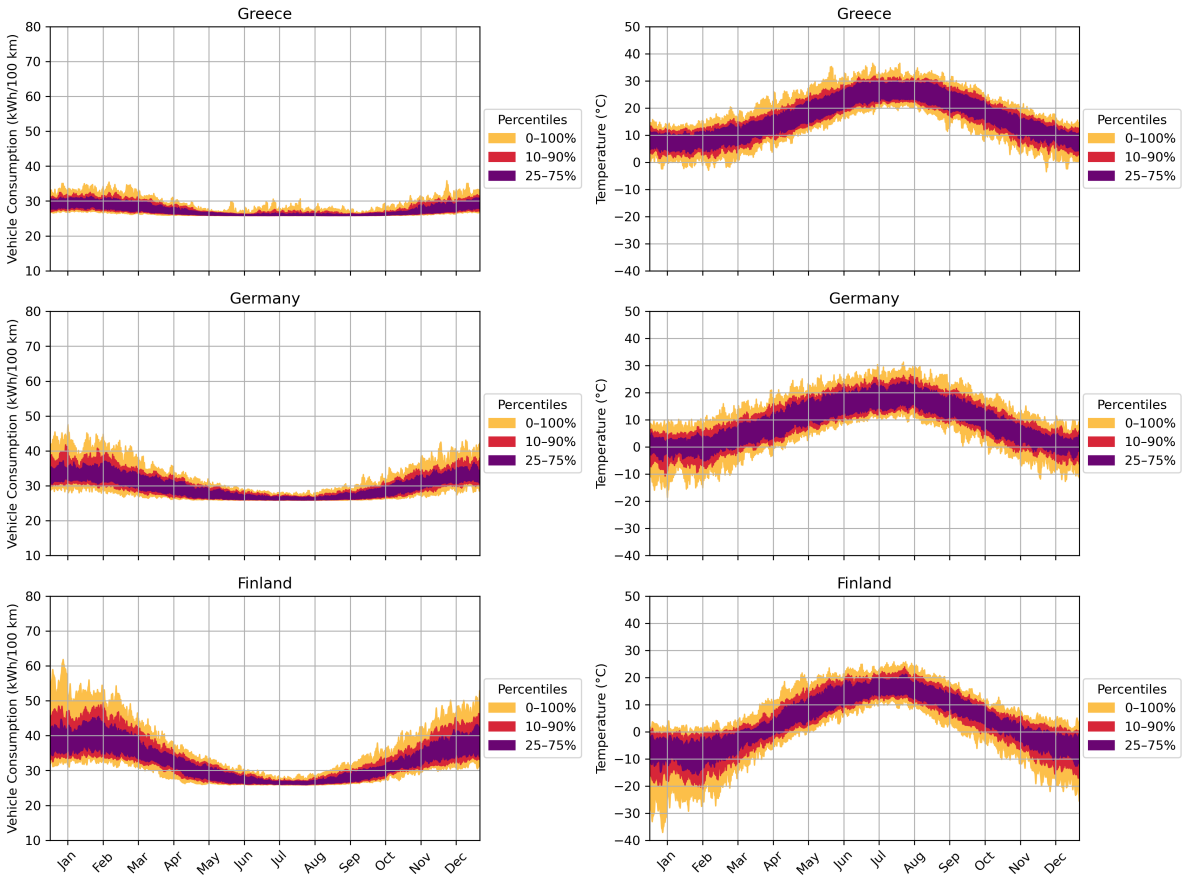

Figure 4.12: Hourly temperature variability (on the right) and hourly temperature effect (on the left) on fuel cell electric vehicle consumption considering different weather years from 1980 to 2019 (on the left). Temperature distribution according to the selected weather years. Colors identify the percentile of temperature occurrence. Driving cycle: WLTP. Reference vehicle: C-segment.

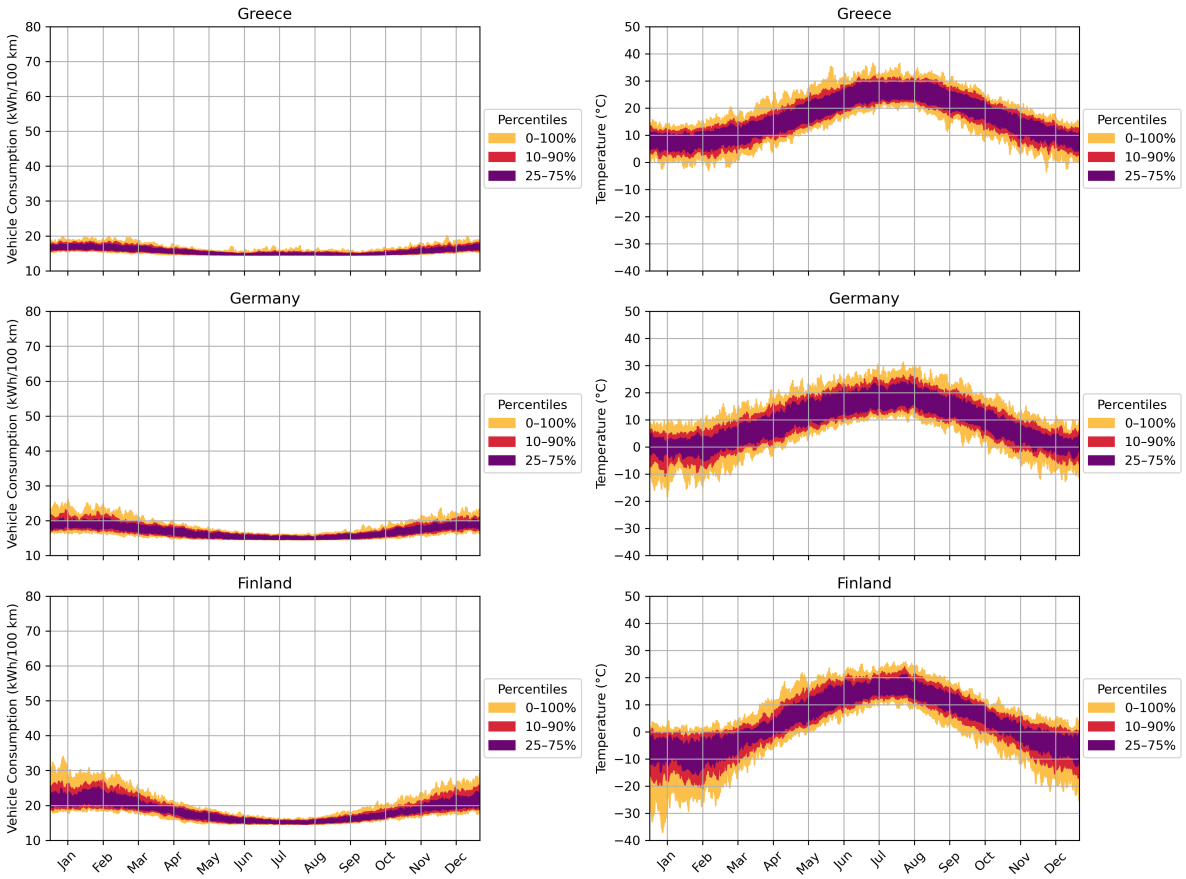

Figure 4.13: Hourly temperature variability (on the right) and hourly temperature effect (on the left) on battery electric vehicle consumption considering different weather years from 1980 to 2019 (on the left). Temperature distribution according to the selected weather years. Colors identify the percentile of temperature occurrence. Driving cycle: WLTP. Reference vehicle: C-segment.

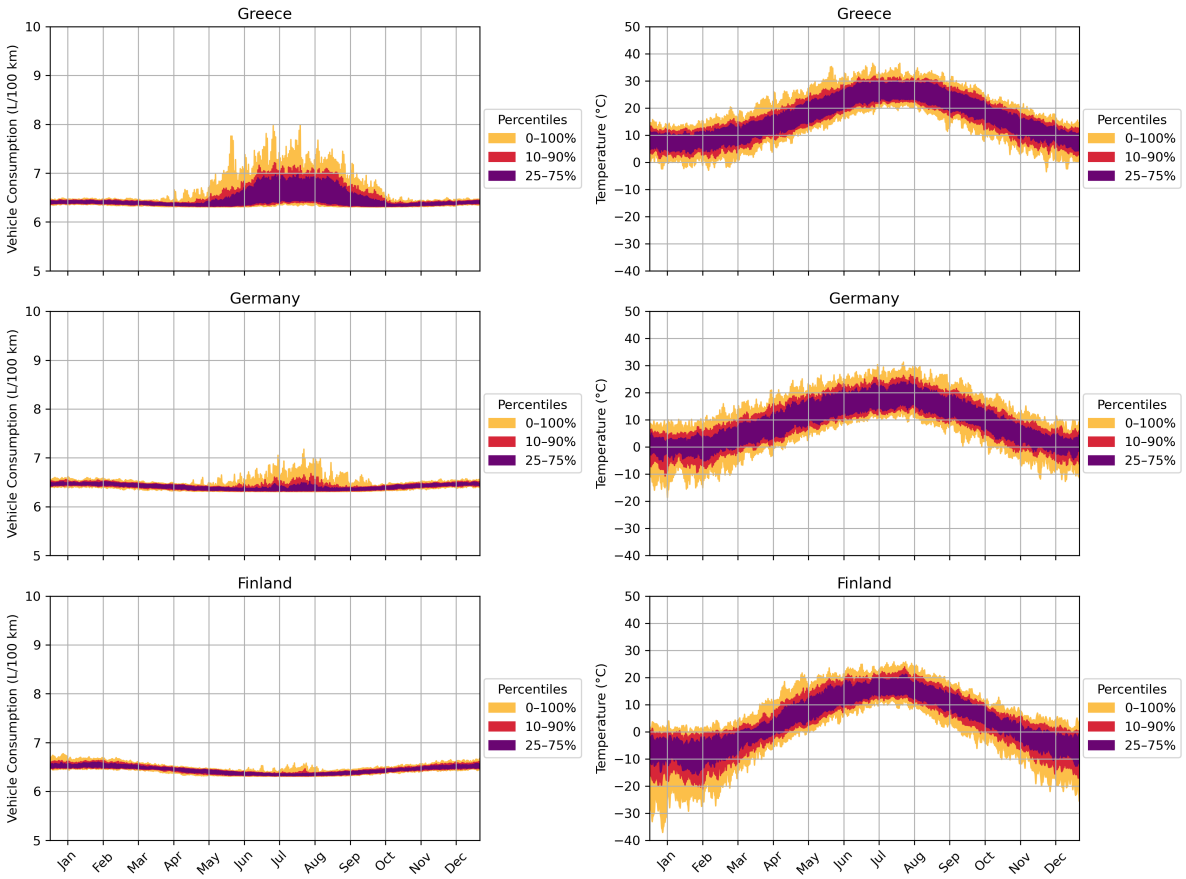

Figure 4.14: Hourly temperature variability (on the right) and hourly temperature effect (on the left) on internal combustion engine vehicle consumption considering different weather years from 1980 to 2019 (on the left). Temperature distribution according to the selected weather years. Colors identify the percentile of temperature occurrence. Driving cycle: WLTP. Reference vehicle: C-segment.

4.3. 2050 scenario analysis

Taking into consideration all the above, this thesis results chapter concludes by making a scenario analysis for the passenger vehicle energy demand in 2050. As already mentioned in Chapter 3, there are three temperature scenarios considered for 2050 according to ICCP, where the global temperature will rise by $1°C$, $1.4°C$, and $2°C$. Furthermore, according to the IEA, there are three policy scenarios for the powertrain technology mix. This sums up to nine scenarios in total, when considering the vehicle share between small, medium, and large cars remains stable over the years. The second part of the scenario analysis considers that there will be an annual growth in the sales of SUVs of about 1%, 1.5%, and 2% under the minimal temperature increase scenario, and the three powertrain mix scenarios. This brings a total of 18 scenarios for the analysis. It is important to note that three European countries are considered, the vehicle kilometers driven are assumed to remain steady, and the WLTP driving cycle has been used for the simulations.

4.3.1. Current passenger vehicle energy demand and future consumption projections

In order to be able to forecast the passenger car energy demand of Greece, Germany, and Finland, first, the energy demand in the current years is computed. Figure 4.15 shows this estimated energy demand for the three countries. As can be seen clearly from the graph, Greece and Finland have similar passenger car energy demand (around 27 TWh for Greece and 29 TWh for Finland), whereas Germany has more than 10 times this number, reaching 379 TWh. This shows that the impact of passenger vehicle electrification in larger countries like Germany, which need more energy, is expected to affect Europe's energy demand on a larger scale.

The European Commission, Joint Research Centre (2021) provides also estimations for the current passenger vehicle energy demand. According to this source, Greece's current passenger vehicle energy demand is 27.6 TWh, a number really close to the estimated one. Same applies for Finland, as the provided energy demand is about two TWh lower than the estimated one, standing at 26.2 TWh. Germany has the highest difference, as the European Commission suggests that the current passenger vehicle energy demand is 340 TWh, which means a 40 TWh offset from the modeled one.

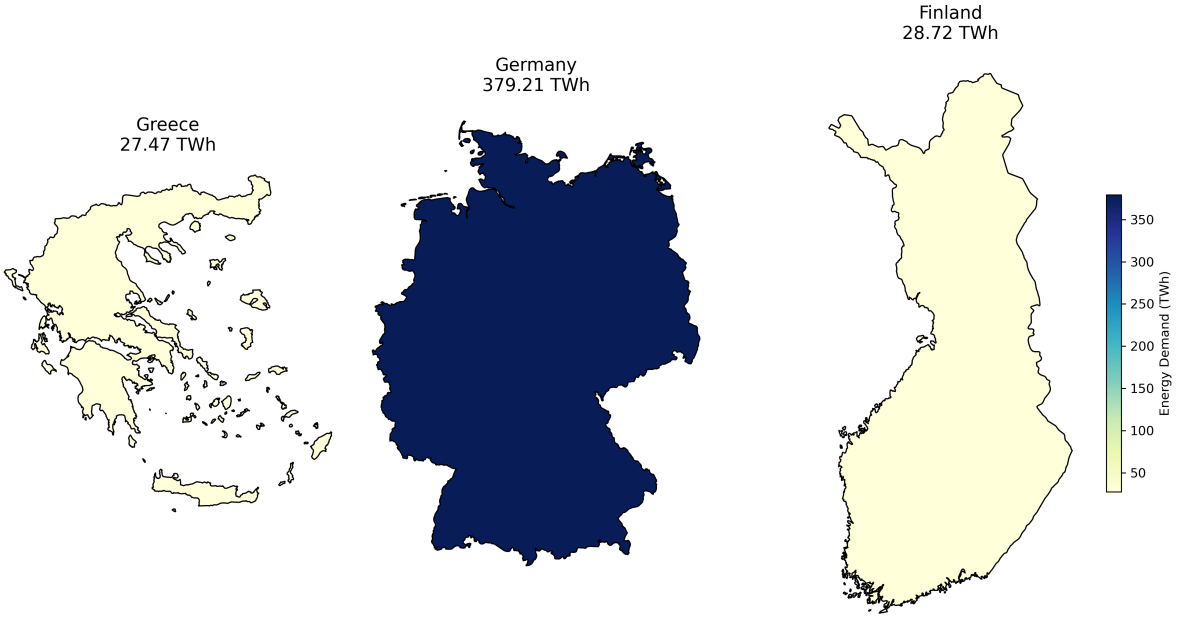

Figure 4.15: Passenger vehicle energy demand in three countries: Greece, Germany, and Finland. Reference driving cycle: WLTP.

In order to be able to predict the passenger car energy demand for 2050, a prediction for the consumption of BEVs, ICEVs, and FCEVs had to be made. In this analysis, it is assumed that there will not be any technological improvement in the powertrains, and their future consumption is computed solely by using the temperature increase that is expected to happen in each country. In order to make this projection, the 40-year period from 1980-2019 has been used, in order to first find a trend that has been followed during this period for the consumption. Figures 4.16 and 4.17 show the annual mean trends for consumption of FCEVs and temperature for Finland and Germany, respectively, whereas Figure 4.18 depicts the ones of Greece. As can be seen from the bottom panels, the temperature has been increasing during the last 40 years, which has the opposite effect on the consumption of FCEVs, since they are more efficient in milder temperatures. This effect is more significant for countries with cold extremes like Finland, where we can see that the historical trend for the consumption is -0.028 kWh/year, while in Germany the slope is about -0.019 kWh/year, and in Greece this drops down to -0.009 kWh/year.

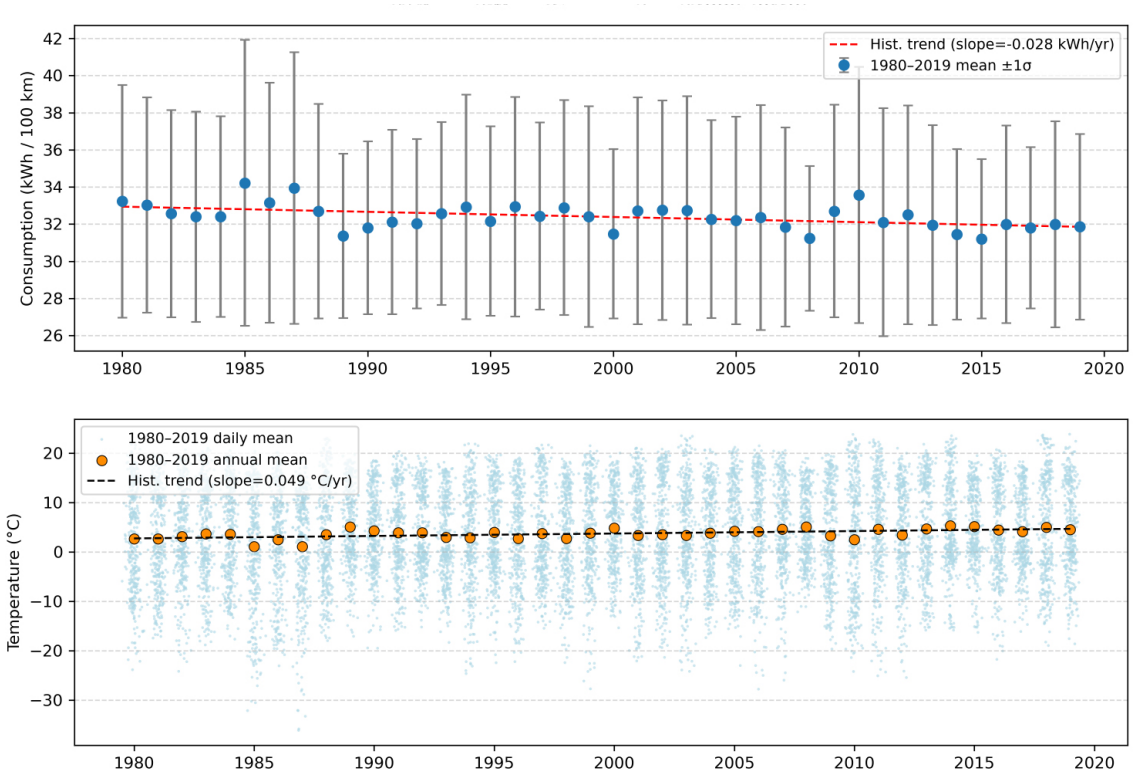

Figure 4.16: Finland: Annual mean consumption (top) and temperature (bottom) trends (1980–2019).

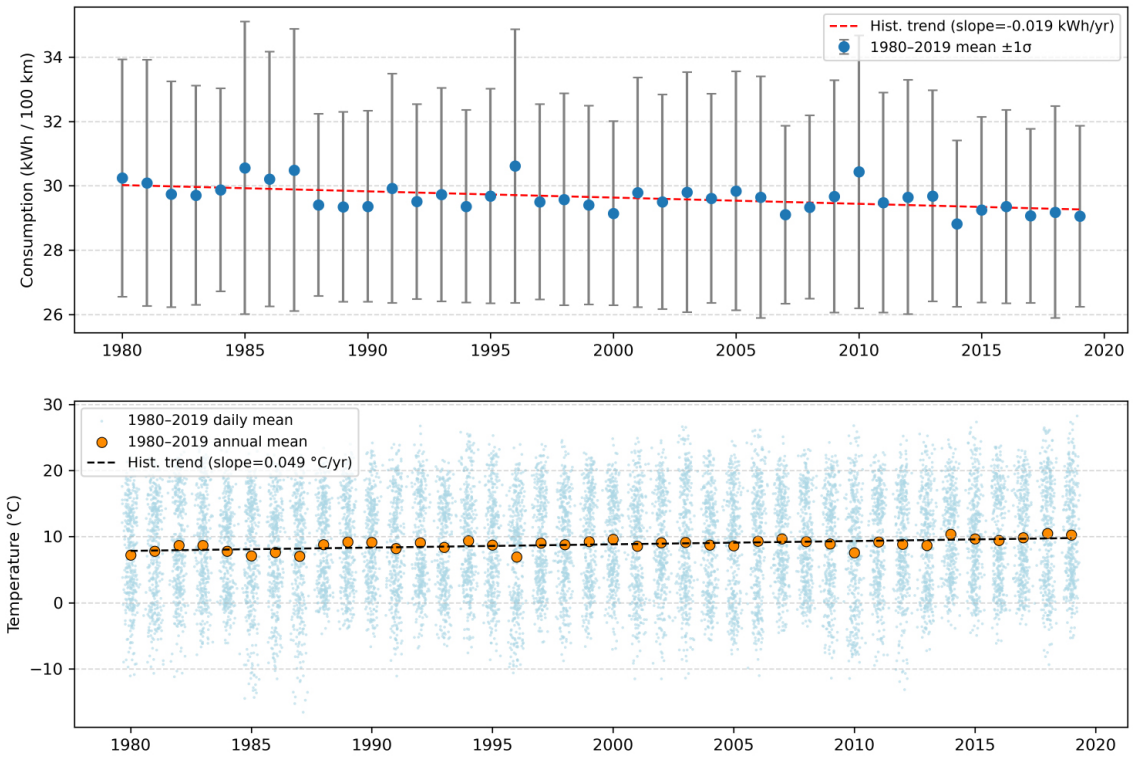

Figure 4.17: Germany: Annual mean consumption (top) and temperature (bottom) trends (1980–2019).

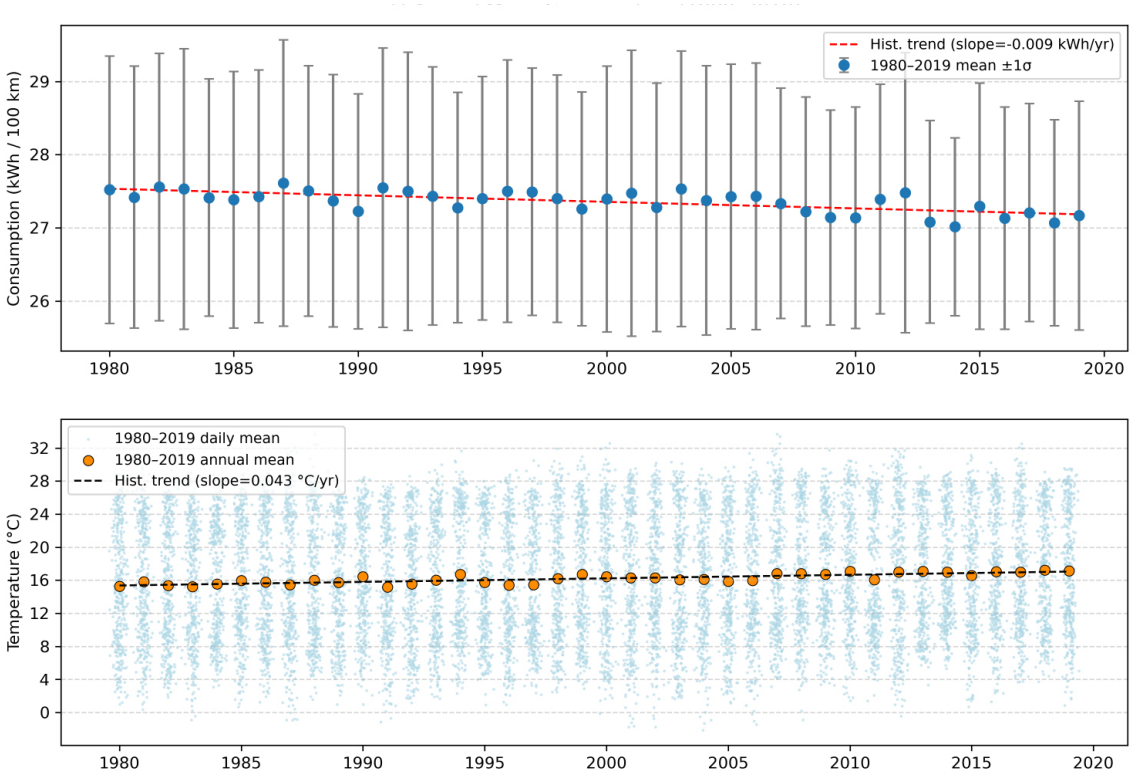

Figure 4.18: Greece: Annual mean consumption (top) and temperature (bottom) trends (1980–2019).

Now, using these trends and the projections for each region's temperature, a projection for the consumption of the FCEVs has been made for 2050. Figure 4.19 presents these projections for the FCEV energy consumption for the three countries. As can be seen clearly from the graphs, as the temperature increases under the different RCP scenarios, the consumption of FCEVs increases. For example, in Finland, the different RCPs are used to forecast a consumption of 31.27 kWh/100km under RCP2.6, 30.88 kWh/100km under RCP4.5, and 28.89 kWh/100km under RCP8.5, which results in a difference of 1.38 kWh/100km for the three scenarios. This difference is almost half in Germany at around 0.55 kWh/100km and even less in Greece, around 0.25 kWh/100km. This reflects the global warming effect in the different climate zones in Europe. This analysis has been made for all three segments of BEVs and ICEVs, and the relevant plots for the projection of the consumption can be found in Appendix A.

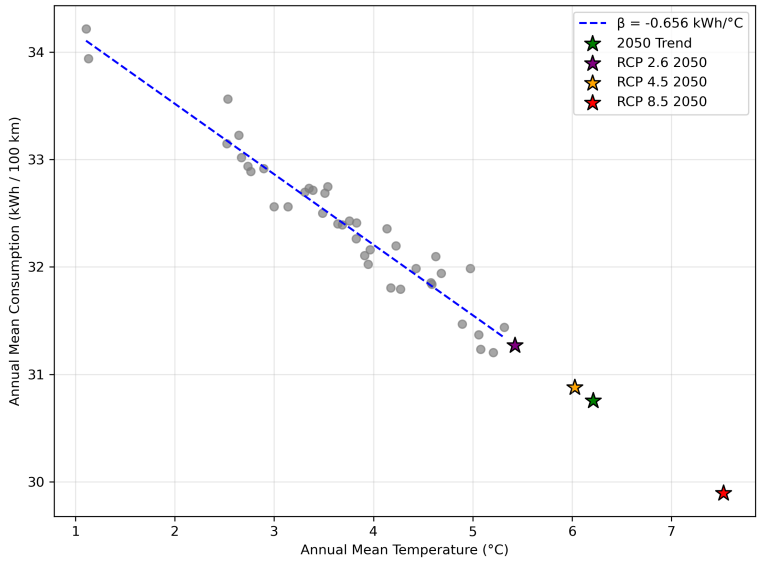

(a) Finland

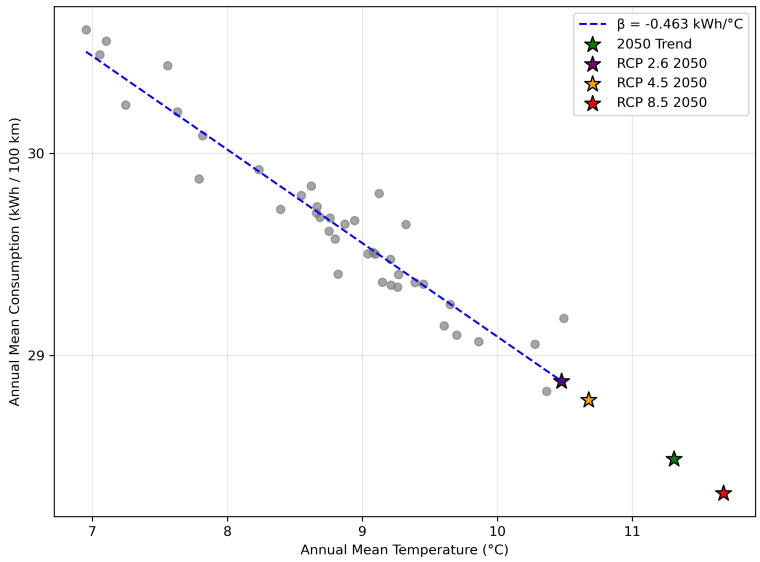

(b) Germany

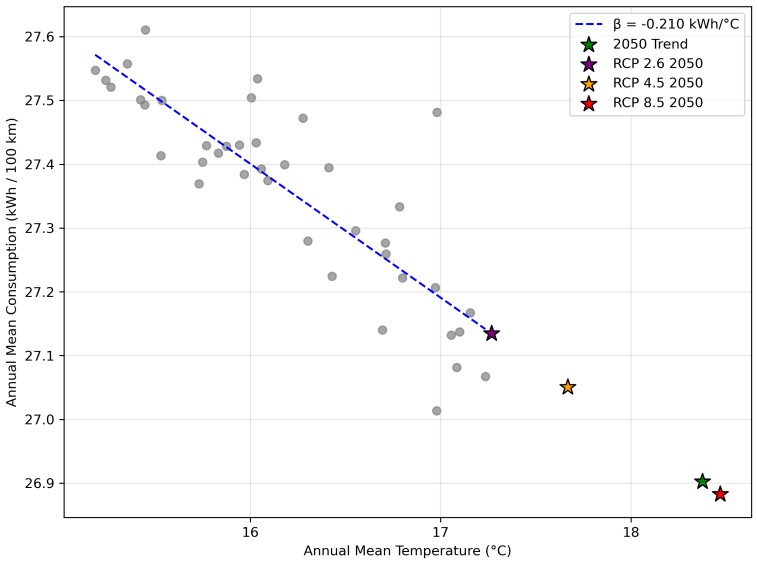

2

(c) Greece

Figure 4.19: Projected 2050 FCEV energy consumption vs. temperature under RCP scenarios for Finland, Germany, and Greece.

4.3.2. Passenger vehicle energy demand projections under different IEA policies and ICCP scenarios

These projections have been used in combination with the scenarios to estimate the average passenger vehicle energy demand in the three European countries in 2050. The first scenario analysis presented estimates the energy demand, while assuming that the vehicle share mix (small, medium, and large) remains steady throughout the years. The results are summarized in Table 4.2. Figure 4.20 presents the forecasted passenger vehicle energy demand for Greece for 2050 under the 9 scenarios.

The most significant source of variation in the energy demand comes from the IEA scenarios applied. To be more specific, under the STEPS scenario, the energy demand remains at the highest level, with values ranging from 11.316 to 11.363 TWh. This reflects a path with lower levels of electrification in the transport sector and only incremental policy progress. In comparison with the aforementioned, the SDS scenario produces lower demand levels, around 9.832 to 9.893 TWh, which reflects the stronger policies and regulations applied and the accelerated adoption of electric vehicles. The NZE scenario predicts an energy demand of around 8.866 to 8.934 TWh, as it assumes that deep decarbonization of the sector will happen.

The influence of the climate pathways (RCPs) on passenger car energy demand is evident but comes secondary to the one of the transport policies. Within the different IEA scenarios, the variation in RCPs produces only a small decrease in energy demand, of around 30-70 GWh. The relationship observed is inverse, and it reflects the impact of ambient temperature in vehicle energy use, especially for cabin heating needs.

Across the total scenario range the projected energy demand in Greece in 2050 varies between 11.4 TWh (STEPS, RCP2.6) and 8.8 TWh (NZE, RCP8.5), which means a nearly 2.5 TWh spread. This variation suggests that the policies followed play a significant role in forming the long-term energy demand. On the other hand, the effect of climate change on consumption is relatively mild, but consistent across policy cases.

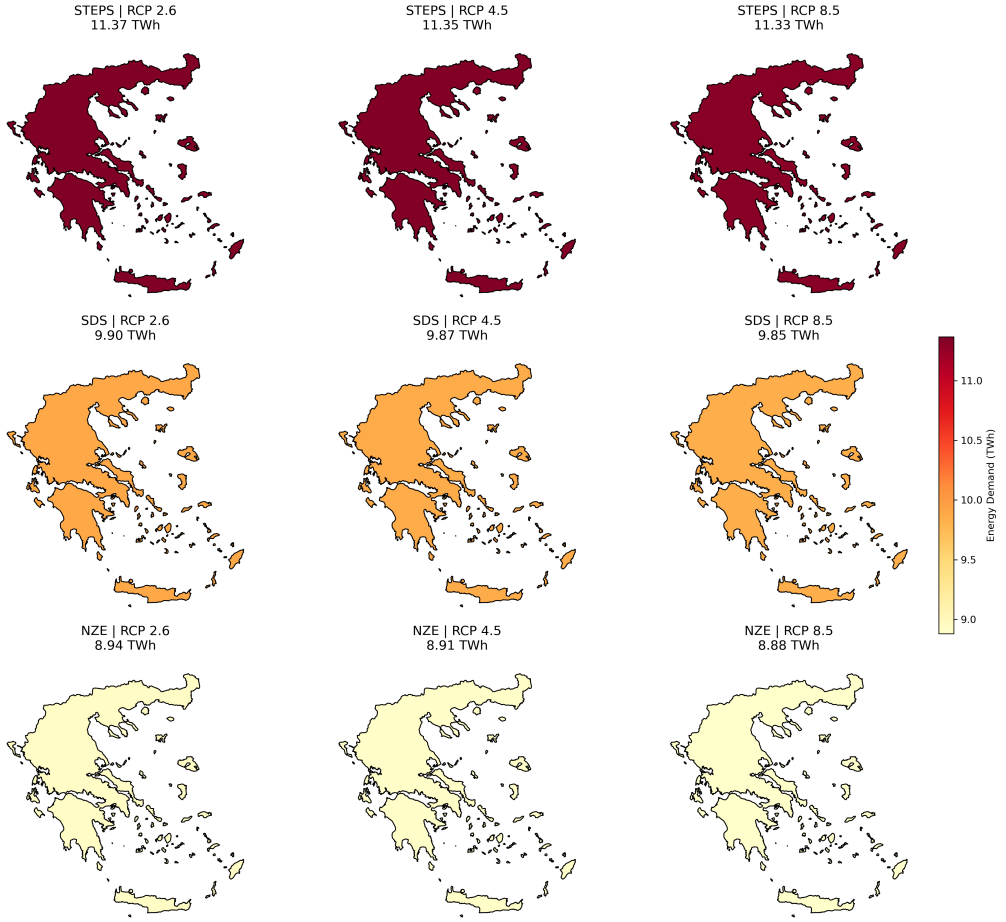

Figure 4.20: Projected passenger vehicle energy demand in Greece in 2050, under three IEA scenarios (STEPS, SDS, NZE) and three IPCC RCPs (2.6, 4.5, 8.5).

Figure 4.21 presents projections of total passenger vehicle energy demand in Germany for the year 2050 under the 9 scenarios defined by the three IEA policies and the three climate futures. In general terms, Germany's projected energy demand is significantly higher than that of Greece, with national totals ranging between around 129 TWh and 164 TWh. reflecting the larger population, the increased vehicle stock, and the more extensive travel demand. The fluctuation between the IEA policy scenarios represents the majority of this range. Under the STEPS scenario, the demand is above 161 TWh in all climate scenarios, whereas under the NZE scenario, it falls to approximately 130 TWh. This means a 30 TWh deviation, which reflects the impact of the energy transition and decarbonization strategies that will be followed.

The role of global warming is also evident in the figure. The temperature rising under the RCP scenarios produces a mild reduction in energy use of around 1-2%, for each policy case. This effect is more evident in Germany than in Greece, because of the colder climate baseline and the larger proportion of energy used in passenger vehicles. However, the climate's influence on interaction with vehicle powertrain technology brings a more significant influence at scale. For example, under the NZE-RCP8.5 scenario, Germany's passenger transport demand is approximately 35 GWh lower than under the NZE-RCP2.6 scenario.

In contrast to the case of Greece, Germany's larger thermal gradient makes the country a more interesting candidate to examine the climate-related shifts in seasonal vehicle energy consumption, but it remains clear that the policies play the most important role in determining the long-term energy consumption.

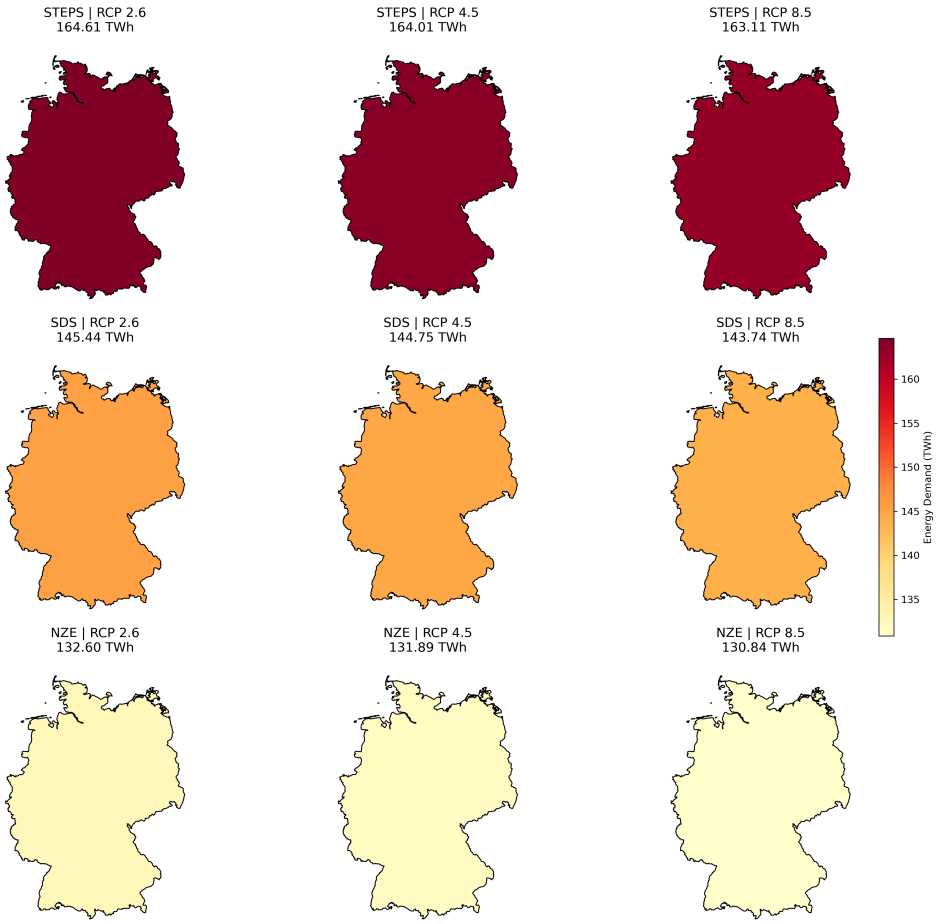

Figure 4.21: Projected passenger vehicle energy demand in Germany in 2050, under three IEA scenarios (STEPS, SDS, NZE) and three IPCC RCPs (2.6, 4.5, 8.5).

Figure 4.22 illustrates Finland's passenger vehicle energy demand in 2050 under the 9 scenarios mentioned previously. In contrast to the larger energy totals of Germany, Finland's absolute demand values are lower, ranging between 10.1 TWh and 12.8 TWh across the different scenarios. This is because of the country's smaller vehicle stock and population. However, Finland shows the most significant variation in projected demand due to climatic factors.

A clear deviation is observed both in the IEA policy axis and in the RCP scenario axis. The energy demand is significantly reduced from STEPS to SDS and to NZE, according to the decarbonization policy ambitions. For example, in STEPS the demand remains at around 12,500 - 12.8 TWh, whereas transitioning to SDS lowers these numbers by around 1.3 - 1.5 TWh, and transitioning to NZE makes a final total of around 10.1 - 10.5 TWh. These values reveal a decline of around 20% of the business-as-usual path.

What differentiates Finland from Germany and Greece is the relative strength of the RCP effect. For each IEA policy scenario, warmer climates consistently produce lower energy demand. The difference between RCP2.6 and RCP8.5 ranges between 200 GWh and 400 GWh, depending to the policy scenario. These differences are more evident than in Greece and slightly larger than in Germany, showing the sensitivity of vehicle energy demand to ambient temperature conditions. Given Finland's long winter periods, heating requirements increase the consumption, and as the climate warms under RCPs, the reduction in this heating demand results in a larger decrease in energy use. This finding further reflects the importance of accounting for regional climatic baselines when evaluating climate mitigation impacts.

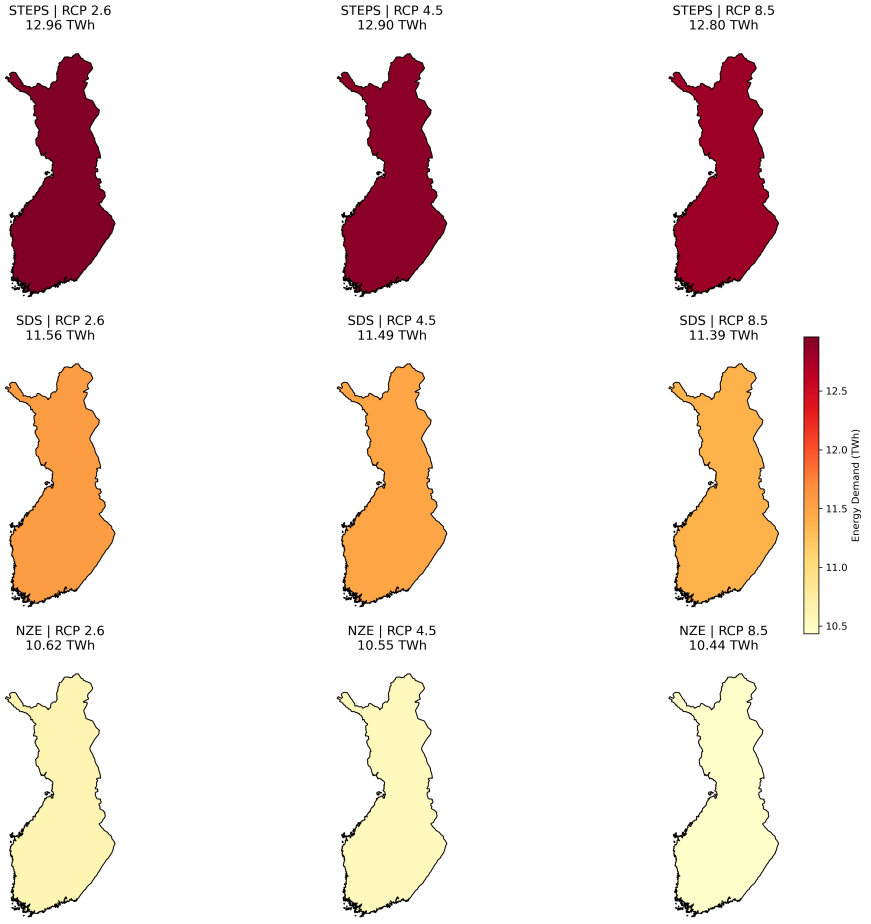

Figure 4.22: Projected passenger vehicle energy demand in Finland in 2050, under three IEA scenarios (STEPS, SDS, NZE) and three IPCC RCPs (2.6, 4.5, 8.5).

Table 4.2: Projected passenger□vehicle energy demand in 2050 (TWh) and percentage reduction from 2019 levels, using both the estimated 2019 baselines and the JRC IDEES 2021 baselines.

Scenario	RCP	Greece	Germany	Finland
STEPS	RCP 2.6	11.36 (–58.6% / –58.8%)	163.61 (–56.9% / –51.9%)	12.85 (–55.3% / –51.0%)
	RCP 4.5	11.35 (–58.7% / –58.9%)	163.31 (–56.9% / –52.0%)	12.76 (–55.6% / –51.3%)
	RCP 8.5	11.32 (–58.8% / –59.0%)	161.81 (–57.3% / –52.4%)	12.52 (–56.4% / –52.2%)
SDS	RCP 2.6	9.89 (–64.0% / –64.2%)	144.31 (–62.0% / –57.6%)	11.44 (–60.2% / –56.3%)
	RCP 4.5	9.87 (–64.1% / –64.2%)	143.97 (–62.0% / –57.6%)	11.33 (–60.6% / –56.7%)
	RCP 8.5	9.83 (–64.2% / –64.4%)	142.27 (–62.5% / –58.2%)	11.07 (–61.5% / –57.7%)
NZE	RCP 2.6	8.93 (–67.5% / –67.6%)	131.43 (–65.3% / –61.3%)	10.49 (–63.5% / –60.0%)
	RCP 4.5	8.91 (–67.6% / –67.7%)	131.08 (–65.4% / –61.4%)	10.38 (–63.9% / –60.4%)
	RCP 8.5	8.87 (–67.7% / –67.9%)	129.31 (–65.9% / –62.0%)	10.11 (–64.8% / –61.4%)

4.3.3. Passenger vehicle energy demand projections under SUV growth scenarios

For the second part of this scenario analysis, passenger vehicle energy demand in 2050 is estimated assuming a steady annual growth rate in SUVs. Different scenarios have been made according to the current sales trend for 1%, 1.5%, and 2% growth. For this analysis, the shares of small and medium cars have been proportionally decreased. The 9 scenarios presented consider the three different percentages of growth rates and the three IEA policy scenarios under RCP 2.6. The results are summarized in Table 4.3.

Figure 4.23 illustrates the expected passenger vehicle energy demand in Greece in 2050 for the different SUV growth rates. As it can be seen clearly from the graph, the increasing penetration of SUVs significantly increases the energy demand across all different policies. According to STEPS scenario, which reflects low electrification, the energy demand increases from 12.6 TWh with 1% SUV growth to 13.8 TWh with 2% growth, which means a relative increase of around 10%. Even according to the ambitious NZE scenario, which leads to decarbonization, the expected energy demand increases from 9.7 TWh to 10.6 TWh, around 8.5%.

This reflects the importance of the vehicle type composition when shaping national energy use, even under transformative policy scenarios. The relatively high sensitivity of the energy demand to the SUV market sales reflects their low efficiency in real-world conditions in comparison with smaller vehicle segments. Moreover, the absolute demand differences between IEA scenarios remain larger than the differences caused by the SUV growth rate alone. For example, at 1.5% growth, demand increases from 13.2 TWh in STEPS to 10.2 TWh in NZE, a decrease of around 23%, compared to the approximately 9% variation which is caused by SUV growth under a certain policy.

This shows the need to coordinate vehicle electrification with polices that target vehicle downsizing. Without measures like these, the benefits of decarbonization could be significantly reduced by shifts in the vehicle fleet that would drive the energy demand upward, even as emissions decline.

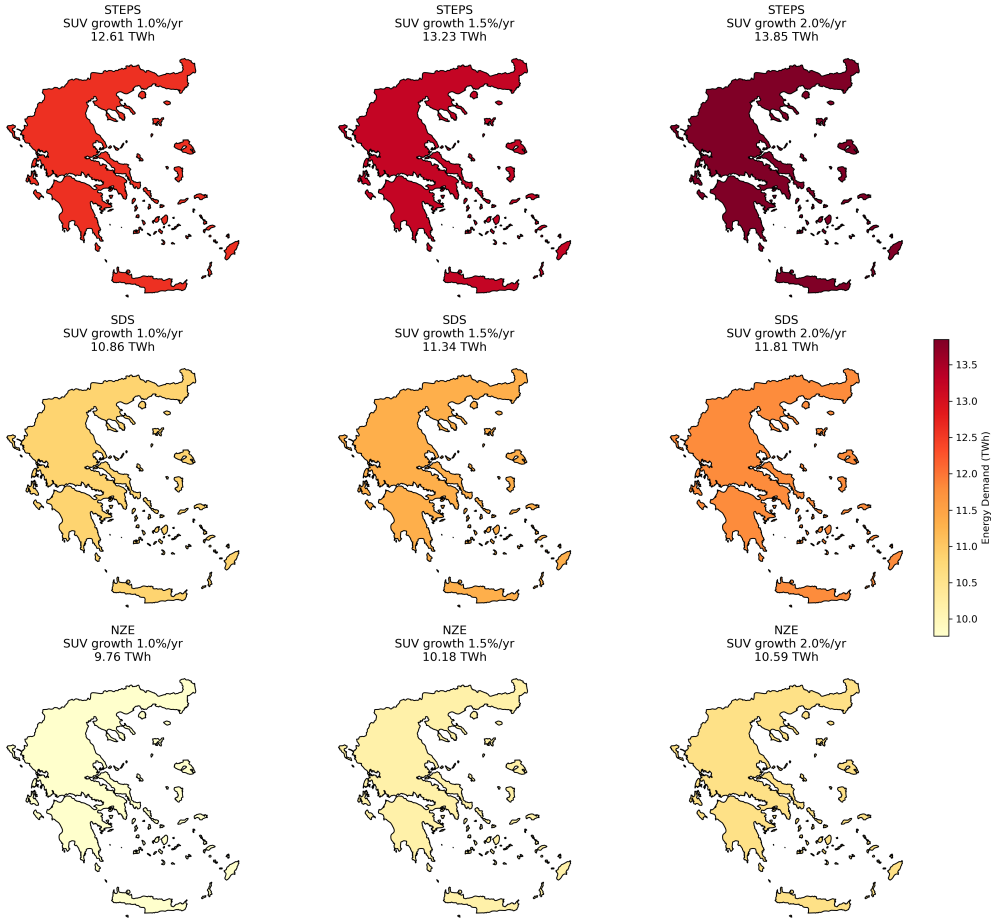

Figure 4.23: Projected passenger vehicle energy demand in Greece in 2050 under three IEA policy scenarios (STEPS, SDS, NZE) and varying SUV market growth rates (1.0%, 1.5%, and 2.0% annually), assuming RCP 2.6 climate conditions.

Figure 4.24 shows how projected passenger vehicle energy demand in Germany responds to varying SUV growth rates. As depicted in the Figure, across all policies, the increased penetration of SUVs in the market leads to increasing energy demand. According to the STEPS scenario, the demand is increased from 181.5 TWh to 199.3 TWh, which means around 10%. Similar results come from the other two scenarios, SDS and NZE, with increases of 8.8% and 8.4% respectively.

Because of Germany's larger vehicle fleet and higher mobility, these percentage shifts mean important absolute differences, which can reach up to 17.8 TWh within a single scenario. Compared to Greece, the energy impact of SUVs growth in Germany is significant in scale, though similar in relative terms.

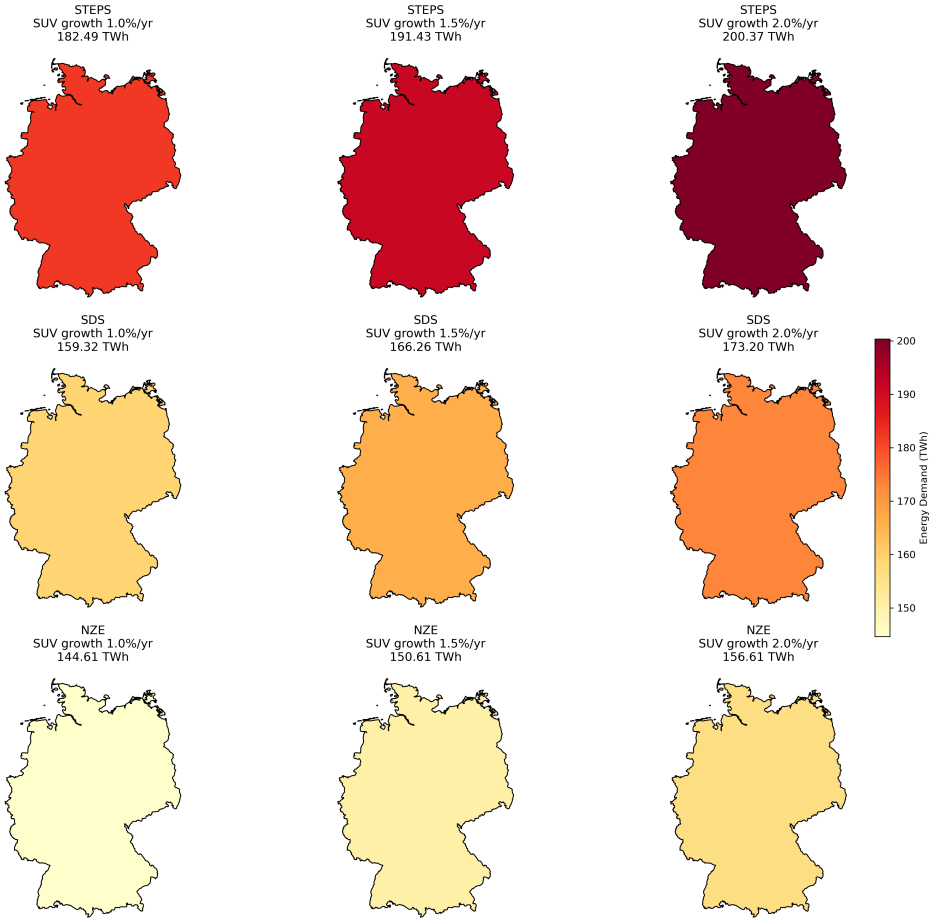

Figure 4.24: Projected passenger vehicle energy demand in Germany in 2050 under three IEA policy scenarios (STEPS, SDS, NZE) and varying SUV market growth rates (1.0%, 1.5%, and 2.0% annually), assuming RCP 2.6 climate conditions.

Figure 4.25 presents the results for the SUV growth scenario for Finland under the different IEA scenarios. As in the other countries, the SUV penetration leads to consistent rises in energy demand. Under the STEPS scenario, demand increases from 14.1 TWh to 15.4 TWh (+9.3%), under the SDS demand increases from 12.4 TWh to 13.5 TWh (+8.1%) and under the NZE demand increases from 11.4 TWh to 12.2 TWh (+7.7%). While percentage increases are comparable to those of Germany and Greece, the absolute impact is smaller due to the country's low baseline mobility. Nonetheless, taking into account Finland's long winters and higher heating energy demands, the cumulative event of heavier, less efficient vehicles remains non-negligible.

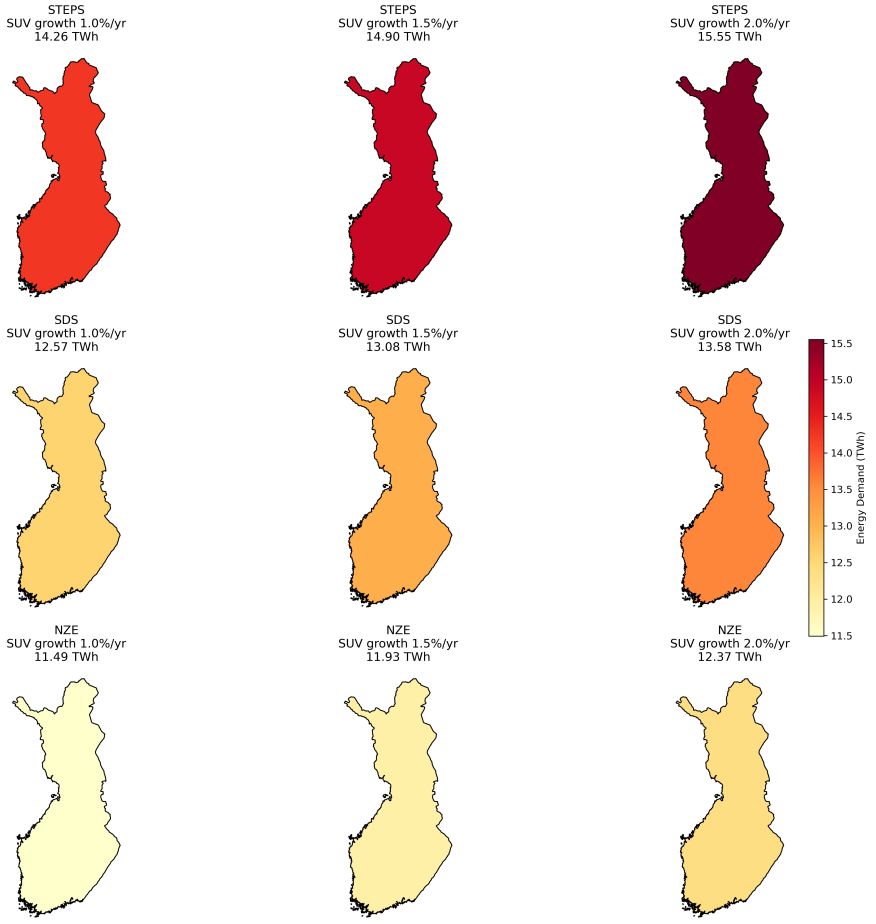

Figure 4.25: Projected passenger vehicle energy demand in Finland in 2050 under three IEA policy scenarios (STEPS, SDS, NZE) and varying SUV market growth rates (1.0%, 1.5%, and 2.0% annually), assuming RCP 2.6 climate conditions.

Table 4.3: Projected 2050 passenger vehicle energy demand (TWh) under RCP 2.6 for varying SUV growth rates, with dual percentage reductions relative to the estimated 2019 baselines and the JRC IDEES 2021 baselines.

Scenario	SUV growth	Greece	Germany	Finland
STEPS	1.0%	12.61 (–54.1% / –54.3%)	181.46 (–52.2% / –46.6%)	14.11 (–50.9% / –46.1%)
	1.5%	13.23 (–51.9% / –52.1%)	190.38 (–49.8% / –44.0%)	14.79 (–48.5% / –43.5%)
	2.0%	13.85 (–49.6% / –49.8%)	199.30 (–47.4% / –41.4%)	15.43 (–46.3% / –41.1%)
SDS	1.0%	10.85 (–60.5% / –60.7%)	158.16 (–58.3% / –53.5%)	12.45 (–56.7% / –52.5%)
	1.5%	11.33 (–58.7% / –58.9%)	165.09 (–56.5% / –51.4%)	12.95 (–54.9% / –50.6%)
	2.0%	11.81 (–57.0% / –57.2%)	172.01 (–54.6% / –49.4%)	13.45 (–53.2% / –48.7%)
NZE	1.0%	9.76 (–64.5% / –64.6%)	143.40 (–62.2% / –57.8%)	11.36 (–60.5% / –56.6%)
	1.5%	10.17 (–62.9% / –63.2%)	149.39 (–60.6% / –56.1%)	11.80 (–58.9% / –55.0%)
	2.0%	10.59 (–61.5% / –61.6%)	155.38 (–59.0% / –54.3%)	12.23 (–57.4% / –53.3%)

5

Discussion

5.1. Interpretation of the main findings

This thesis investigated the effect of powertrain technologies, vehicle characteristics, and ambient weather conditions on the passenger vehicle energy demand in Europe. The enhanced VCAM tool allowed the simulation for BEVs, FCEVs, and ICEVs in various vehicle segments and European regions.

The findings confirm the ambition that BEVs are the most energy-efficient powertrain technology under standard conditions. However, their consumption and range are sensitive to temperature, especially under below-zero temperature conditions. At -20 degrees Celsius, BEVs presented an increase in consumption of around 80%, in comparison with their optimal consumption, significantly reducing their autonomy. This confirms and extends the observations previously made from empirical studies, such as the DOE and NAF reports, revealing the thermal limitations of battery and heating systems.

FCEVs presented the most stable thermal behavior, but with their increased baseline energy consumption as a cost. Because modern BEVs and FCEVs typically offer comparable ranges on a single charge or fill, the biggest benefit of FCEVs in cold or hot climates is this lower percentage drop in efficiency.

ICEVs showed low sensitivity to temperature during winter because of the availability of waste heat, but had low performance under extreme hot conditions, when the HVAC and engine cooling loads increased the energy use. Under all climate conditions, ICEVs remained the least efficient technology, supporting the policies that suggest their phase-out.

Vehicle segment analysis showed a steady increase in consumption as vehicle size increases. This effect was bigger in BEVs and FCEVs under extreme temperature conditions due to higher HVAC loads and auxiliary power needs. These results highlight the importance of vehicle downsizing as a possible policy design.

Regarding the different regions, the simulations showed that the climate diversity shapes the different national energy demand standards. Finland. where long and harsh winters are experienced, presented a peak seasonal demand of more than 30% of that of Greece. The scenario analysis showed that while policy interventions play the most important role in shaping the future passenger vehicle energy demand, the effects of vehicle fleet composition and global warming are still notable.

In summary, the findings suggest the need for regional and temperature-oriented energy planning towards the decarbonization of the passenger transport sector. The efficiency gains of the sector's electrification can be undermined by poor vehicle performance, vehicle sales trends, or poor climatic adaptation.

5.2. Comparison with literature

The findings of this thesis are broadly consistent with existing literature on vehicle energy modeling, especially in relation to climate sensitivity, fuel cell electric vehicle performance, and the broader system

implications of electric vehicle demand.

Various European studies confirm that BEVs are particularly sensitive to the ambient temperature variations. M. Al-Wreikat et al. (2022) showed that when the temperature drops from $25\,^{\circ}\mathrm{C}$ to $0\,^{\circ}\mathrm{C}$ BEV range can decrease by 28%, mainly because of the increased HVAC loads and battery inefficiency. Similarly, Bicer et al. (2023) observed that energy consumption can increase by up to 40% in below-zero conditions based on real-world data. This thesis confirms these findings by using 40 years of climate data in three European countries and showing that seasonal and regional temperature variations lead to big variations in BEV energy demand. In contrast with many previous studies that evaluate only static or ideal testing conditions, this thesis offers a more dynamic and regionally detailed perspective.

Regarding FCEVs, this research contributes to a less explored sector. While many modeling tools exclude hydrogen vehicles or oversimplify them, this thesis integrates detailed thermal and operational modeling. Hydrogen Insight (2024) reports that in very cold climates (e.g., $-6\,^{\circ}\mathrm{C}$ in Québec) FCEVs can show significant consumption increases up to 40%. This thesis expands this knowledge by systematically comparing FCEV performance across different climate zones and driving cycles in Europe.

From a system perspective, the results underline the importance of accurate EV demand modeling in order to plan the electricity system. The thesis supports the conclusions of International Council on Clean Transportation (ICCT) (2024), which highlight that smart charging and vehicle-to-grid strategies can offer significant grid flexibility, especially for handling peak loads. However, it also addresses more extreme challenges, such as the “Dunkelflaute” phenomenon, where low wind and solar availability during winter can severely constrain supply. As highlighted by Energy Central (2024), failing to accurately model EV load during these periods can lead to a significant underestimation of system stress, especially in regions that are highly dependent on imports or lack storage. Including FCEVs in this context adds another layer of value, as they offer the possibility to geographically transfer electricity demand by producing hydrogen in uncongested regions.

Overall, this thesis not only confirms many of the already existing observations but also expands the literature by offering a long-term, geographically differentiated modeling of passenger vehicle energy demand under realistic European conditions. It connects the detailed vehicle performance analysis to energy system planning, contributing to bridging the gap between transport models and infrastructure investment strategies.

5.3. Implications

The results of this thesis have several important implications for energy system planning, transport policy, and sustainable mobility strategies. Besides the validation of already known trends, this thesis offers new, applicable insights that can inform the way in which the electrification strategies are formed.

First, it is worth noting that efficiency is not enough without thermal robustness, which is the ability to keep the range up when temperatures stray far from 20 degrees Celsius. While BEVs outperform all other powertrains under optimal conditions, they suffer up to 80% range loss in extreme cold, in the worst case scenario, making temperature sensitivity a limiting factor in their wide adoption.

Second, it is important to keep in mind that vehicle size can seriously undermine decarbonization. Proliferation of SUVs significantly offsets the efficiency gain from electrification. Even with the adoption of the most ambitious policy scenarios, such as NZE, the SUV growth of only 1.5% can increase the national energy demand by 8-10% in 2050, which in scale has a crucial impact on the demand. Downsizing polices are necessary to avoid falling back on climate goals.

Third, although FCEVs are not the absolute winner in raw consumption, they can play crucial roles that BEVs struggle to. By pairing a relatively small battery with a hydrogen fuel cell stack, FCEVs reduce the need for really large batteries, thus reducing vehicle cost, weight, and charging footprint. At the same time, they refuel in a few minutes and maintain long ranges, making them suitable for heavy-duty transportation, where BEVs requirements for battery size and charging time can be prohibitive. Furthermore, because FCEVs use only modest power for on-board battery charging, they help to decongest the grid and the public fast-charging infrastructure, helping to smooth peak electricity demand as vehicle electrification emerges.

Last, it is important to note that while warming climates may slightly reduce the vehicle energy use, this passive effect cannot substitute for transitioning to efficient powertrains. Decarbonization is driven by policies and not by temperature alone. Relying on future warming to reduce energy demand creates the risk of having a false sense of progress. Robust transitions towards more efficient powertrains and smart fleet management strategies should remain a priority to decarbonize the sector.

5.4. Limitations of the study

Despite its contributions, this study has several limitations, mainly related to the assumptions made and the available data. First, the simulation of fuel cell electric vehicles was limited by the availability of actual power split strategies, as the current FCEV algorithm did not consider a dynamic or variable power split, but static options were used. This thesis followed a fixed power split strategy based on the literature. A more robust approach could involve an optimization technique to determine the ideal power split control strategy under various constraints, thereby reducing the modeling error.

Second, the FCEV modeling used a system efficiency to represent the entire fuel cell system. Incorporating each component of the fuel cell system with its specific efficiencies could enhance the accuracy of the simulations, especially under high-load or extreme temperature scenarios. Third, because of the lack of FCEV HVAC performance data, the thermal modeling has been based on BEV performance. Although this provides a reasonable approximation, it introduces an error during temperatures when the HVAC system is turned on. This is also depicted in the validation results, where the error with the HVAC system turned on can reach 10-13%. Additionally, the number of validated FCEV configurations was limited. The lack of sufficient experimental data restrained the ability to generalize findings for all FCEV types.

Finally, the use of the WLTP driving cycle for the scenario analysis introduces another limitation. While WLTP provides a good basis for the analysis, it does not show the localized driving behavior, such as regional traffic, road grade, or regional speed profiles. The inclusion of site-specific or empirically recorded driving cycles would provide a more accurate representation of actual consumption, in particular in spatial modeling of energy demand.

5.5. Recommendations for further research

Future work should focus, as a priority, on refining FCEV modeling by using more accurate and robust optimization to form the power split control strategies, and finding more accurate HVAC designs based on hydrogen-specific systems. Expanding the validation could also increase robustness. Furthermore, integrating region-specific driving profiles would allow for regional assessments beyond the WLTP standard. This could enhance the accuracy of the passenger vehicles' energy demand projections for both urban and rural mobility. Last, because FCEVs combine a compact battery pack with a hydrogen fuel cell stack, they can achieve fast refueling and increased autonomy without the increased battery cost and weight. This makes them increasingly attractive for long-distance transportations and heavy-duty vehicles, where the charging time and the grid congestion are critical. Consequently, future work should develop detailed models for FCEV-powered trucks and commercial fleets, exploring optimal battery sizing, hydrogen infrastructure needs, and impacts on electricity demand, in order to clarify the role of hydrogen in decarbonizing the full spectrum of the transport sector.

6

Conclusion

This thesis research aims to investigate how different powertrain technologies, vehicle types, and environmental conditions affect the passenger car energy demand, with a specified focus on the European territory. By enhancing the Vehicle Consumption Assessment model (VCAM) to incorporate hydrogen fuel cell electric vehicles (FCEVs) and taking into consideration the temperature variability and the regional fleet composition, this research aimed to cover crucial gaps in current vehicle energy consumption models. The following sections present conclusive answers to the research questions posed in the beginning by summarizing the key findings and their implications.

What are the quantified differences in consumption and range between various powertrain technologies across vehicle segments?

The results of the simulations made during this thesis indicate significant and quantifiable differences both in passenger vehicle energy consumption and in driving range between the different powertrain technologies. The battery electric vehicles (BEVs) consistently presented the highest energy efficiency, with the energy consumption values ranging from around 14 kWh/100km to 20 kWh/100km in A, C, and E segments under WLTP driving conditions. This increased efficiency is a result of the increased drivetrain efficiency of the electric motors and the capability of regenerative braking.

Regarding fuel cell electric vehicles (FCEVs), which were added to VCAM through this research, they presented a relatively intermediate energy efficiency. To be more specific, at optimal temperatures between 15 and 25 degrees celcius, C-Segment FCEVs achieved energy consumption levels of around 21 to 23 kWh/100km, corresponding to ranges near 800 km for a standard tank. However, during cold conditions the consumption rises significantly, reaching values of more than 45 kWh/100km due to the increased thermal demand, which reduce range by more than 20%. These results show that while FCEVs offer longer ranges than BEVs, they are also significantly affected by ambient temperature conditions. The segment-specific analysis made during this research confirmed that the vehicle mass and the aerodynamic characteristics strongly influence both energy use and range.

As far as internal combustion engine vehicles (ICEVs) are concerned, they presented the highest energy consumption levels across all segments. Their specific fuel consumption differed a lot with varying driving cycles and vehicle segments, but it was always higher than that of FCEVs and BEVs, thus reflecting the relatively low thermal efficiency of the combustion process and the absence of energy recovery technologies.

It is worth noting here the nonlinear relationships that exist between vehicle segments and energy consumption as a result of the interacting effects of mass, frontal area, drivetrain sizing, and thermal demand. To be more specific, while increased mass generally means higher consumption, the extent of this impact varies depending on the driving cycle and temperature.

In summary, BEVs offer higher efficiency, but they are suffering from the limited thermal resilience and range. FCEVs offer an attractive balance between range and efficiency, but require effective strategy

planning to manage operating under extreme temperature conditions. ICEVs remain the least efficient, but they are less sensitive to cold. These findings underline the need to plan the energy systems according to climate sensitivity to deploy low-carbon emission technologies in Europe.

To what degree does weather variability impact the energy consumption of passenger vehicles with different powertrains?

The impact of weather variability on passenger vehicle energy demand is crucial, especially for electrified powertrain technologies. This thesis assessed the sensitivity of fuel cell electric vehicles, the battery electric vehicles, and the internal combustion engine vehicles to ambient temperature variations, using historical hourly weather data for the period 1980 - 2019 in three European countries: Greece, Germany, and Finland, which represent three different climate zones present in Europe.

Quantitatively, BEVs and FCEVs present increased sensitivity to ambient temperature, especially in colder climates. This is indicated by the ”cold penalty” values of 83.3% and 87.0% for BEVs and FCEVs, respectively in -20 degrees in comparison with their consumption at 20 degrees. ICEVs, on the other hand, present a moderate increase in consumption in cold climates (5.0%), which is the result of their capability to use engine waste heat to cover the cabin’s heating demand. However, ICEVs still present increased consumption in warmer conditions, even up to 25%, because of the cooling demand.

Beyond point-based assessments, the study used a time-series analysis for 40 years of weather data to evaluate both the seasonal and the inter-annual variability in consumption. The heatmap analyses of hourly energy consumption patterns revealed that FCEVs in colder countries, such as Finland, presented consistently increased hydrogen consumption during winter months, with clear peaks during years when long winters were experienced. In contrast, in Mediterranean countries like Greece, the consumption remains relatively steady throughout the year, with small increases during the summer months when the cabin cooling loads are high.

What is worth noting is that the results show that the mean annual temperature alone is not enough to explain the inter-annual variation in consumption. The distribution, frequency, and duration of extreme temperature events have a larger impact on the overall energy consumption than the annual averages. For example, one year with short but severe cold periods could result in higher overall energy consumption than a year with generally lower average temperatures.

The seasonal distributions presented in the results section of this thesis further depict the increased difference in consumption during winter months for BEVs and FCEVs, especially in colder regions. The 90th percentile values of the winter period consumption are significantly higher than the median, highlighting the importance of modeling weather extremes and not relying on average conditions

In conclusion, temperature conditions variability, including both seasonal and annual fluctuations, plays a key role in shaping the energy consumption profile of electrified vehicles. FCEVs and BEVs are particularly sensitive to ambient temperature extremes, a fact that leads to significant operational uncertainty and challenges when planning infrastructure. The findings underline the need to integrate detailed weather data when planning long-term energy and mobility, especially when evaluating the resilience and resource requirements of vehicle fleets that emit less in Europe.

To what extend does the energy demand for passenger mobility differ across European regions, and what role do vehicle fleet compositions and climate zones play?

The passenger vehicle energy demand in Europe presents significant regional differences, which is shaped by a combination of demographic, climatic, technological, and behavioral factors. This research investigated the future landscape of vehicle energy demand in 2050 for three representative countries, Greece, Germany, and Finland, where each one of them was selected to reflect distinct climate zones and fleet characteristics.

The scenario analysis, which combines International Energy Agency (IEA) policies and Representative Concentration Pathways (RCPs) revealed that the national energy demand is driven mainly by two

factors: the degree of decarbonization achieved through the policy implementation and the temperature profiles, which are connected with climate change pathways.

Germany, with its large population and high vehicle stock, presented the highest absolute demand projections, ranging between 129 and 164 TWh depending on the scenario. In contrast, Greece and Finland showed significantly lower values because of the smaller fleet and the less intensive travel demand. However, the influence of climate and fleet composition was more evident in Finland, where cold winters and extended heating demands enhance the impact of policy and climatic changes.

For all the countries, the IEA policy scenarios represent the majority of the variation, with the energy demand being decreased by over 30% when moving from STEPS to NZE. For example, in Finland, the demand under the STEPS-RCP 2.6 scenario was approximately 12.8 TWh, and it dropped to around 10 TWh under the NZE-RCP 8.5 scenario, which means a 20% reduction solely by policy ambitions. RCP-related changes produced smaller but still notable effects. Warmer climates resulted in lower energy demand for all policy scenarios because of the reduced heating needs, with Finland showing the highest sensitivity, followed by Germany and then Greece.

In addition, fleet composition, and especially the growth of SUVs, appeared to be a critical factor that influences future energy demand. The simulations considered different SUV sales growth rates, according to market trends, and this revealed an upward pressure on energy use, even under the most ambitious policy scenarios. For instance, in Germany under the NZE scenario, the energy demand was increased by 12 TWh between the 1.0% and 2.0% SUV growth cases. These results are important in scale, and they are opposing the decarbonization efforts.

These findings indicate that the regional differences in energy demand are determined by different factors, including policy design and technological choices. As the climate gets colder across European regions, it plays a more important role, whereas in warmer climates, policies are the key influencers. However, the interaction between the variables must be addressed to ensure that electrification and decarbonization strategies produce the expected outcomes.

To what extent is the energy demand from passenger mobility influenced by variations in powertrain technologies, vehicle types, and weather conditions?

The passenger vehicle energy demand is significantly influenced by the interaction of selecting the powertrain system, the vehicle configuration, and environmental conditions. This thesis demonstrates that these factors operate in a cooperative way to shape the future energy demand landscape of the European transport sector.

First, the powertrain technology has a foundational impact on the energy demand. TO be more specific, BEVs offer the highest efficiency under optimal conditions, but they have unstable consumption rates, because of their temperature sensitivity. Furthermore, FCEVs are less efficient in absolute terms, but they present a smoother energy consumption pattern for different driving conditions, because of their hybrid architecture and better thermal load management. On the other hand, ICEVs are the least affected by temperature, but they present the highest energy requirements and lowest overall system efficiency, and thus, they confirm the need to phase them out in the future.

Second, both the vehicle segment and the fleet composition play an important role. Larger and heavier vehicles have significantly higher energy consumption because of the increased mass, aerodynamic resistance, and auxiliary power needs. The trend to multiply SUVs represents a structural challenge that could alter the energy gains of the electrification of the transport sector and they need to be offset by downsizing policies or stricter efficiency regulations.

Third, the weather variability produces crucial temporal and regional variation in energy demand. Both BEVs and FCEVs show important nonlinear responses to extreme cold and hot temperature events, which lead to increased seasonal requirements, especially in northern climates. These effects, which are connected to the temperature, are getting worse over time, due to the increased inter-annual climatic fluctuations and the long-term global warming scenarios, highlighting the need to integrate dynamic weather modeling into energy system planning.

Finally, the regional context is in the middle of the outcome of these factors. Countries such as Finland, Germany, and Greece show how demographic scale, climate zone, and vehicle use interact with policies and technology selection to produce different energy demand pathways. Even under similar powertrain changes, different countries can face different infrastructure needs and storage requirements due to the localized effects.

In conclusion, this research confirms that the future passenger vehicle energy demand in Europe does not solely depend on the electrification rate or the powertrain technology adoption. It is the complex interaction of powertrain efficiency, vehicle fleet mix, and climate profile that will decide the final energy demand needs of the transport sector. Consequently, the effective decarbonization requires an integrated planning that combines powertrain innovation, behavioral change, climatic resilience, and specific policy interventions both at regional and European levels.

References

(ACEA), E. A. M. A. (2024). *Charging ahead: Accelerating the roll-out of eu electric vehicle charging infrastructure* (Analysis report using EAFO data, accessed May 2024). https://alternative-fuels-observatory.ec.europa.eu/transport-mode/road/electric-vehicles/charts-and-data/infrastructure-progress

Agency, E. E. (2023). Greenhouse gas emissions from transport in europe [Accessed: 2025-03-24]. https://www.eea.europa.eu/en/analysis/indicators/greenhouse-gas-emissions-from-transport

Agency, E. E. (2024). New registrations of electric vehicles in europe (indicator) [Published 31 Oct 2024]. https://www.eea.europa.eu/en/analysis/indicators/new-registrations-of-electric-vehicles

Agency, E. E. (2025). Transport and mobility (in-depth topic) [Modified 10 Feb 2025]. https://www.eea.europa.eu/en/topics/in-depth/transport-and-mobility

Ahn, K., Rakha, H., Trani, A., & Van Aerde, M. (2004). Development of vt-micro model for estimating hot stabilized light duty vehicle fuel consumption and emissions. *Transportation Research Part D: Transport and Environment*, *9*(1), 49–74.

Ahn, K., Rakha, H., Trani, A. A., & Van Aerde, M. (2002). Estimating vehicle fuel consumption and emissions based on instantaneous speed and acceleration levels. *Journal of Transportation Engineering*, *128*(2), 182–190. https://doi.org/10.1061/(ASCE)0733-947X(2002)128:2(182)

Akçelik, R., & Biggs, D. (1989). Efficiency and drag in the power-based model of fuel consumption. *Transportation Research Part B: Methodological*, *23*(5), 376–385.

Al-Wreikat, M., Abduljabbar, R., & Dia, H. (2022). Effects of ambient temperature and trip characteristics on the energy consumption of an electric vehicle. *Energy*, *239*, 122230. https://doi.org/10.1016/j.energy.2021.122230

Al-Wreikat, Y., Serrano, C., & Sodré, J. R. (2022). Effects of ambient temperature and trip characteristics on the energy consumption of an electric vehicle. *Energy*, *238*, 122028. https://doi.org/10.1016/j.energy.2021.122028

An, F., & Ross, M. (1993). *A model of fuel economy and driving patterns* (Technical Paper No. 930328). SAE International. https://doi.org/10.4271/930328

Argonne National Laboratory. (2016). D3: 2016 toyota mirai [Technology Assessment and Policy Studies (TAPS) Program, Argonne National Laboratory]. https://www.anl.gov/taps/d3-2016-toyota-mirai

Basso, D., et al. (2014, February). *Premium efficiency motor selection and application guide* (tech. rep. No. DOE/GO-102014-4107). U.S. Department of Energy. Washington, D.C. https://www.energy.gov/sites/prod/files/2014/04/f15/amo_motors_handbook_web.pdf

Bi, Y., Zhang, G., & Hu, J. (2021). Strategies for the modelisation of electric vehicle energy consumption: A review. *Elsevier*. https://doi.org/10.1016/j.rser.2021.111620

Bicer, Y., Dincer, I., Khalid, H., & Sadeghzadeh, M. (2023). Impact of ambient temperature on electric vehicle energy consumption and range: Analysis based on real-world data. *Energies*, *18*(8), 1994. https://doi.org/10.3390/en18081994

Blog, M. D. S. (2019). *Root mean square error and its normalization*. https://www.marinedatascience.co/blog/2019/01/07/normalizing-the-rmse

Boriboomsin, K., Barth, M., Zhu, W., & Vu, A. (2012). Eco-routing navigation system based on multi-source historical and real-time traffic information. *Transportation Research Board 91st Annual Meeting*. https://www.researchgate.net/publication/260305181_Eco-Routing_Navigation_System_Based_on_Multisource_Historical_and_Real-Time_Traffic_Information

Brooker, A., et al. (2015). Fastsim: A model to estimate vehicle efficiency, cost and performance. *SAE Technical Paper*, 2015-01–0973. https://doi.org/10.4271/2015-01-0973

Car and Driver. (2015). *2015 hyundai tucson fuel cell first drive review* [Accessed: 2025-06-14]. Car and Driver. https://www.caranddriver.com/reviews/a15107787/2015-hyundai-tucson-fuel-cell-first-drive-review/

Car and Driver. (n.d.). *2024 hyundai nexo review, pricing, and specs* [Accessed: 2025-06-14]. Car and Driver. https://www.caranddriver.com/hyundai/nexo

Chen, Y., Li, S., & Li, Y. (2024). A review on quantitative energy consumption models from road transportation. *Energies*, *17*(1), 2. https://doi.org/10.3390/en17010002

Commission, E. (2023a). Co emission performance standards for cars and vans. https://climate.ec.europa.eu/eu-action/transport/road-transport-reducing-co2-emissions-vehicles/co2-emission-performance-standards-cars-and-vans_en

Commission, E. (2023b). Fit for 55 – delivering the eu's 2030 climate target on the way to climate neutrality [Accessed: 2025-03-24]. https://climate.ec.europa.eu/eu-action/european-green-deal/delivering-european-green-deal/fit-55_en

Energy Central. (2024). *Dunkelflaute and storage solutions: Uncomfortable truths in germany's energy transition* [Accessed: 2025-06-30]. https://www.energycentral.com/energy-biz/post/dunkelflaute-and-storage-solutions-uncomfortable-truths-germanys-energy-xYIpjKdYPNH6seT

Europe, H. (2023). *Clean hydrogen monitor 2023* (FCEV deployment data (European Alternative Fuels Observatory)). Hydrogen Europe. https://hydrogeneurope.eu/wp-content/uploads/2023/10/Clean_Hydrogen_Monitor_11-2023_DIGITAL.pdf

European Commission, Joint Research Centre. (2021). JRC IDEES 2021 v1: Infrastructure for Data and Energy Efficiency Simulation [Accessed: 2025-06-30]. https://jeodpp.jrc.ec.europa.eu/ftp/jrc-opendata/JRC-IDEES/JRC-IDEES-2021_v1/

Eurostat. (2025). Passenger cars in the eu - statistics explained [Accessed: March 13, 2025]. https://ec.europa.eu/eurostat/statistics-explained/index.php?title=Passenger_cars_in_the_EU

Fiori, C., Ahn, K., & Rakha, H. A. (2016). Power-based electric vehicle energy consumption model: Model development and validation. *Applied Energy*, *168*, 257–268. https://doi.org/10.1016/j.apenergy.2016.01.097

Giechaskiel, B., Komnos, D., & Fontaras, G. (2021). Impacts of Extreme Ambient Temperatures and Road Gradient on Energy Consumption and CO_2 Emissions of a Euro 6d-Temp Gasoline Vehicle. *Energies*, *14*(19), 6195. https://doi.org/10.3390/en14196195

Grubwinkler, B., Varnhagen, G., & Lienkamp, M. (2016). Crowd-sourced digital maps for energy consumption estimation of evs. *Journal of Advanced Automotive Technology*.

Guzzella, L., & Sciarretta, A. (2013). *Vehicle propulsion systems: Introduction to modeling and optimization* (3rd). Springer.

He, Z., Peng, H., Gao, Y., Yang, J., Hao, S., Han, G., & Wang, J. (2023). Approximate global energy management based on macro–micro mixed traffic model for plug-in hybrid electric vehicles. *Applied Sciences*, *13*(20), 11196. https://doi.org/10.3390/app132011196

Henning, M., Thomas, A. R., & Smyth, A. (2019). *An analysis of the association between changes in ambient temperature, fuel economy, and vehicle range for battery electric and fuel cell electric buses* (tech. rep.) (Report funded by the National Fuel Cell Bus Program (FTA)). Cleveland State University, Energy Policy Center. https://engagedscholarship.csuohio.edu/urban_facpub/1630/

Holden, J., Gonder, J., & Grewe, T. (2015). *Enhanced trip-based energy consumption model: Adding road grade and turn types to fastsim* (tech. rep.). National Renewable Energy Laboratory (NREL). https://www.nrel.gov/docs/fy15osti/energy-model.pdf

Hydrogen Cars Now. (n.d.). *Hyundai tucson fcev* [Accessed: 2025-06-14]. Hydrogen Cars Now. https://www.hydrogencarsnow.com/index.php/hyundai-tucson-fcev/

Hydrogen Insight. (2024). *Hydrogen-powered cars also struggle to deal with cold weather: Study* [Accessed: 2025-06-30]. https://www.hydrogeninsight.com/transport/hydrogen-powered-cars-also-struggle-to-deal-with-cold-weather-study/2-1-1721868

IEA. (2019a). Car market share by powertrain in selected countries and globally in the stated policies scenario, 2019–2030 and 2050 [Accessed: 2025-06-11].

IEA. (2019b). Car market share by powertrain in selected countries and globally in the sustainable development scenario, 2019–2030 and 2050 [Accessed: 2025-06-11].

IEA. (2021). *Net zero by 2050: A roadmap for the global energy sector* (tech. rep.) (Accessed: 2025-06-11). International Energy Agency. https://iea.blob.core.windows.net/assets/deebef5d-0c34-4539-9d0c-10b13d840027/NetZeroby2050-ARoadmapfortheGlobalEnergySector_CORR.pdf?utm_source=chatgpt.com

IEA. (2023). Global ev outlook 2023 [Accessed: 2025-03-24]. https://www.iea.org/reports/global-ev-outlook-2023

IEA. (2024). Global co emissions from transport by subsector, 2000–2030 [Accessed: 2025-03-24].

International Council on Clean Transportation (ICCT). (2024). *Smart charging for cars and trucks in europe* [Accessed: 2025-06-30]. https://theicct.org/publication/smart-charging-cars-trucks-europe-mar25/

IPCC. (2014). Annex i: Atlas of global and regional climate projections [In: Climate Change 2014: Working Group I Contribution to the IPCC Fifth Assessment Report]. https://www.ipcc.ch/report/ar5/wg1/atlas-of-global-and-regional-climate-projections/

Jimenez-Palacios, J. L. (1999). *Understanding and Quantifying Motor Vehicle Emissions with Vehicle Specific Power and TILDAS Remote Sensing* [Ph.D. thesis]. Massachusetts Institute of Technology [Available on Google Scholar].

Kan, Z., Tang, L., Kwan, M.-P., Ren, C., Liu, D., Pei, T., Liu, Y., Deng, M., & Li, Q. (2018). Fine-grained analysis on fuel-consumption and emission from vehicles trace. *Journal of Cleaner Production*, *203*, 340–352. https://doi.org/10.1016/j.jclepro.2018.08.222

Lajunen, A. (2017). Energy efficiency and performance of cabin thermal management in electric vehicles. *SAE Technical Paper*, 2017-01–0192. https://doi.org/10.4271/2017-01-0192

Mądziel, M. (2023). Vehicle emission models and traffic simulators: A review. *Energies*, *16*(9), 3941. https://doi.org/10.3390/en16093941

Mangipinto, A., Lombardi, F., Sanvito, F., Pavičević, M., Quoilin, S., & Colombo, E. (2022). Impact of mass-scale deployment of electric vehicles and benefits of smart charging across all european countries. *Applied Energy*, *322*, 118676. https://doi.org/10.1016/j.apenergy.2022.118676

Markel, T., Brooker, A., Hendricks, T., Johnson, V., Kelly, K., Kramer, B., O'Keefe, M., Sprik, S., & Wipke, K. (2002). Advisor: A systems analysis tool for advanced vehicle modeling. *Journal of Power Sources*, *110*, 255–266. https://doi.org/10.1016/S0378-7753(02)00189-1

Martin, P. (2024). Hydrogen-powered cars also struggle to deal with cold weather: Study. *Hydrogen Insight*. https://www.hydrogeninsight.com/transport/hydrogen-powered-cars-also-struggle-to-deal-with-cold-weather-study/2-1-1721868

Masclans Abelló, P. (2021). *Design and validation of a consumption framework for mixed fleets* [Master's thesis, Technical University of Munich].

Muneer, T., Asif, M., & Kubie, J. (2004). *Future hydrogen economy: Clean and sustainable energy*. Springer.

Norwegian Automobile Federation. (n.d.). Ev winter range test: Electric cars vs winter – the truth about evs' range in cold weather [Accessed via CarMagazine article on EV winter range]. https://www.naf.no/elbil/aktuelt/elbil-og-vinter-test-av-rekkevidde-og-lading/

Ntziachristos, L., Gkatzoflias, D., Kouridis, C., & Samaras, Z. (2009). Copert 4: Computer program to calculate emissions from road transport. *Information Technologies in Environmental Engineering*, 491–504.

on Clean Transportation, I. C. (2023). Phase-out targets for combustion engine vehicles by country [Accessed: 2025-03-24]. https://theicct.org/global-ice-phaseout/

on Climate Change, I. P. (2014). *Climate change 2014: Synthesis report. summary for policymakers* (tech. rep.). IPCC. https://www.ipcc.ch/report/ar5/syr/

OWD. (2021). Co emissions from transport [Accessed: 2025-03-24].

Park, S., Rakha, H. A., Ahn, K., & Moran, K. (2013). Virginia tech comprehensive power-based fuel consumption model (vt-cpfm): Model validation and calibration considerations [Open access under CC BY-NC-ND license.]. *International Journal of Transportation Science and Technology*, *2*(4), 317–336. https://doi.org/10.1260/2046-0430.2.4.317

Post, K., Kent, J., & Dulla, R. (1984). Fuel consumption and emission modeling by power demand and a comparison with other models. *Transportation Research Part A: General*, *18*(3), 191–213.

Purnima, P., & Jayanti, S. (2020). Optimal sizing of a fuel processor for a fuel cell-powered passenger car. *Unknown Journal*, Unknown Pages.

Rajamani, R. (2012). *Vehicle dynamics and control* (2nd). Springer Science & Business Media.

Rakha, H., Ding, Y., & Hao, P. (2011). Virginia tech comprehensive power-based fuel consumption model: Model development and testing. *Transportation Research Part D: Transport and Environment*, *16*(7), 492–503.

Sanvito, F. D. (2022). *Assessment of sector-coupling synergies between electric vehicles and energy systems in decarbonization scenarios* [Doctoral dissertation, Politecnico di Milano, Department of Energy] [Doctoral Thesis].

Scora, G., & Barth, M. (2006). *Comprehensive modal emissions model (cmem), version 3.01 user's guide* (tech. rep.). University of California, Riverside.

Tate, E. D., & Boyd, S. P. (2000). Finding ultimate limits of performance for hybrid electric vehicles. *SAE Technical Paper*, (2000-01-3099).

U.S. Department of Energy. (2024). Fuel Economy in Cold Weather [Accessed 24 March 2025]. https://www.energy.gov/energysaver/fuel-economy-cold-weather

Wong, J. Y. (2001). *Theory of ground vehicles* (3rd ed.). John Wiley & Sons.

Wu, Q., Dong, Z., Zhang, X., Zhang, C., Iqbal, A., & Chen, J. (2025). Towards more efficient pem fuel cells through advanced thermal management: From mechanisms to applications. *Sustainability*, *17*, 943. https://doi.org/10.3390/su17030943

Wu, X., & Peng, H. (2005). A hierarchical coordinated control strategy for optimizing the fuel economy of a power-split hybrid electric bus. *Proceedings of the American Control Conference*, 1318–1323.

Ye, Q., Chen, X., Liao, R., & Yu, L. (2019). Development and evaluation of a vehicle platoon guidance strategy at signalized intersections considering fuel savings. *Transportation Research Part D: Transport and Environment*, *77*, 120–131. https://doi.org/10.1016/j.trd.2019.10.020

Yue, Y., He, X., & Zhang, Y. (2013). Mesoscopic traffic modeling and its application in energy consumption analysis. *Transportation Research Part C: Emerging Technologies*, *35*, 182–193. https://doi.org/10.1016/j.trc.2013.07.001

A

Projections for consumption

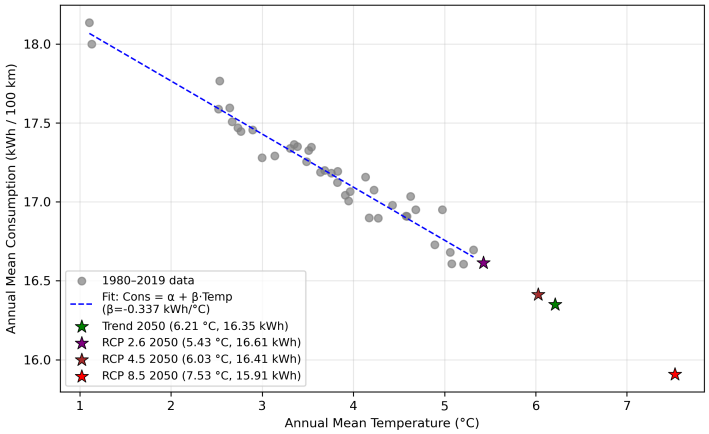

(a) Segment A

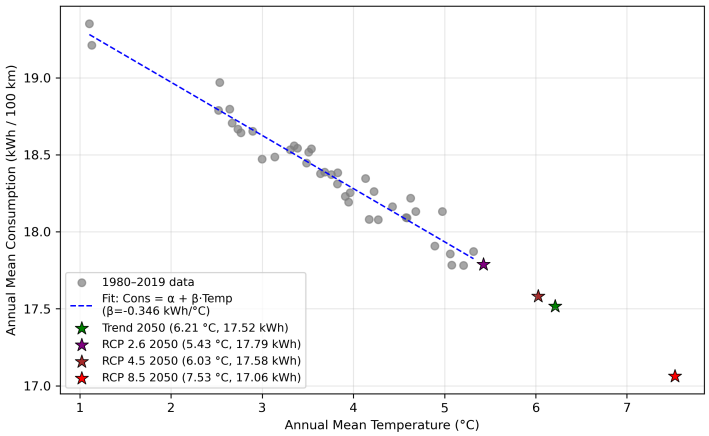

(b) Segment C

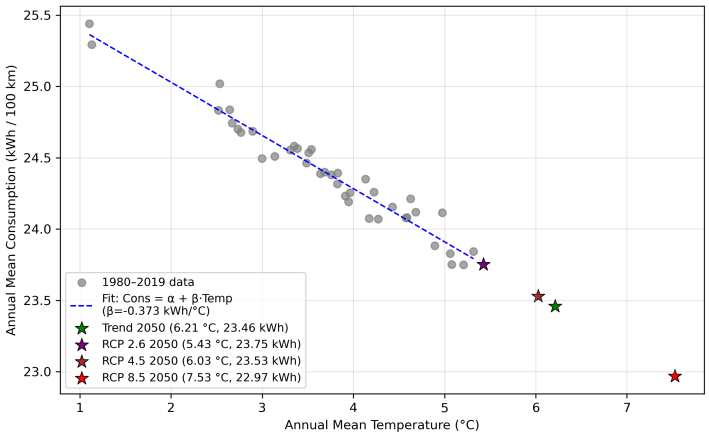

(c) Segment E

Figure A.1: Finland BEV consumption vs. temperature projections by vehicle segment under RCP scenarios.

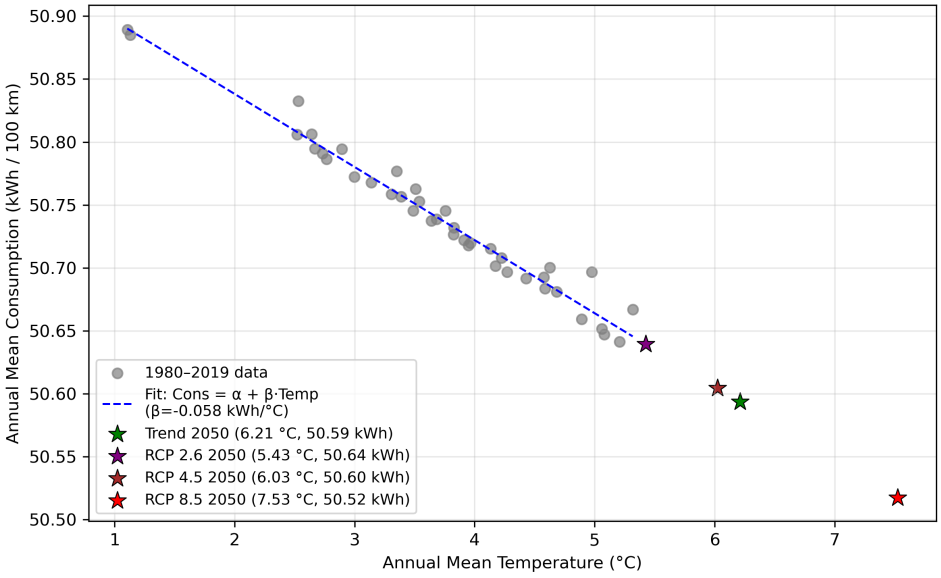

(a) Segment A

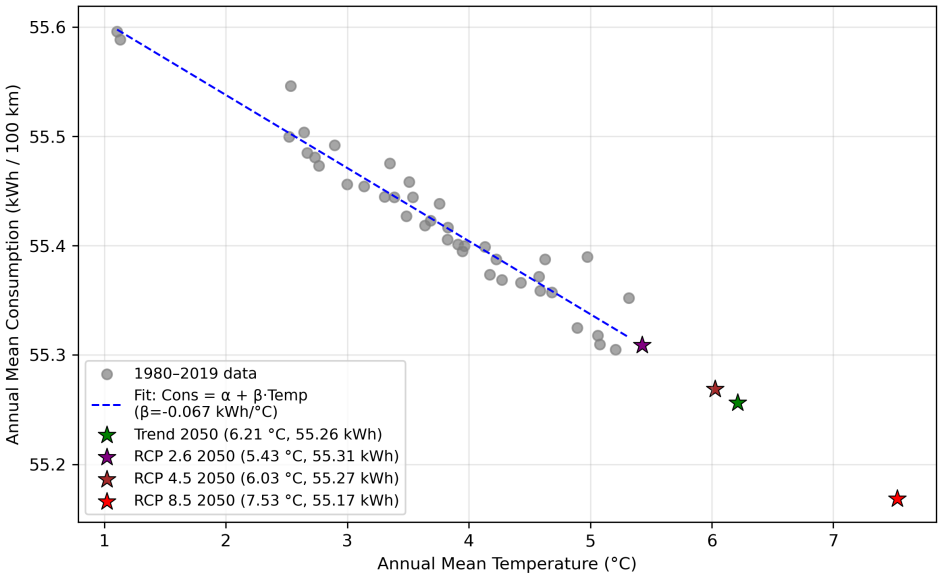

(b) Segment C

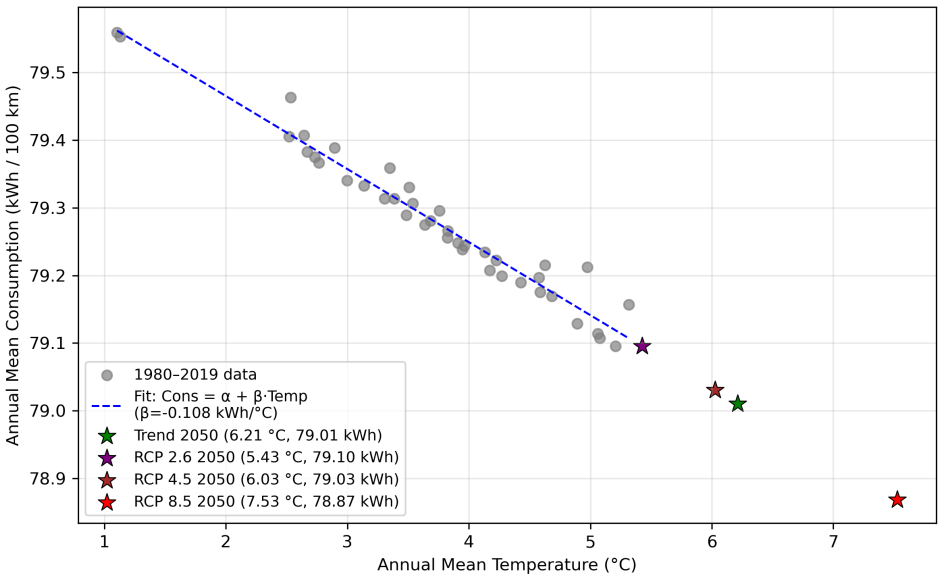

(c) Segment E

Figure A.2: Finland ICEV consumption vs. temperature projections by vehicle segment under RCP scenarios.

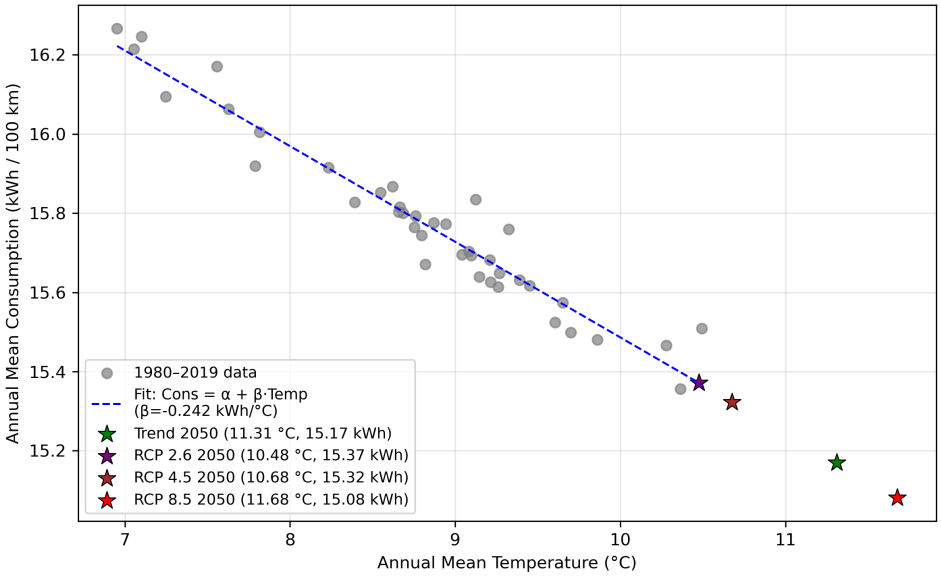

(a) Segment A

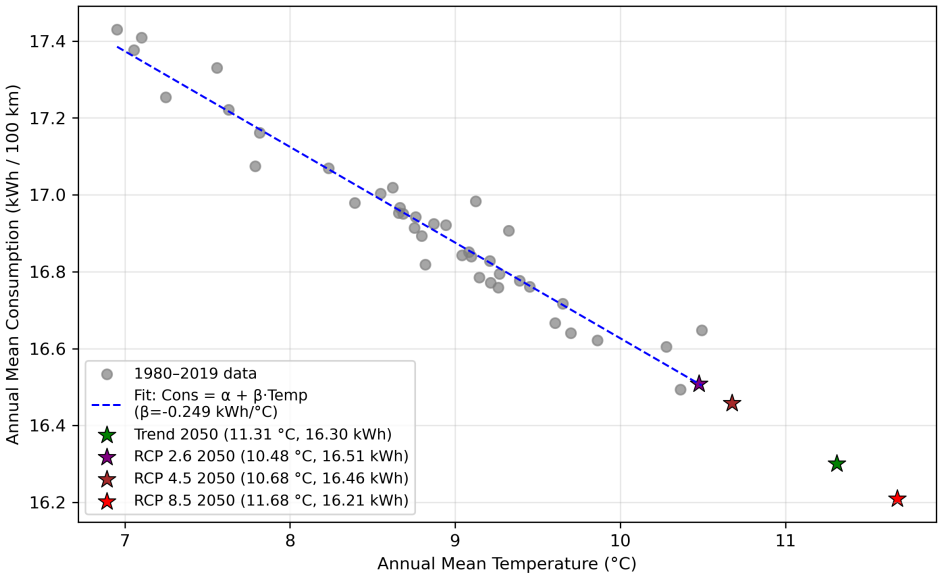

(b) Segment C

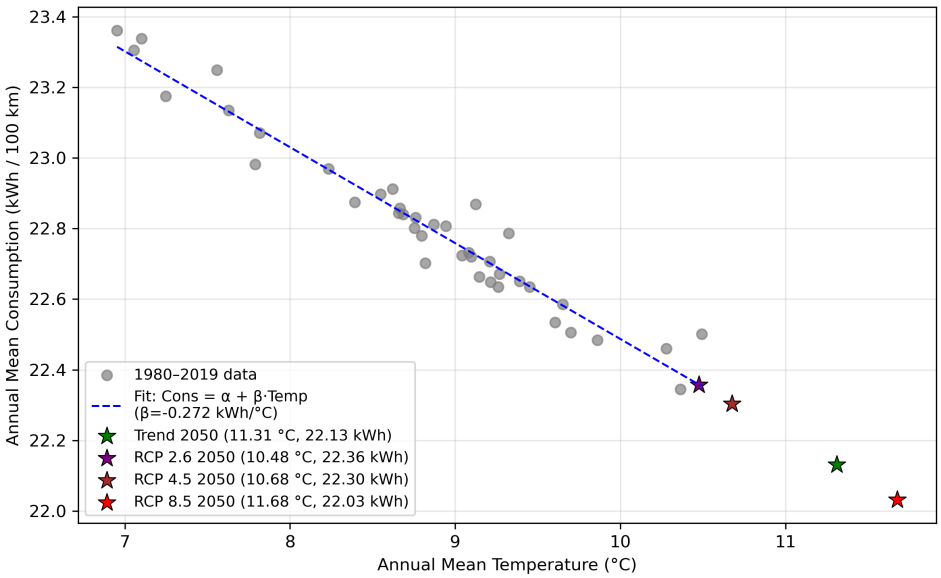

(c) Segment E

Figure A.3: Germany BEV consumption vs. temperature projections by vehicle segment under RCP scenarios.

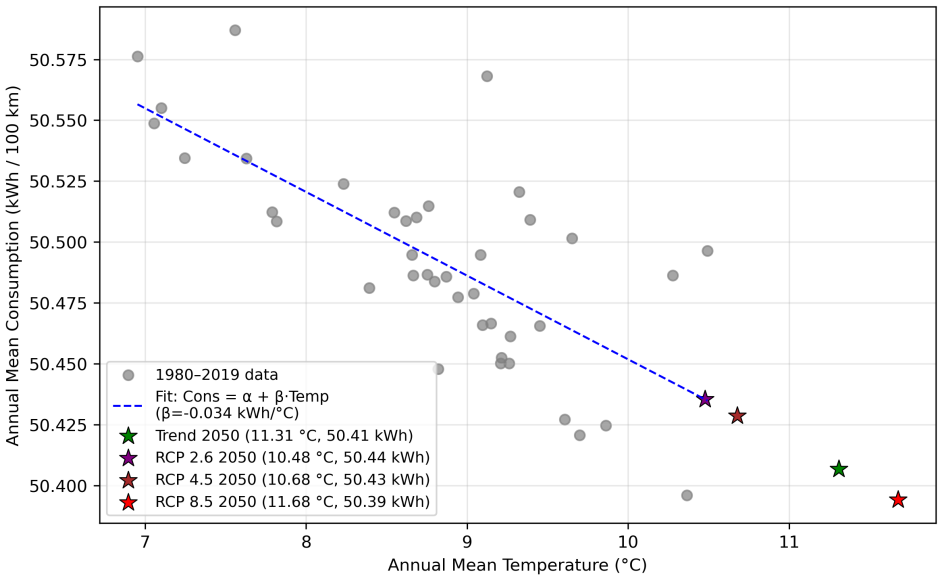

(a) Segment A

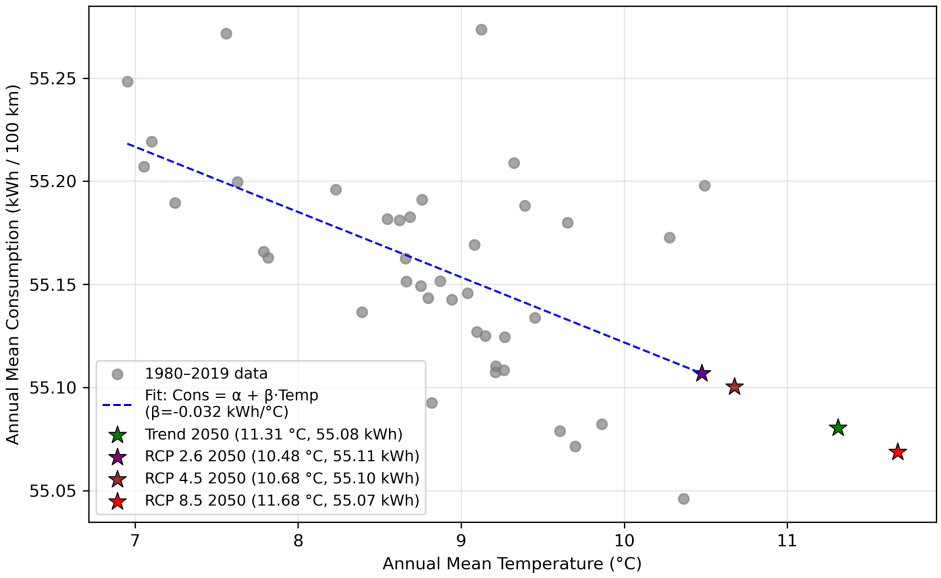

(b) Segment C

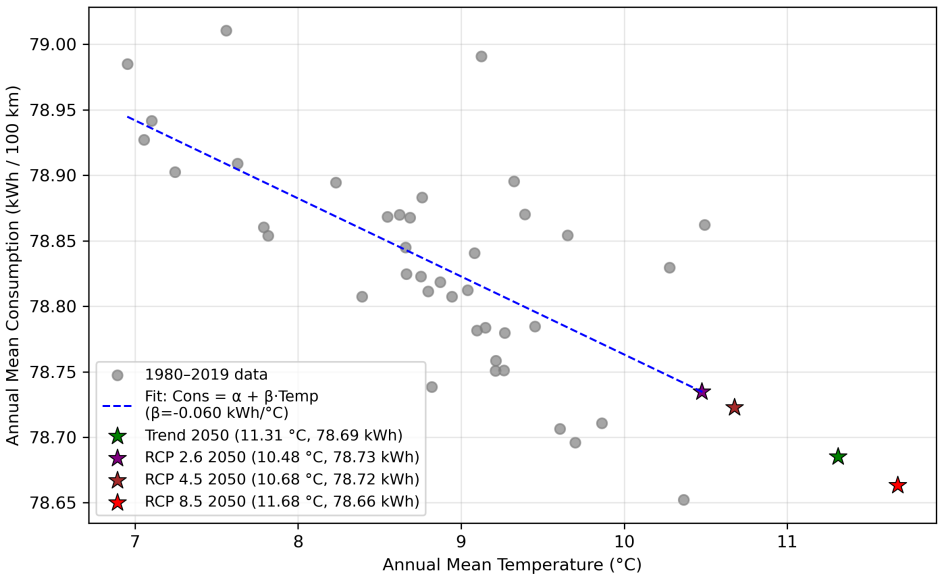

(c) Segment E

Figure A.4: Germany ICEV consumption vs. temperature projections by vehicle segment under RCP scenarios.

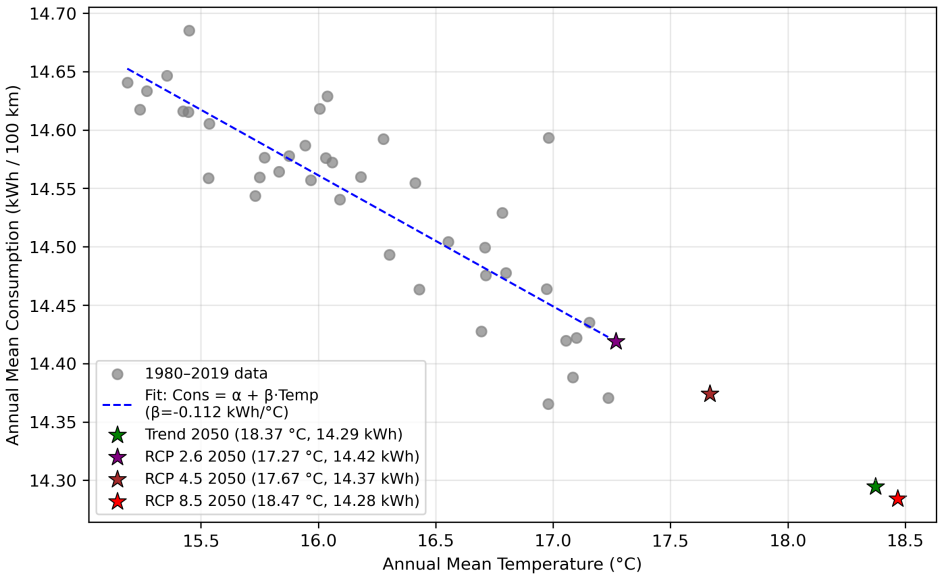

(a) Segment A

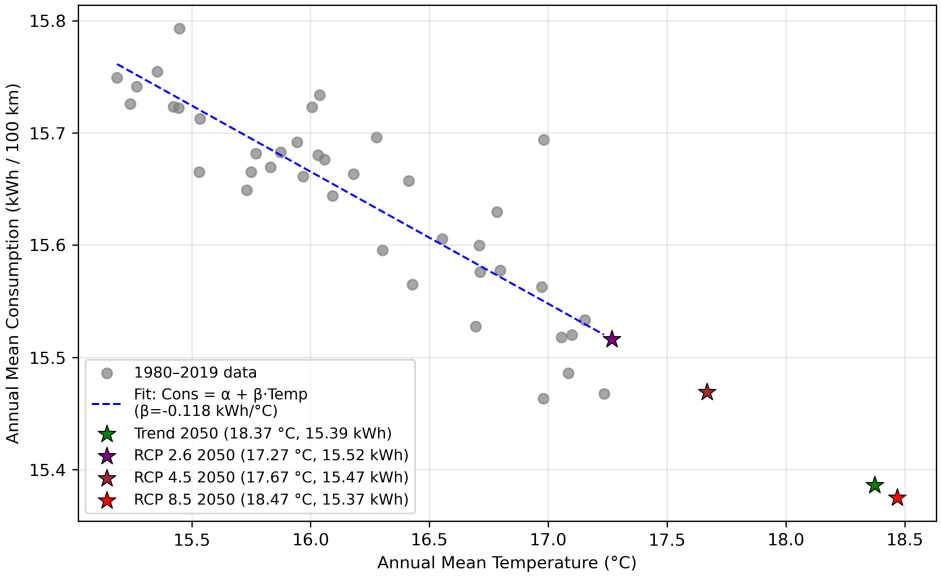

(b) Segment C

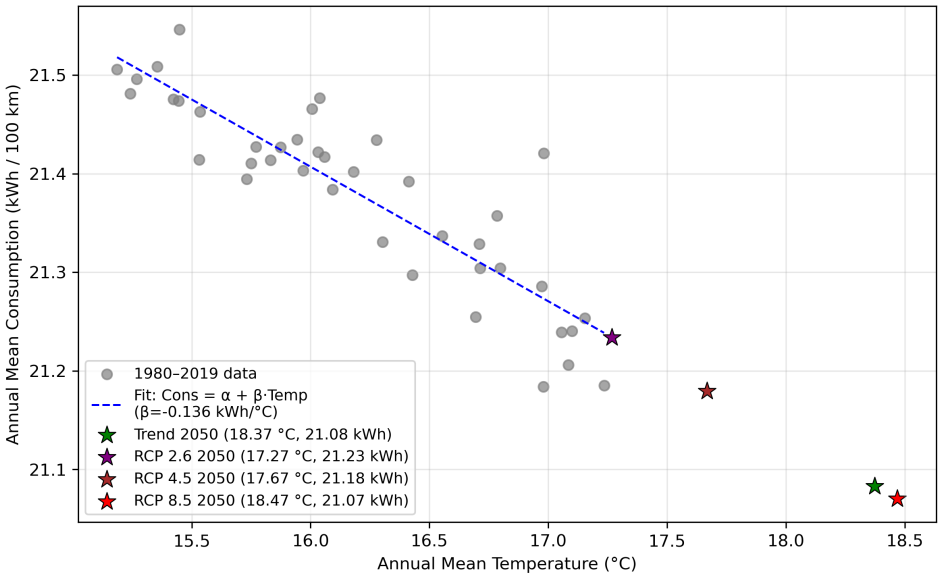

(c) Segment E

Figure A.5: Greece BEV consumption vs. temperature projections by vehicle segment under RCP scenarios.

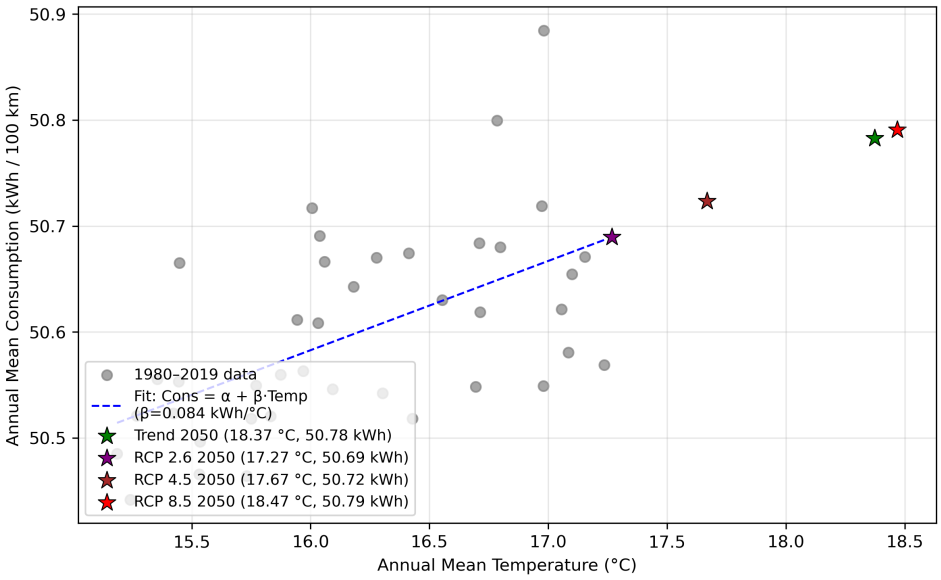

(a) Segment A

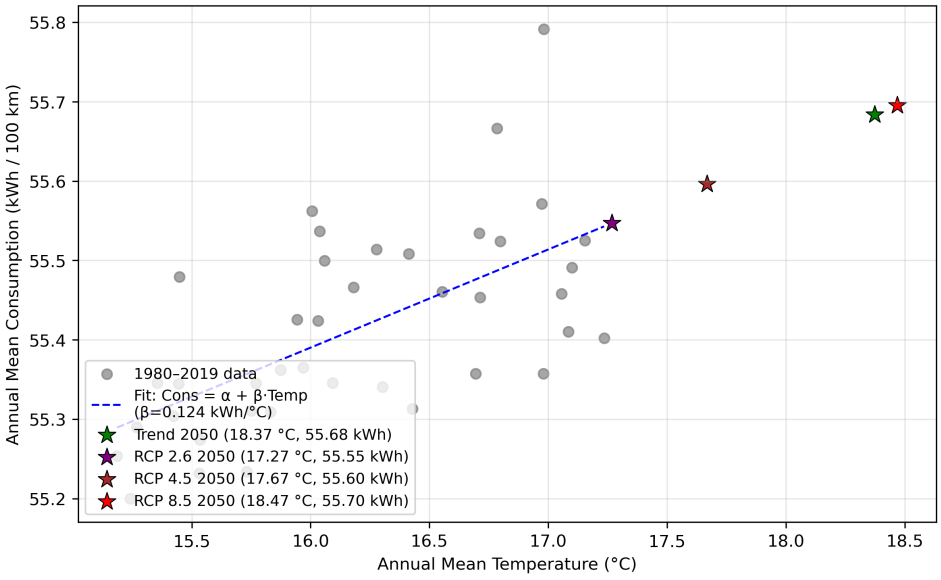

(b) Segment C

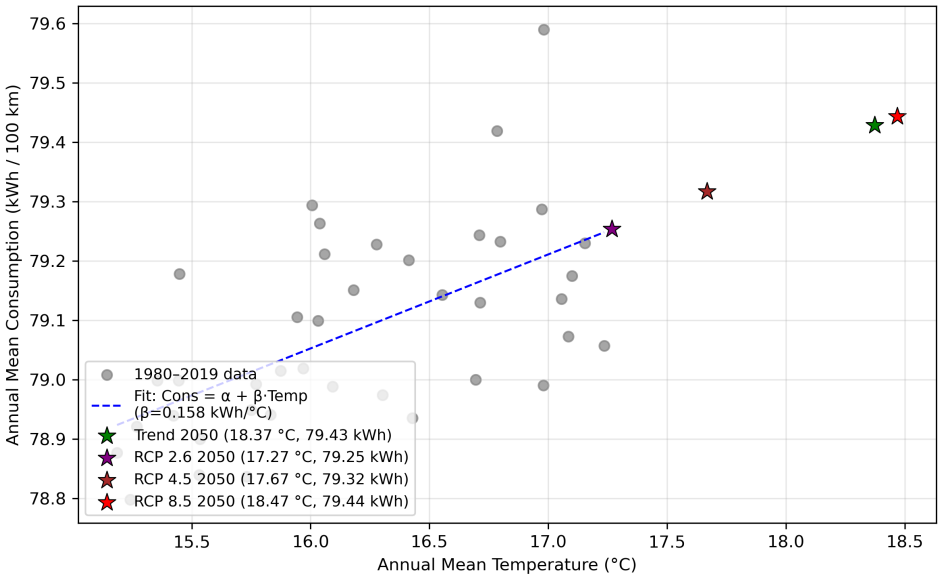

(c) Segment E

Figure A.6: Greece ICEV consumption vs. temperature projections by vehicle segment under RCP scenarios.

B

Small vehicle policy scenario

An additional scenario for a promising small vehicle policy has been made and is presented here. Figures B.1, B.2, and B.3 present the results for Finland, Germany, and Greece, respectively. Table B.1 summarizes the results.

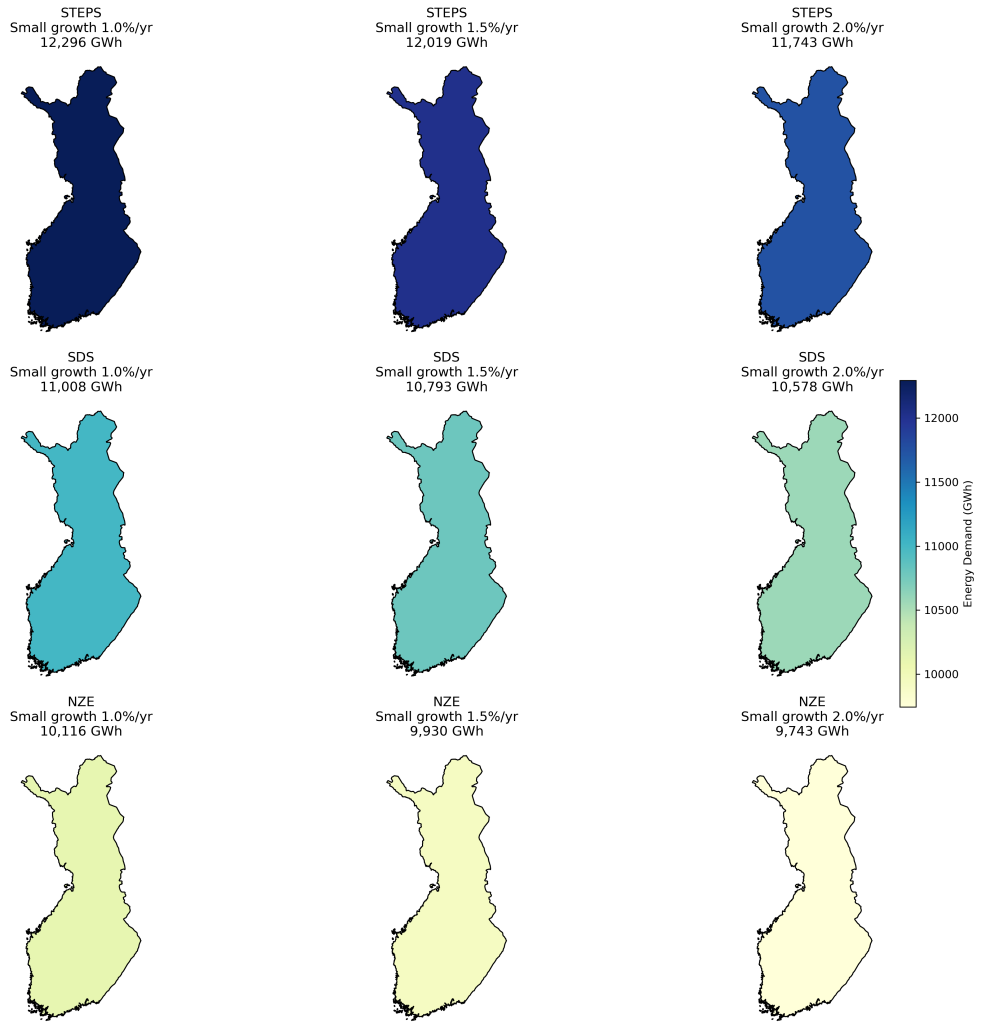

Figure B.1: Projected passenger vehicle energy demand in Finland in 2050 under three IEA policy scenarios (STEPS, SDS, NZE) and varying small vehicle growth rates (1.0%, 1.5%, and 2.0% annually), assuming RCP 2.6 climate conditions.

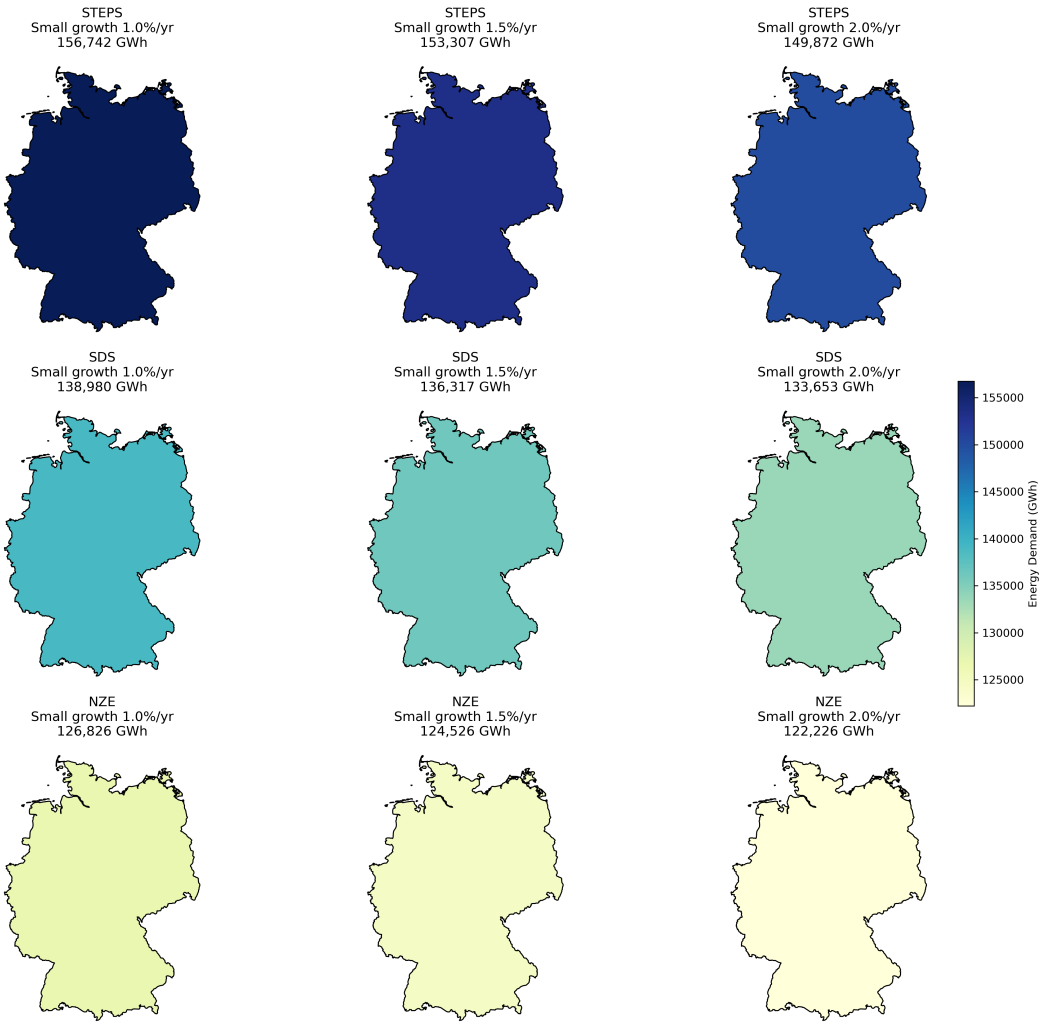

Figure B.2: Projected passenger vehicle energy demand in Germany in 2050 under three IEA policy scenarios (STEPS, SDS, NZE) and varying small vehicle growth rates (1.0%, 1.5%, and 2.0% annually), assuming RCP 2.6 climate conditions.

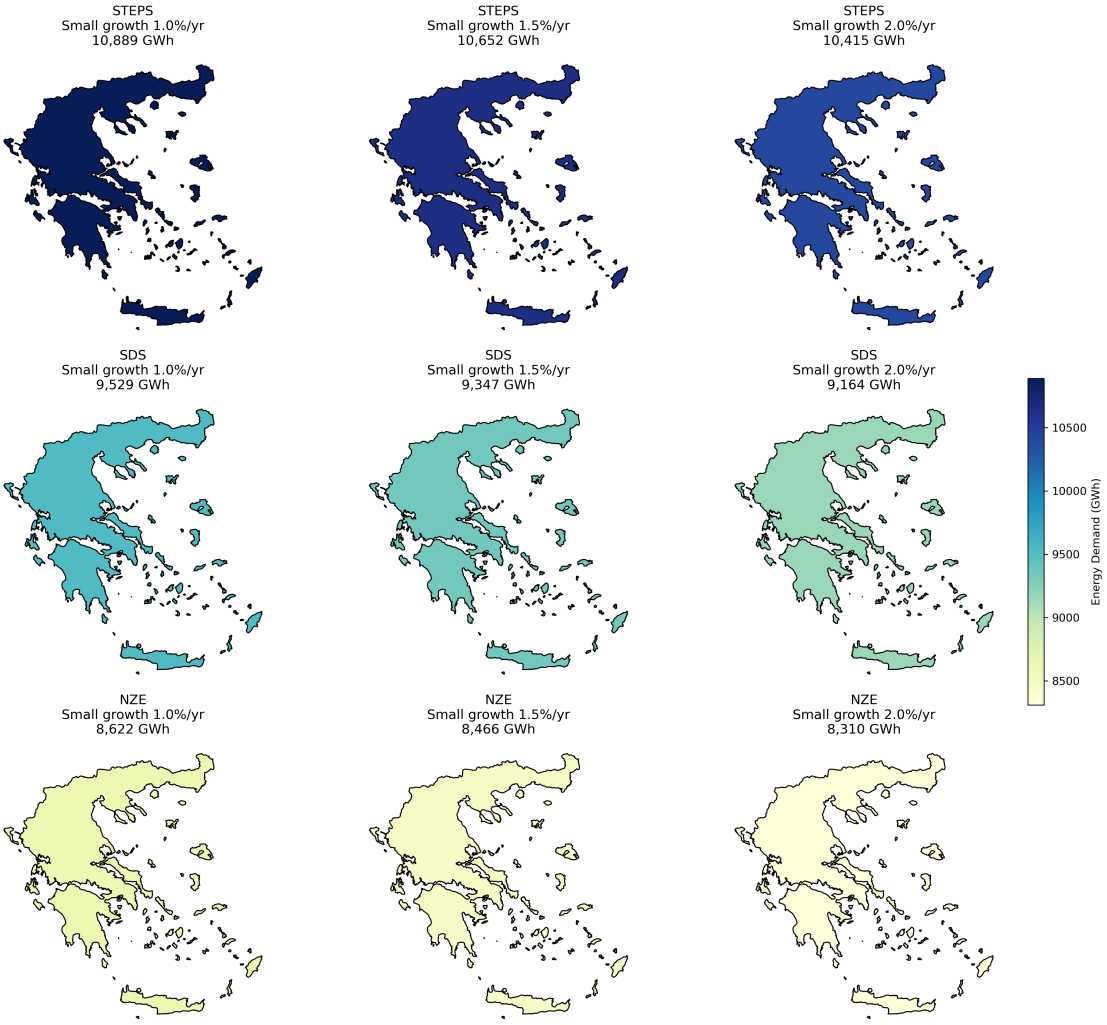

Figure B.3: Projected passenger vehicle energy demand in Greece in 2050 under three IEA policy scenarios (STEPS, SDS, NZE) and varying small vehicle growth rates (1.0%, 1.5%, and 2.0% annually), assuming RCP 2.6 climate conditions.

Table B.1: Energy demand in 2050 under Small Vehicle Growth scenarios, relative to 2019 baseline

Scenario	Small Growth	Greece	Germany	Finland
STEPS	1.0%	10,889 (–60.4%)	156,742 (–58.7%)	12,296 (–57.2%)
	1.5%	10,652 (–61.2%)	153,307 (–59.6%)	12,019 (–58.2%)
	2.0%	10,415 (–62.1%)	149,872 (–60.5%)	11,743 (–59.2%)
SDS	1.0%	9,529 (–65.3%)	138,980 (–63.4%)	11,008 (–61.7%)
	1.5%	9,347 (–66.0%)	136,317 (–64.1%)	10,793 (–62.5%)
	2.0%	9,164 (–66.6%)	133,653 (–64.8%)	10,578 (–63.2%)
NZE	1.0%	8,622 (–68.6%)	126,826 (–66.6%)	10,116 (–64.8%)
	1.5%	8,466 (–69.2%)	124,526 (–67.2%)	9,930 (–65.5%)
	2.0%	8,310 (–69.7%)	122,226 (–67.8%)	9,743 (–66.1%)